IntechOpen

Peripheral Membrane Proteins

Edited by Shihori Tanabe

PERIPHERAL MEMBRANE PROTEINS

Edited by **Shihori Tanabe**

Peripheral Membrane Proteins
http://dx.doi.org/10.5772/intechopen.71809
Edited by Shihori Tanabe

Contributors

Yolanda Sanchez, Tomas Edreira, Elvira Manjon, Meera Srivastava, Ximena Leighton, Harvey B Pollard, Jun Ishii, Yasuyuki Nakamura, Akihiko Kondo, Jia Song, Michael Testa, Pero Lučin, Hana Mahmutefendić, Gordana Blagojević Zagorac, Senka Maćešić, Noriyuki Ishii, Shihori Tanabe

Notice

First published in London, United Kingdom, 2018 by IntechOpen
eBook (PDF) Published by IntechOpen, 2019
IntechOpen is the global imprint of INTECHOPEN LIMITED, registered in England and Wales, registration number: 11086078, The Shard, 25th floor, 32 London Bridge Street
London, SE19SG – United Kingdom
Printed in Croatia

British Library Cataloguing-in-Publication Data
A catalogue record for this book is available from the British Library

Additional hard and PDF copies can be obtained from orders@intechopen.com

Peripheral Membrane Proteins
Edited by Shihori Tanabe

p. cm.

Print ISBN 978-1-78923-512-8

Online ISBN 978-1-78923-513-5

eBook (PDF) ISBN 978-1-83881-617-9

Meet the editor

Dr. Shihori Tanabe, PhD, is a senior researcher at the Division of Risk Assessment, Biological Safety Research Center, National Institute of Health Sciences. She completed her doctorate in the field of molecular biology and pharmacology from the Graduate School of Pharmaceutical Sciences, University of Tokyo. She also performed the research mainly focused on biochemistry and cellular biology at the Department of Pharmacology, College of Medicine, University of Illinois at Chicago. She is a delegate of the Japanese Society for Regenerative Medicine, a councilor of the Society for Regulatory Science of Medical Products, and an editorial board member of the *Journal of Toxicological Sciences*, *Fundamental Toxicological Sciences*, *World Journal of Stem Cells*, *World Journal of Gastrointestinal Oncology*, and *Journal of Medical Genomics and Biomarkers*.

Contents

Preface

The peripheral membrane proteins transduce the extracellular signaling into the cells. The membrane proteins exist in the cellular membranes and are associated with lipids. The membrane proteins include G protein-coupled receptors, receptor tyrosine kinases, channels and transporters and other mysterious proteins.

This book introduces peripheral membrane proteins and their characteristics. The chapters describe the functions and signaling of G proteins, as well as kinases related to cancer signaling, the mechanism of membrane protein recycling, and the structure of the immune-related membrane protein. The signaling and molecular networks mediated by membrane proteins are associated with diseases and therapeutics, which indicate the importance of the investigation in membrane proteins.

In the first chapter, peripheral membrane proteins are introduced in general. The second chapter describes the function of yeast RhoGEF protein related to cellular responses in cell growth and cell division control. The third chapter describes the biosensing techniques in yeast utilizing G protein signaling as a mediator of ligand stimulation-induced gene transcription. The fourth chapter describes the function of a small G protein, Rab35 GTPase, in development and disease. The fifth chapter describes the transcription and network of a serum- and glucocorticoid-inducible kinase, SGK1, in cancer regulated by TGF-beta1. The sixth chapter describes the mechanism in rapid endosomal recycling of membrane proteins. The seventh chapter describes the folding and binding properties and structure of human complement receptor type 1 extracellular domain.

This book intends to provide the readers with mechanism, function and molecular network of membrane proteins. The scope of the book includes insights into peripheral membrane proteins with various roles and conformations in signaling the diseases and biofunctions.

Dr. Shihori Tanabe
Division of Risk Assessment
Biological Safety Research Center
National Institute of Health Sciences
Japan

Chapter 1

Introductory Chapter: Invitation for Peripheral Membrane Proteins

Shihori Tanabe

Additional information is available at the end of the chapter

http://dx.doi.org/10.5772/intechopen.79512

1. Introduction

The peripheral membrane proteins transduce the outer membrane signaling into the cells. The molecules include trimetric G proteins that consist of alpha, beta, and gamma subunits; transporters; and channels. These proteins trigger the intercellular signaling by the stimulations such as ligands including proteins and chemicals. The signaling which is transduced via the peripheral membrane proteins activates several pathways including the G protein signaling, mitogen-activated protein kinase (MAPK) signaling, tumor necrosis factor (TNF) signaling, transforming growth factor (TGF) beta signaling, Wnt signaling, and Hedgehog signaling. Meanwhile, the peripheral membrane proteins, such as cadherins, transduce the signaling from the extracellular ligands into the cells. This book intends to provide the readers with a comprehensive overview of the features and signaling of membrane proteins, which includes the molecular structure and interaction. The insights in membrane proteins associated with diseases and the therapeutics and the effects of the drugs and chemicals are also in the scope of the book.

2. Peripheral membrane proteins

The peripheral membrane proteins exist in the cellular membranes, usually hydrophobic domains are embedded in the lipid membrane and the hydrophilic domains transduce the intercellular signaling. The peripheral membrane proteins include the G protein-coupled receptors (GPCRs), receptor tyrosine kinases (RTKs), channels, and the transporters. The cell-cell communications are mediated with cell adhesion molecules such as cadherins or interactions of antigen and antibody through T cell receptors (TCRs). Transmembrane signaling is mediated via molecular complexes such as dimers, multimers of the receptors, and

colocalized signaling proteins [1–3]. The transmembrane proteins can be classified into receptors, transporters, enzymes, and others [2]. Among receptors, human G-protein-coupled and seven transmembrane receptors include rhodopsin, adhesion, secretin, glutamate, V1R, frizzled, and taste2 [2]. RTKs include epidermal growth factor (EGF) receptors, fibroblast growth factor (FGF) receptors, Ephrin receptors, Ser/Thr kinase receptor family, Axl, neurotrophin receptors, insulin receptors, receptor guanylate cyclases, and platelet-derived growth factor (PDGF) receptors [2]. Furthermore, receptors of the immunoglobulin (Ig) superfamily include TCRs, killer cell Ig-like receptors, leukocyte Ig-like receptors, Fc receptor, netrin receptors, and cytokine receptors [2]. The other receptors include TNF/nerve growth factor (NGF) receptors, integrins, receptor-like protein tyrosine phosphatases, low-density lipoprotein (LDL) receptors, Toll-like receptors, plexins, contactin-associated protein, notch, interleukin (IL) 17 receptors, neurexins, selectin, syndecan, neuropilins, transferrin receptors, adiponectin and progestin, and patched receptors [2]. The transporters contain channels including ion channels and aquaporins, solute carrier superfamily, and active transporters [2]. Ion channels are further classified into chloride channels, voltage-gated-like ion channels, and ligand-gated ion channels [2]. Enzymes include oxidoreductases such as nicotinamide adenine dinucleotide (NADH)/nicotinamide adenine dinucleotide phosphate (NADPH), cytochrome c, and oxygenases; transferases such as acyltransferases transferring other groups than aminoacyl groups, glycosyltransferases, transferring phosphorus-containing groups; and hydrolases such as protein tyrosine phosphatases (non-receptors), O- and S-glycosylases, peptidases, and nucleoside diphosphatases [2]. Miscellaneous class includes ligands such as major histocompatibility complex (MHC), semaphorins, delta, neuroligin, and ephrin B and structural/adhesion proteins such as Ig superfamily, cadherin, and claudin [2].

3. Signaling mediated by peripheral membrane proteins

Membrane proteins mediate signal transduction [4]. EphrinA1 linked to the membrane by glycosylphosphatidylinositol (GPI) anchor or by a single transmembrane segment that triggers Eph signaling which is important for development and cancer via EphA2 RTK [4]. G protein transduces extracellular signaling to inside of the cells via the binding and dissociation of GPCRs [5]. The G protein signaling consists of the cascades from stimulus of the receptor leading to the dissociation of the G protein from the receptor to transduce the downstream pathways to activate various cellular responses. The signaling pathways activated by G protein include MAPK signaling and small G protein signaling [1]. It is very important to elucidate G protein functions and characteristics to know the various cellular activities induced by receptor stimulus. Membrane structure consists of varieties of lipids, which mediates essential functions of gases as substrates or ligands to proteins [6]. Plasma membrane phospholipids are reorganized by membrane potential and induce K-Ras-dependent MAPK signaling [7]. The membrane proteins bind lipids, which leads to the changes in the protein structure and function [8]. The transportomes of eukaryotes which consist of transporters exhibit the energetic evolution [9].

The immune signaling is mediated via transmembrane proteins such as TCRs and B cell receptors [10]. The ligands outside of the cells bind to the extracellular binding domain of the receptor, which leads to the activation of the intracellular signaling via the signaling domain

of the receptor [10]. Multichain immune recognition receptors including TCRs, glycoprotein VI, natural killer (NK) receptors and Fc receptors such as FcεRI, FcαRI, FcγRI, and FcγRIII have a binding subunit and a signaling subunit, both of which are membrane proteins, and assemble together via transmembrane interactions [10]. Upon the ligand binding towards the binding subunit, the signaling subunits form homooligomers to activate downstream signals in signaling chain homooligomerization model [10]. The targeting of the transmembrane interactions between the binding subunit and the signaling subunit has therapeutic potential in which the interference with the transmembrane agent leads to modulate the intracellular signaling [10]. The inhibition of TCRs has the potential in arthritis and skin disease, whereas the inhibition of FcRs targets allergy or asthma [10].

The RTK signaling is induced by the binding of the extracellular ligands leading to oligomerization of the receptors [10]. Among transmembrane RTKs, erb-b2 receptor tyrosine kinase 2 (ErbB2) receptor and epidermal growth factor receptor (EGFR) are targets for cancer treatment, whereas the targeting β-2 adrenergic receptor (β-2AR) has the therapeutic potential for cardiovascular disease or asthma [10].

4. Conclusion

In conclusion, the peripheral membrane proteins regulate and are regulated by several signaling molecules. These proteins transduce signaling triggered by the outside stimulus into the cells, which leads to the regulation of gene and protein expression via transcription of the modulated DNA. The peripheral membrane proteins consist of the several classes and activate the downstream signaling pathways involving in cellular changes and diseases. The new approach to treat diseases might be possible by targeting the peripheral membrane proteins.

Acknowledgements

The author acknowledges the people who are involved in the research.

Conflict of interest

The author declares no conflict of interest.

Author details

Shihori Tanabe

Address all correspondence to: stanabe@nihs.go.jp

National Institute of Health Sciences, Kawasaki, Japan

References

[1] Hanna S, Sl-Sibai M. Signaling networks of Rho GTPases in cell motility. Cellular Signalling. 2013;**25**:1955-1961. DOI: 10.1016/j.cellsig.2013.04.009

[2] Almén MS, Nordström KJV, Fredriksson R, Schiöth HB. Mapping the human membrane proteome: A majority of the human membrane proteins can be classified according to function and evolutionary origin. BMC Biology. 2009;**7**:50. DOI: 10.1186/1741-7007-7-50

[3] Wang Y, Bugge K, Kragelund BB, Lindorff-Larsen K. Role of protein dynamics in transmembrane receptor signalling. Current Opinion in Structural Biology. 2018;**48**:74-82. DOI: 10.1016/j.sbi.2017.10.017

[4] Groves JT, Kuriyan J. Molecular mechanisms in signal transduction at the membrane. Nature Structural & Molecular Biology. 2010;**17**:659-665. DOI: 10.1038/nsmb.1844

[5] Radhakrishnan K, Halsz A, McCabe MM, Edwards JS, Wilson BS. Mathematical simulation of membrane protein clustering for efficient signal transduction. Annals of Biomedical Engineering. 2012;**40**:2307-2318. DOI: 10.1007/s10439-012-0599-z

[6] Mayne CG, Arcario MJ, Mahinthichaichan P, Baylon JL, Vermaas JV, Navidpour L, Wen PC, Thangapandian S, Tajkhorshid E. The cellular membrane as a mediator for small molecule interaction with membrane proteins. Biochimica et Biophysica Acta. 2016;**1858**:2290-2304. DOI: 10.1016/j.bbamem.2016.04.016

[7] Zhou Y, Wong CO, Cho K, van der Hoeven D, Liang H, Thakur DP, Luo J, Babic M, Zinsmaier KE, Zhu MX, Hu H, Venkatachalam K, Hancock JF. Membrane potential modulates plasma membrane phospholipid dynamics and K-Ras signaling. Science. 2015;**349**:873-876. DOI: 10.1126/science.aaa5619

[8] Laganowsky A, Reading E, Allison TM, Ulmschneider MB, Degiacomi MT, Baldwin AJ, Robinson CV. Membrane proteins bind lipids selectively to modulate their structurer and function. Nature. 2014;**510**:172-175. DOI: 10.1038/nature13419

[9] Darbani B, Kell DB, Borodina I. Energetic evolution of cellular Transportomes. BMC Genomics. 2018;**19**:418. DOI: 10.1186/s12864-018-4816-5

[10] Sigalov AB. New therapeutic strategies targeting transmembrane signal transduction in the immune system. Cell Adhesion & Migration. 2010;**4**:255-267. DOI: 10.4161/cam.4.2.10746

Chapter 2

The Function of Fission Yeast Rho1- of Cell Growth and Division

Tomás Edreira, Elvira Manjón and Yolanda Sánchez

Additional information is available at the end of the chapter

http://dx.doi.org/10.5772/intechopen.75913

Abstract

Guanine nucleotide exchange factors (GEFs) are directly responsible for the activation of Rho-family GTPases in response to physical and chemical stimuli and ultimately regulate numerous cellular responses such as polarized growth, morphogenesis, and movement. The GEF proteins are characterized by a Dbl-homology (DH) domain that contacts the Rho GTPases, to catalyzing nucleotide exchange, and an associated Pleckstrin homology (PH) domain, which fine-tunes the exchange process by a variety of mechanisms related to the binding of phosphoinositides. Most GEFs are divergent in regions outside the DH/PH module and contain additional protein-protein or lipid-protein interaction domains that presumably dictate unique cellular functions. Fission yeast Rho1-GEFs act as a link between growth processes and the cell cycle machinery. In this chapter, we focus on the recent leaps in our understanding of how Rho1-GEFs control interphase and cytokinesis in fission yeast. Furthermore, we will go beyond mitosis and highlight the unexpected roles of Rho1-GEFs in the DNA damage response.

Keywords: guanine nucleotide exchange factor (GEF), small GTPases, morphogenesis, fission yeast, genome integrity

1. Introduction: fission yeast Rho1p regulates actin dynamics and cell integrity

Rho GTPases are key regulators of the actin cytoskeleton dynamics in eukaryotic cells. Moreover, they also regulate diverse cellular functions including cell cycle, gene expression, vesicle trafficking, and cell polarity [1–3]. In response to physical and chemical stimuli, most Rho GTPases switch between an active GTP-bound conformation, which interacts with downstream

effectors, and an inactive GDP-bound conformation. Because GDP is in general tightly bound and GTP is hydrolyzed very slowly, small GTPases require the helping hand of guanine nucleotide exchange factors (GEFs) that facilitate GDP dissociation, as well as the help of GTPase-activating proteins (GAPs) that stimulate GTP hydrolysis [4, 5]. For certain small GTPases that carry a farnesyl or a geranylgeranyl group in their C-terminus, GDP/GTP alternation combines with cytosol/membrane alternation, which is mediated by guanine dissociation inhibitors (GDIs) that sequester the GTPase within the cytosol in an inactive conformation by shielding their lipid moiety. In addition, the fine-tuning of Rho GTPases is achieved at the posttranscriptional level by microRNA (miRNA) and at posttranslational level by covalent modifications that affect its intracellular distribution, stability, and turnover, among others [6].

Fission yeast Rho GTPase Rho1p is essential and is a functional homolog of human RhoAp and budding yeast Rho1p [7]. Rho1p is present on the plasma membrane (PM) and at internal membranes (unpublished results). Prior to the septum invagination, the protein slightly concentrates to the middle cortex of the cell. As the actomyosin ring shrinks, Rho1p signals continue to invaginate and finally split into two closely associated discs [7, 8].

Depletion for Rho1p activity in growing cells causes cells to lyse, and the cells shrink and die in a kind of "apoptosis" accompanied by the disappearance of polymerized actin. An increase in Rho1p expression produces larger actin dots, randomly distributed throughout the cell [7, 9] and a thick cell wall [10]. Thus, a proper balance of Rho1p activity is important for regulating the actin cytoskeleton and the cell wall polymers. To date, there is no likely effector(s) of Rho1p in the regulation of the actin cytoskeleton. However, the protein regulates cell integrity through its interaction with at least three different targets: the β(1,3)-glucan synthase, which is responsible for the synthesis of β-glucan, the major cell wall component [11–14], and the kinases Pck1p and Pck2p (the orthologs of *Saccharomyces cerevisiae* Pkc1p and human PKC). Pck1p and Pck2p operate in a redundant fashion to control essential functions in morphogenesis and cell wall biosynthesis [15–17]. Rho1p, Pck1p, and Pck2p function upstream of the mitogen-activated protein kinase (MAPK) module (Mkh1p, Skh1p/Pek1p, and Pmk1p/Spm1p) of the cell integrity signaling pathway (CIP) [18–21]. This signaling cascade becomes activated under adverse conditions and regulates cell separation, morphogenesis, cell wall construction, or ionic homeostasis [22, 23]. Pck2p elicits the activation of the MAP kinase Pmk1p in response to most environmental stimuli, whereas Pck1p plays a minor role as a positive regulator of Pmk1p during vegetative growth and cell wall stress [21, 24].

Regarding upstream components of Rho1p signaling, two proteins Mtl2p (Mid two like 2) and Wsc1p, with the characteristics of cell wall stress sensor-like proteins, act by turning on the GTPase. Both proteins are required to maintain the physiological levels of Rho1-GTP under the chronic cell wall stress produced by antifungal agents [25]. Interestingly, signaling through the MAPK Pmk1p remained active in the *mtl2*Δ and *wsc1*Δ disruptants exposed to cell wall stress.

2. Structure and features of fission yeast Rho1p-GEFs

Fission yeast Rho1p acts as a hub for the integration of different signals, and only recently have conditional mutants been described for studying its central role in cell integrity signaling

[26]. In fact, much of what is known about the function of Rho1p comes from studying its regulators, GEFs and GAPs. Rho1p activity is regulated by three GEFs: Rgf1p, Rgf2p, and Rgf3p [8, 27–30]. Other members of the Rho-GEF family in *S. pombe* are the Cdc42p-specific GEFs: Scd1p and Gef1p [31, 32], and Gef3p specific for Rho4p [33, 34]. Gef2p [35, 36] and Mug10p have not yet been assigned to any known GTPase (https://www.pombase.org).

Rho1p-GEFs (Rgf1-3), like most Rho-GEFs, are multidomain proteins and contain a Dbl-homology (DH) domain, which contacts the Rho GTPase followed by a Pleckstrin homology (PH) domain (reviewed in Ref. [37]). The DH domain stabilizes GTP-free Rho intermediates, leading to GTP loading, owing to high levels of intracellular GTP [38, 39]. The nature of this interaction has emerged from crystallography or nuclear magnetic resonance studies of DH domain-containing GEF constructs in complex with their cognate GTPase [5, 40]. DH binding induces conformational changes in the switch regions and the P loop of the GTPase, while leaving the remainder of the structure largely unperturbed [4, 39]. DH domains contain three conserved regions (CR1, CR2, and CR3) and form structures similar to elongated bundles of α-helices arranged in a "chaise longue" shape. Amino acid substitutions within these conserved regions adversely affect nucleotide exchange activity. In *S. pombe*, a point mutation located on helix H8 (CR3) of Rgf3p or the deletion of four amino acids in the same region of the Rgf1p- and Rgf2p-DH domain produces a lack-of-function phenotype [27, 30]. PH domains in DH-PH RhoGEFs are endowed with a variety of regulatory functions and can be autoinhibitory, assist in the exchange reaction, and influence the targeting of RhoGEFs to phosphoinositide-containing membranes [41]. In *S. pombe, rgf3*$^{+}$, a mutation that falls between the PH and Citron and NIK1-like kinase homology (CNH) domains (*lad1-1* mutant), prevents Rgf3p from localizing to the medial ring during cytokinesis [29]. Similarly, in the Rgf1pΔPH mutant, the normal localization of Rgf1p at the two tips is disrupted, and the signal becomes mainly monopolar [42]. Both mutations, *lad1-1* and the Rgf1pΔPH, phenocopy the lack-of-function phenotype.

Apart from the DH-PH module, Rgf1p, Rgf2p, and Rgf3p contain protein-protein interaction domains. Rgf1p and Rgf2p hold a DEP domain that was first discovered in flies (***D****isheveled*), worms (***E****GL-10*), and mammalians (***P****leckstrin*). The DEP domain is a globular domain of about 100 residues that is present in a limited number of protein families with diverse functions related to signal transduction. The best-known function of the DEP domain is plasma membrane anchoring, but DEP domains are also involved in signal termination, intradomain binding, and in dimerization [43–45]. It is worth noting that Rgf1p and Rgf2p, the two proteins containing a DEP domain, localize to both poles and the septum, while Rgf3p, which lacks the DEP domain, localizes exclusively to the septum [8, 29, 30]. Accordingly, in the Rgf1pΔDEP mutant, which lacks 26 internal amino acids of the DEP domain, the protein partially disappears from the poles. However, in this mutant, Rgf1p strongly accumulated inside the nucleus [42]. This finding suggests that the DEP domain of Rgf1p could mediate membrane anchoring and suggests a function for DEP domains in the intramolecular interactions that drive changes in localization (see next section).

The three Rho1p GEFs bear a C-terminal regulatory domain termed the citron homology domain or CNH. Structurally, the CNH domain belongs to the super-family of β-propellers [46] and is present near the C-terminus of several kinases implicated in the regulation of the actin cytoskeleton [e.g., citron, nck-interacting kinase (NIK) and TNIK (traf-2 and nck-interacting kinase)] and

in the regulation of Rom1p and Rom2p (the *S. cerevisiae* orthologous of *S. pombe* Rgf1p/2). This CNH domain is of unknown function but might be a protein-protein interaction domain [47, 48]. The CNH domain is essential for Rgf1p function in cell integrity and cell polarity [42]. Moreover, cells carrying mutations in the CNH domain of Rgf3p are inviable, and swapping of the CNH domain of Rgf3p for its counterpart in Rgf1p did not rescue the lethality in the *rgf3*Δ/*rgf3*$^{+}$ diploid (unpublished data). These observations suggest that the CNH domain of Rgf1p and Rgf3p may mediate its interaction with different proteins, thus providing signal specificity.

3. Recruitment of Rgf1p, Rgf2p, and Rgf3p to different subcellular sites

The essential localization of Rho1p to the cellular membranes makes it difficult to understand the specific tasks of this protein in polarized growth, secretion, and gene expression. In many cases, it is the specific localization of the corresponding GEFs and GAPs that activate/inactivate the GTPase in time and space, allowing the GTPase to function in different signaling pathways [49]. Most Rho-GEFs localize either to the cytoplasm or to the plasma membrane (PM), and only a few of them are seen in the nucleus.

In *S. pombe,* Rgf1p shows a dynamic localization during an unperturbed cell cycle. Its distribution mirrors that of the cortical actin patches that accumulate at actively growing tips during interphase and relocalize to a central ring during mitosis (**Figure 1**) [8, 27, 29, 30]. Accordingly, the localization of Rgf1p-GFP to cell tips was strongly affected by the disruption of the actin filaments with Latrunculin A (an actin-depolymerizing agent), but was unaffected by acute disruption of the microtubules with methyl benzimidazole carbamate (MBC). In fission yeast, the actomyosin ring is assembled before anaphase A, whereas its constriction occurs after completion of anaphase B [50]. Rgf1p-GFP appears in the midzone membrane in early anaphase. As the ring constricts, Rgf1p is detected near the actomyosin ring as well as in the developing membrane forming a double-filled disc.

Rgf2p localizes uniformly at the periphery of the spore, probably associated with the forespore inner membrane. Rgf2p-GFP fluorescence appears in the fraction of cells that have already undergone meiosis I and II, where the spore outline is perfectly defined [51]. The fluorescence signal is hardly seen in vegetative wild-type cells. However, when expressed in a multicopy plasmid with its own promoter, Rgf2p fluorescence localizes to the growing ends, the septum, and across the whole cell surface [8, 29, 51].

Rgf3p-GFP localizes exclusively to the contractile ring (**Figure 1**) [8, 29, 30]. Rgf3p appears in the contractile ring when SPBs are ~3 μm apart and contracts with the ring until the signal reaches the center of the cell and then fades. Rgf3p fluorescence is at the trailing edge of the myosin II-regulatory light-chain Rlc1p, which may indicate that Rgf3p is closer to the plasma membrane than myosin II [8]. Recently, super-resolution microscopy was used to determine the spatial localization of contractile ring components relative to the membrane. These experiments have showed that Rgf3p localizes to an intermediate layer of the ring that

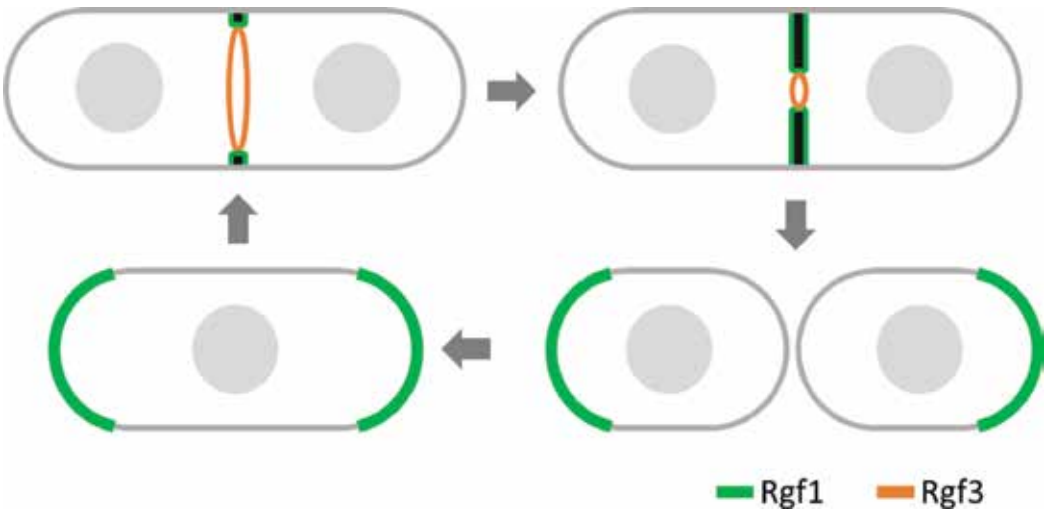

Figure 1. A schematic representation of Rgf1p and Rgf3p localization along the fission yeast cell cycle. See text for details.

includes Pxl1p, Fic1p, Spa2p, Pck1p, Clp1p, Pom1p, and Cyk3. This layer is sandwiched by the membrane-bound scaffolds Mid1p, Cdc15p, and Imp2p on the outer side and by F-actin and motor proteins on the inner side [52]. Interestingly, Cdc15p and Imp2p recruit Rgf3p, Pxl1p, Fic1p, and Cyk3p to preconstriction CRs [53–55]. Rgf3p localization also depends on the CR-localized arrestin Art1p [56]. Art1p and Rgf3p physically interact and are interdependent for localization to the division site. Moreover, both proteins are involved in the maintenance of active Rho1p levels at the division site [56].

Many signaling pathways are activated under stress conditions, and a change in the localization of the GEFs may be crucial for inhibiting or redirecting polarized growth under the new situation. For instance, Rgf1p is released from the cellular poles and enriched in the cytoplasm under osmotic stress (sorbitol and KCl 1.2 M). This situation is transient, and the protein returns to the cell tips 2 h after treatment, even in the presence of stress (unpublished observations). On the contrary, cell wall stress induced by caspofungin, an antifungal agent that inhibits β-glucan biosynthesis, increases the level of Rgf1p at the cell tips at least threefold. Unexpectedly, Rgf1p accumulates in the nucleus in response to DNA replication damage caused by hydroxyurea (HU, an inhibitor of the ribonucleotide reductase that blocks DNA replication). This is characteristic of Rgf1p, since neither Rgf2p nor Rgf3p is observed to undergo altered cellular localization under DNA replication-stressed cells [42]. During a normal cell cycle, Rgf1p continuously shuttles between the nucleus and the cytoplasm. Import to the nucleus is mediated by a nuclear localization sequence (NLS) at the N-terminus, whereas release into the cytoplasm requires two leucine-rich nuclear export sequences (NES1 and NES2) at the C-terminus of the protein. When cells are subject to replication stress, the nuclear accumulation of Rgf1p depends on the DNA replication checkpoint kinase Cds1p and the 14-3-3 chaperone Rad24p. Both proteins control the nuclear accumulation of Rgf1p by inhibiting its nuclear export [42].

4. Rho1p-GEFs at the cell tips

Rgf1p localizes to the growing ends and the septum, where Rho1p and its effectors Pcks and the GSs are known to function. Rgf1p and Rho1p interact by co-immunoprecipitation, and deletion of Rgf1p greatly decreases the amount of GTP-bound Rho1p, suggesting that Rgf1p is responsible for most of the GTP-bound Rho1p available in the cell [19, 27]. Approximately 15% of the *rgf1*Δ cells lyse and the mutants are hypersensitive to cell wall-damaging agents and other types of stress [19, 27, 42, 57]. The lysis phenotype of *rgf1* null cells is similar to that seen after depletion of Rho1p. However, while *rho1*$^{+}$-depleted cells die in pairs (^) that lose their integrity mainly during the division process, in *rgf1*Δ cells lysis occurs mainly in single cells and in pairs of lengthy cells (^). These observations indicate that *rgf1*Δ cells do not lose their integrity during septation.

Rgf1p regulates cell integrity directly through Rho1p by activating the β-GS complex containing the catalytic subunit Bgs4p [27] and indirectly (also through Rho1p) by signaling upstream from the Pmk1p mitogen-activated protein kinase pathway (CIP, cell integrity pathway) [19]. Rgf1p positively regulates the activation of the CIP in cells stressed by cell wall damage and osmotic shock. Moreover, Rgf1p mainly acts alone in this process since Pmk1p activation was largely independent of the other two Rho1p-GEFs, Rgf2p and Rgf3p [19]. Thus, Rgf1p is important for cell wall remodeling at the cellular poles during an unperturbed cycle, acting through Rho1p-Bgs4p, and under stress conditions through Pck2p-Pmk1p.

Another characteristic of the *rgf1*Δ cells is that they are monopolar because after mitosis they fail to activate bipolar growth. In *S. pombe*, both cell ends are different at least in terms of the time of growth activation [58–60]. In wild-type cells, it is always the old end (the one that preexisted before cell division) that initiates growth after cell division. Then, after a period of approximately 50 min, each cell initiates bipolar growth in a process called New End Take-Off (NETO) [61]. This growth transition is triggered by the activation of CDK1 on spindle pole bodies at mid-G2 phase [62] and requires correct completion of the last stages of cytokinesis to render the new cell pole growth competent [63]. Moreover, transient depolymerization of actin has been shown to promote NETO in G1-arrested cells, suggesting that the reorganization of actin may be sufficient to initiate NETO [64]. How the cell cycle signal is transmitted to the cytoskeletal proteins inducing growth initiation at the second cell pole is unknown.

NETO is directed by specific polarity proteins, the kelch-repeat protein Tea1p, the SH3 domain-containing protein Tea4p, and the DYRK (dual-specificity tyrosine phosphorylation-regulated) kinase, Pom1p [65–67]. Tea1p and Tea4p are deposited at cell poles by microtubules where they form protein complexes that recruit and activate the GTPase Cdc42p, a key protein for actin reorganization [68–70]. Similar to Tea1p, Tea4p, and Pom1p, Rgf1p is required for NETO. In the absence of Rgf1p, Cdc42p and the actin patches localize exclusively to the growing end (data not shown and [27]). Thus, Rgf1p could be a good candidate to promote the actin reorganization required to initiate growth at the second end. In line with this, it has been recently shown that Rgf1p is phosphorylated by the MARK/PAR-1 family kinase Kin1p [71]. Kin1p regulates cell polarity and cell wall biosynthesis through unknown mechanisms [72–74]. Moreover, the same authors have shown that Kin1p is a substrate of the CaMKK-like

(Ca2+/calmodulin-dependent protein kinase) Ssp1p [71], also known to contribute to NETO through its function in actin remodeling [64, 75]. Additional substrates for Kin1p are Tea4p, Mod5p, Rga2p, Rng10p, and Chr4p [71]. Thus, Rgf1p could form part of the Ssp1p-Kin1p-signaling pathway for cell polarity and cytokinesis (see subsequent text).

Rgf2p localizes at the cell poles and the septum and plays a minor role in β-glucan biosynthesis during vegetative growth [8, 51]. *rgf2*Δ cells grow like wild-type cells at high and low temperatures and in the presence of heat, osmotic, and genotoxic stresses. However, the disruption of *rgf1*$^{+}$ in an *rgf2*Δ background is lethal, suggesting that Rgf2p shares with Rgf1p an essential function during vegetative growth [8, 51]. Mild overexpression of *rgf2*$^{+}$ (driven by its own promoter or the *rgf1*$^{+}$ promoter in a multicopy plasmid) fully rescues the lysis of *rgf1*Δ cells and partially rescues their bipolar growth defect [51]. The overexpression of the lack of function allele, *rgf2-PTTR*Δ [51], under the control of the *nmt1* promoter increases the percentage of lysis and monopolar cells in the wild-type strain (unpublished results). Therefore, a high level of Rgf2p phenocopies the absence of Rgf1p and suggests that both proteins may compete for the same substrates. In the absence of Rgf1p, Rgf2p takes over the essential functions for Rho1p during vegetative growth.

5. Rho1p-GEFs in cell separation (mitosis and cytokinesis)

S. pombe cells divide similar to mammalian cells, utilizing an actin- and myosin-based contractile ring (CAR) [50, 76]. However, as cell-walled organisms, cytokinesis in *S. pombe* also requires the synthesis of a septum between daughter cells [77, 78]. This septum is composed of three layers. The central layer is the primary septum (PS) that is synthesized in a centripetal manner as the actomyosin contractile ring constricts and is sandwiched on both sides by the secondary septa (SS) [79, 80]. After septum formation, glucanases are secreted to break down the inner primary septum which splits the daughter cells [81, 82].

Septum synthesis is carried out by the GS complex, which includes a regulatory subunit (Rho1p) [83] and three essential catalytic subunits, Bgs1p, Bgs3p, and Bgs4p. It is known that Bgs1p forms linear β-glucans and is essential for PS formation [11] and Bgs4p forms branched β-glucans and is responsible for SS [14]. The function of Bgs3p in β-glucan biosynthesis is unknown. However, cells depleted for Bgs3p are shorter and rounder than wild-type cells and do not lyse, suggesting that the protein must be important for cell polarity and not directly involved in the preservation of cell integrity [84].

Among the Rho1p GEFs, Rgf3p localizes to the CAR and is the main candidate for the role of a positive regulator of Rho1p function during cell separation [8, 30, 85]. First, *lad1-1* cells (a mutant allele of *rgf3*) undergo cell lysis specifically at cell division; electron microscopy analysis indicates that lysis occurs only as the primary septum begins to be degraded [29]. Second, echinocandin hypersensitivity in *ehs2-1* (a mutant allele of *rgf3*) cells is suppressed by mild overexpression of Bgs1p, Bgs2p, and Bgs3p in multi-copy plasmids [30, 84] and third, Rgf3p interacts with GDP-Rho1p, and cells overexpressing Rgf3p have increased GS activity [30].

Ring maturation and constriction also takes longer in *rgf3* mutants [8, 56]. It is possible that Rgf3p acts as a physical link between components of the CAR and the membrane-bound Bgs-mediated septum growth [52]. As previously pointed out, CAR-localized proteins, such as Cdc15p, Imp2p, and Art1p, recruit Rgf3p, which activates the regulatory subunit of the β-GS [53, 56]. The same proteins may also have a role in the trafficking of the catalytic subunits, the Bgs enzymes (β-GS). For instance, Cdc15p participates in the transport of Bgs1p from the late Golgi to the septum membrane, while Rga7p (a Rho GAP) contributes to the transfer of the Bgs4p to the same area [86, 87]. Therefore, cell lysis in *rgf3* cells could be due to a defect in the newly formed cell wall, but whether it is involved in PS or SS biosynthesis is not yet known.

Another point that remains uncertain is the relationship between Rgf3p-Rho1p and the septation initiation network (SIN), the signaling pathway that coordinates mitosis with cytokinesis. SIN signaling requires three protein kinases Cdc7p, Sid1p and Sid2p, and the GTPase Spg1p, and is required for CAR constriction and for septum formation [88, 89]. Overexpression of Rho1p or Rgf3p, but not Rgf1p, partially rescues the lethality of *sid2* mutants at a low restrictive temperature [90, 91]. Based on these results, it has been proposed that SIN activates Rho1p, which in turn activates the Bgs enzymes [91]. However, the SIN target(s) remains unknown. A systematic search for Sid2p substrates has exploited the fact that phosphorylation of the Sid2p consensus site, RxxS [92], creates a binding site for 14-3-3 proteins. The comparison of the proteins that associate with Rad24p when the SIN is switched on or off has generated a list of potential Sid2p targets [93]. Although both Rgf1p and Rgf3p contain several RxxS consensus sites (10 and 7, respectively), only Rgf1p and not Rgf3p appeared in the search [93]. Rgf3p could be directly phosphorylated by Sid2p or another NDR kinase, but that has not been tested. Finally, Rho1p is essential for the feedback activation of Spg1p during actomyosin ring constriction [90].

In animal cells that enter mitosis, RhoA (Rho1p in yeast) and Ect2p (RhoA GEF) play important roles in the remodeling of the actomyosin cortex critical for accurate cell division [94, 95]. In addition, several RhoGEFs have been implicated in the process of chromosome segregation. ARHGEF10 controls centrosome duplication by activation of RhoA [96]. More recently, Net1p, the closest homolog of Rgf1p in mammals, has been shown to be required for chromosome alignment during metaphase and for the generation of stable kinetochore-microtubule attachments; its inhibition results in SAC activation. However, these functions are independent of its nucleotide exchange activity [97].

In *S. cerevisiae*, Cdc5p (polo-like kinase) regulates contractile ring formation via Tus1p and Rom2p, two Rho-GEF proteins and orthologs of Rgf3p and Rgf1p, respectively, that activate the GTPase Rho1p [98]. Rho1p regulates formin-mediated contractile ring assembly [99].

In *S. pombe*, the lytic phenotype displayed by *rho1* and *rgf3* mutants has proven problematic for identifying a possible role for Rho1p in the early stages of cell division. In addition, Rgf1p and Rgf2p also appear at the division site. Rgf1p accumulates in the nucleus of cells treated with HU, except in those cells that have already entered mitosis [42]. However, little is known about a possible role for Rgf1p and Rgf2p in cell division. Double-mutant and phenotypic complementation results suggest that Rgf1p and Rgf3p are not functionally exchangeable. Disruption of *rgf1*$^{+}$ in an *rgf3* mutant (*ehs2-1*) produced viable cells at 28°C but not at 37°C,

a temperature which allows both mutants to grow on plates [27]. In addition, the moderate expression of *rgf1*$^{+}$ does not suppress the lysis of *ehs2-1* cells at 37°C [30]. However, it still needs to be tested whether cell death in the *rgf1Δehs2-1* occurs during cell separation and it is not a consequence of the sum of tip growth defects plus septation defects. Regarding Rgf2p, cells of the double *rgf2Δehs2-1* mutant are viable at all temperatures and phenotypically similar to *ehs2-1* cells.

6. Role of Rho1-GEFs in the maintenance of genome integrity

Besides their classical role as membrane-bound signal-transducing molecules, it has recently been shown that Rho GEFs, Rho GTPases, and downstream components are found in the nucleus, suggesting that Rho-related-signaling processes may also take place in this cellular compartment [100, 101]. Nuclear Rho GEFs, Net1p and Ect2p, regulate, respectively, RhoA- and RhoB-mediated cell death after DNA damage [102–104]. Net1p-knockdown cells fail to activate the nuclear RhoA fraction in response to ionizing radiation [105], and Ect2p regulates epigenetic centromere maintenance by stabilizing newly incorporated CENP-A (a histone H3 variant that acts as the epigenetic mark defining centromere loci [106]).

As pointed out earlier, Rgf1p is accumulated in the cell nucleus during the stalled replication caused by hydroxyurea and is important for tolerance to chronic exposure to the drug [42]. HU causes deoxyribonucleoside triphosphate starvation by inactivating ribonucleotide reductase and blocks the progression of replication forks from early firing origins, activating the DNA replication checkpoint pathway [107]. The central sensor of the DNA replication checkpoint pathway is Rad3p, the fission yeast homolog of human ATR. Rad3p phosphorylates and activates the checkpoint kinases Cds1p or Chk1p, depending on the stage of the cell cycle and the nature of the upstream signal. DNA damage inflicted during S phase leads to the activation of Cds1p, whereas DNA damage activates Chk1p during the G2 phase. Once activated, Cds1p and Chk1p phosphorylate downstream targets to slow down cell-cycle progression and implement DNA repair mechanisms [108, 109].

Nuclear accumulation of Rgf1p after replication stress depends on the replication checkpoint kinases, Rad3p and Cds1p, and on the chaperone Rad24p that belongs to the 14-3-3 family. In the proposed model, when cells are subject to replication stress, Cds1p activation recruits Rgf1p through phosphorylation priming its interaction with Rad24p. This interaction would hide the NES sequence, reducing its association with the exportin Crm1p and thus blocking its exit from the nucleus [42].

While the mechanism for Rgf1p nuclear accumulation is outlined, much less is known about the function of Rgf1p in replication stress, as both processes seem to be directly related. An Rgf1p mutant, Rgf1p-9A, which substitutes nine serine potential phosphorylation Cds1p sites for alanines, (1) does not interact with endogenous Rad24p, (2) fails to accumulate in the nucleus in response to replication stress, and (3) displays a severe defect in survival in the presence of HU. Moreover, the Rgf1p-9A cells do not show the phenotypes characteristic of the *rgf1Δ* cells such as monopolar growth, sensitivity to caspofungin, and the *vic* phenotype

(viable in the presence of immunosuppressant and chlorine ion) [19, 27]. These results suggest that the interaction with Cds1p-Rad24p is required specifically for tolerance to replication stress. Thus, Rgf1p could be part of the mechanism by which Cds1p and Rad24p promote survival in the presence of chronic replication stress [42].

Rgf1p is also involved in tolerance to genotoxic agents other than HU [57]. *rgf1*Δ cells are sensitive to camptothecin (CPT, a topoisomerase inhibitor) and highly sensitive to exposure to phleomycin (Phl, a derivative of bleomycin); both agents induce DNA double-strand brakes (DSBs) [110–112].

DSBs are repaired by two major pathways non-homologous end joining (NHEJ) in G1 and homologous recombination (HR) in S and G2, when the sister chromatid is accessible for use as a template for repair. HR is largely error-free and is the preferred method in yeast. HR initiates when the DSB is resected by nucleases and helicases, generating 3′ single-stranded DNA (ssDNA) overhangs onto which the Rad51p recombinase, with the help of Rad52p, assembles as a nucleoprotein filament [113]. This structure can invade homologous duplex DNA, which is used as a template for DNA synthesis [114, 115].

It has been recently shown that Rgf1p is involved in the repair of DNA double-strand breaks induced by Phl treatment [57]. The deletion of Rgf1p does not prevent the imposition of the checkpoint, but it does prevent recovery from DNA damage, resulting in permanent activation of Chk1p and permanent arrest of the cells in G2/M. This phenotype correlates with the inability of *rgf1*Δ cells to efficiently repair fragmented chromosomes after Phl treatment and with the presence of long-lasting, unrepaired, Phl-induced Rad52p foci in *rgf1*Δ cells.

Moreover, Rho1p and some of the proteins involved in Rho1p signaling also function in the recovery from a DNA-damage G2-induced arrest induced by Phl. Similar to the *rgf1*Δ mutant cells, the *rho1-596* mutant [26] is sensitive to CPT and Phl. The dissolution rate of Phl-induced Rad52p-YFP foci in *rho1-596* and *rgf1*Δ *rho1-596* cells at 28°C (permissive temperature) is very similar to that of the *rgf1*Δ cells, suggesting that Rho1p functions in DSB repair [57]. Future studies defining the interaction of Rgf1p/Rho1p with other DSB repair proteins at Rad52p factories may help to delineate its role in completing DSB repair.

Acknowledgements

We apologize to all authors whose work has not been cited because of space limitation. We thank R. Barrios for the technical help and E. Keck for editing the English language. Elvira Manjón and T. Edreira were supported by a contract from the Regional Government of Castile and Leon cofinanced by the European Social Fund. This work was supported by grants BFU2011-24683/BMC from the CICYT, Spain, and SA073U14 from the Regional Government of Castile and Leon.

Conflict of interest

The authors declare that there is no conflict of interest.

Author details

Tomás Edreira[1,2], Elvira Manjón[1,2] and Yolanda Sánchez[1,2]*

*Address all correspondence to: ysm@usal.es

1 Instituto de Biología Funcional y Genómica, CSIC, Universidad de Salamanca, Salamanca, Spain

2 Departamento de Microbiología y Genética, Universidad de Salamanca, Salamanca, Spain

References

[1] Cook DR, Rossman KL, Der CJ. Rho guanine nucleotide exchange factors: Regulators of Rho GTPase activity in development and disease. Oncogene. 2014;**33**:4021-4035. DOI: 10.1038/onc.2013.362

[2] Hall A. Rho family GTPases. Biochemical Society Transactions. 2012;**40**:1378-1382. DOI: 10.1042/BST20120103

[3] Ridley AJ. Rho GTPase signalling in cell migration. Current Opinion in Cell Biology. 2015;**36**:103-112. DOI: 10.1016/j.ceb.2015.08.005

[4] Bos JL, Rehmann H, Wittinghofer A. GEFs and GAPs: Critical elements in the control of small G proteins. Cell. 2007;**129**:865-877. DOI: 10.1016/j.cell.2007.05.018

[5] Cherfils J, Zeghouf M. Regulation of small GTPases by GEFs, GAPs, and GDIs. Physiological Reviews. 2013;**93**:269-309. DOI: 10.1152/physrev.00003.2012

[6] Liu M, Bi F, Zhou X, Zheng Y. Rho GTPase regulation by miRNAs and covalent modifications. Trends in Cell Biology. 2012;**22**:365-373. DOI: 10.1016/j.tcb.2012.04.004

[7] Nakano K, Arai R, Mabuchi I. The small GTP-binding protein Rho1 is a multifunctional protein that regulates actin localization, cell polarity, and septum formation in the fission yeast Schizosaccharomyces pombe. Genes to Cells. 1997;**2**:679-694. DOI: 10.1046/j.1365-2443.1997.1540352.x

[8] Mutoh T, Nakano K, Mabuchi I. Rho1-GEFs Rgf1 and Rgf2 are involved in formation of cell wall and septum, while Rgf3 is involved in cytokinesis in fission yeast. Genes to Cells. 2005;**10**:1189-1202. DOI: 10.1111/j.1365-2443.2005.00908.x

[9] Arellano M, Duran A, Perez P. Localisation of the Schizosaccharomyces pombe rho1p GTPase and its involvement in the organisation of the actin cytoskeleton. Journal of Cell Science. 1997;**110**(Pt 20):2547-2555

[10] Perez P, Rincon SA. Rho GTPases: Regulation of cell polarity and growth in yeasts. The Biochemical Journal. 2010;**426**:243-253. DOI: 10.1042/BJ20091823

[11] Cortes JC, Konomi M, Martins IM, Munoz J, Moreno MB, Osumi M, et al. The (1,3)beta-D-glucan synthase subunit Bgs1p is responsible for the fission yeast primary septum formation. Molecular Microbiology. 2007;**65**:201-217. DOI: 10.1111/j.1365-2958.2007.05784.x

[12] Martin V, Garcia B, Carnero E, Duran A, Sanchez Y. Bgs3p, a putative 1,3-beta-glucan synthase subunit, is required for cell wall assembly in *Schizosaccharomyces pombe*. Eukaryotic Cell. 2003;**2**:159-169. DOI: 10.1128/EC.2.1.159-169.2003

[13] Martin V, Ribas JC, Carnero E, Duran A, Sanchez Y. bgs2+, a sporulation-specific glucan synthase homologue is required for proper ascospore wall maturation in fission yeast. Molecular Microbiology. 2000;**38**:308-321. DOI: 10.1046/j.1365-2958.2000.02118.x

[14] Munoz J, Cortes JC, Sipiczki M, Ramos M, Clemente-Ramos JA, Moreno MB, et al. Extracellular cell wall beta(1,3)glucan is required to couple septation to actomyosin ring contraction. The Journal of Cell Biology. 2013;**203**:265-282. DOI: 10.1083/jcb.201304132

[15] Arellano M, Valdivieso MH, Calonge TM, Coll PM, Duran A, Perez P. *Schizosaccharomyces pombe* protein kinase C homologues, Pck1p and Pck2p, are targets of Rho1p and Rho2p and differentially regulate cell integrity. Journal of Cell Science. 1999;**112**(Pt 20):3569-3578. PMID: 10504305. ISSN: 0021-9533 (Print) 0021-9533 (Linking)

[16] Sayers LG, Katayama S, Nakano K, Mellor H, Mabuchi I, Toda T, et al. Rho-dependence of *Schizosaccharomyces pombe* Pck2. Genes to Cells. 2000;**5**:17-27. DOI: 10.1046/j.1365-2443.2000.00301.x

[17] Toda T, Shimanuki M, Yanagida M. Two novel protein kinase C-related genes of fission yeast are essential for cell viability and implicated in cell shape control. The EMBO Journal. 1993;**12**:1987-1995. DOI: 10.1002/j.1460-2075.1993.tb05848.x

[18] Barba G, Soto T, Madrid M, Nunez A, Vicente J, Gacto M, et al. Activation of the cell integrity pathway is channelled through diverse signalling elements in fission yeast. Cellular Signalling. 2008;**20**:748-757. DOI: 10.1016/j.cellsig.2007.12.017

[19] Garcia P, Tajadura V, Sanchez Y. The Rho1p exchange factor Rgf1p signals upstream from the Pmk1 mitogen-activated protein kinase pathway in fission yeast. Molecular Biology of the Cell. 2009;**20**:721-731. DOI: 10.1091/mbc.E08-07-0673

[20] Madrid M, Jimenez R, Sanchez-Mir L, Soto T, Franco A, Vicente-Soler J, et al. Multiple layers of regulation influence cell integrity control by the PKC ortholog Pck2 in fission yeast. Journal of Cell Science. 2015;**128**:266-280. DOI: 10.1242/jcs.158295

[21] Sanchez-Mir L, Soto T, Franco A, Madrid M, Viana RA, Vicente J, et al. Rho1 GTPase and PKC ortholog Pck1 are upstream activators of the cell integrity MAPK pathway in fission yeast. PLoS One. 2014;**9**:e88020. DOI: 10.1371/journal.pone.0088020

[22] Madrid M, Soto T, Khong HK, Franco A, Vicente J, Perez P, et al. Stress-induced response, localization, and regulation of the Pmk1 cell integrity pathway in *Schizosaccharomyces pombe*. The Journal of Biological Chemistry. 2006;**281**:2033-2043. DOI: 10.1074/jbc.M506467200

[23] Perez P, Cansado J. Cell integrity signaling and response to stress in fission yeast. Current Protein & Peptide Science. 2010;**11**:680-692. DOI: 10.2174/138920310794557718

[24] Madrid M, Vazquez-Marin B, Soto T, Franco A, Gomez-Gil E, Vicente-Soler J, et al. Differential functional regulation of protein kinase C (PKC) orthologs in fission yeast. The Journal of Biological Chemistry. 2017;**292**:11374-11387. DOI: 10.1074/jbc.M117.786087

[25] Cruz S, Munoz S, Manjon E, Garcia P, Sanchez Y. The fission yeast cell wall stress sensor-like proteins Mtl2 and Wsc1 act by turning on the GTPase Rho1p but act independently of the cell wall integrity pathway. Microbiology. 2013;**2**:778-794. DOI: 10.1002/mbo3.113

[26] Viana RA, Pinar M, Soto T, Coll PM, Cansado J, Perez P. Negative functional interaction between cell integrity MAPK pathway and Rho1 GTPase in fission yeast. Genetics. 2013;**195**:421-432. DOI: 10.1534/genetics.113.154807

[27] Garcia P, Tajadura V, Garcia I, Sanchez Y. Rgf1p is a specific Rho1-GEF that coordinates cell polarization with cell wall biogenesis in fission yeast. Molecular Biology of the Cell. 2006;**17**:1620-1631. DOI: 10.1091/mbc.E05-10-0933

[28] Garcia P, Tajadura V, Garcia I, Sanchez Y. Role of rho GTPases and rho-GEFs in the regulation of cell shape and integrity in fission yeast. Yeast. 2006;**23**:1031-1043. DOI: 10.1002/yea.1409

[29] Morrell-Falvey JL, Ren L, Feoktistova A, Haese GD, Gould KL. Cell wall remodeling at the fission yeast cell division site requires the Rho-GEF Rgf3p. Journal of Cell Science. 2005;**118**:5563-5573. DOI: 10.1242/jcs.02664

[30] Tajadura V, Garcia B, Garcia I, Garcia P, Sanchez Y. *Schizosaccharomyces pombe* Rgf3p is a specific Rho1 GEF that regulates cell wall beta-glucan biosynthesis through the GTPase Rho1p. Journal of Cell Science. 2004;**117**:6163-6174. DOI: 10.1242/jcs.01530

[31] Coll PM, Trillo Y, Ametzazurra A, Perez P. Gef1p, a new guanine nucleotide exchange factor for Cdc42p, regulates polarity in *Schizosaccharomyces pombe*. Molecular Biology of the Cell. 2003;**14**:313-323. DOI: 10.1091/mbc.E02-07-0400

[32] Hirota K, Tanaka K, Ohta K, Yamamoto M. Gef1p and Scd1p, the two GDP-GTP exchange factors for Cdc42p, form a ring structure that shrinks during cytokinesis in *Schizosaccharomyces pombe*. Molecular Biology of the Cell. 2003;**14**:3617-3627. DOI: 10.1091/mbc.E02-10-0665

[33] Munoz S, Manjon E, Sanchez Y. The putative exchange factor Gef3p interacts with Rho3p GTPase and the septin ring during cytokinesis in fission yeast. The Journal of Biological Chemistry. 2014;**289**:21995-22007. DOI: 10.1074/jbc.M114.548792

[34] Wang N, Wang M, Zhu YH, Grosel TW, Sun D, Kudryashov DS, et al. The Rho-GEF Gef3 interacts with the septin complex and activates the GTPase Rho4 during fission yeast cytokinesis. Molecular Biology of the Cell. 2015;**26**:238-255. DOI: 10.1091/mbc.E14-07-1196

[35] Ye Y, Lee IJ, Runge KW, Wu JQ. Roles of putative Rho-GEF Gef2 in division-site positioning and contractile-ring function in fission yeast cytokinesis. Molecular Biology of the Cell. 2012;**23**:1181-1195. DOI: 10.1091/mbc.E11-09-0800

[36] Zhu YH, Ye Y, Wu Z, Wu JQ. Cooperation between rho-GEF Gef2 and its binding partner Nod1 in the regulation of fission yeast cytokinesis. Molecular Biology of the Cell. 2013;**24**:3187-3204. DOI: 10.1091/mbc.E13-06-0301

[37] Rossman KL, Der CJ, Sondek J. GEF means go: Turning on RHO GTPases with guanine nucleotide-exchange factors. Nature Reviews Molecular Cell Biology. 2005;**6**:167-180. DOI: 10.1038/nrm1587

[38] Alemany L, de Sanjose S, Tous S, Quint W, Vallejos C, Shin HR, et al. Time trends of human papillomavirus types in invasive cervical cancer, from 1940 to 2007. International Journal of Cancer. 2014;**135**:88-95. DOI: 10.1002/ijc.28636

[39] Buchsbaum RJ. Rho activation at a glance. Journal of Cell Science. 2007;**120**:1149-1152. DOI: 10.1242/jcs.03428

[40] Dvorsky R, Ahmadian MR. Always look on the bright site of Rho: Structural implications for a conserved intermolecular interface. EMBO Reports. 2004;**5**:1130-1136. DOI: 10.1038/sj.embor.7400293

[41] Rossman KL, Sondek J. Larger than Dbl: New structural insights into RhoA activation. Trends in Biochemical Sciences. 2005;**30**:163-165. DOI: 10.1016/j.tibs.2005.02.002

[42] Munoz S, Manjon E, Garcia P, Sunnerhagen P, Sanchez Y. The checkpoint-dependent nuclear accumulation of Rho1p exchange factor Rgf1p is important for tolerance to chronic replication stress. Molecular Biology of the Cell. 2014;**25**:1137-1150. DOI: 10.1091/mbc.E13-11-0689

[43] Consonni SV, Maurice MM, Bos JL. DEP domains: Structurally similar but functionally different. Nature Reviews Molecular Cell Biology. 2014;**15**:357-362. DOI: 10.1038/nrm3791

[44] Gammons MV, Renko M, Johnson CM, Rutherford TJ, Bienz M. Wnt signalosome assembly by DEP domain swapping of Dishevelled. Molecular Cell. 2016;**64**:92-104. DOI: 10.1016/j.molcel.2016.08.026

[45] Xu W, He X. DEEP insights through the DEP domain. Structure. 2010;**18**:1223-1225. DOI: 10.1016/j.str.2010.09.007

[46] Chen CK, Chan NL, Wang AH. The many blades of the beta-propeller proteins: Conserved but versatile. Trends in Biochemical Sciences. 2011;**36**:553-561. DOI: 10.1016/j.tibs.2011.07.004

[47] Bassi ZI, Audusseau M, Riparbelli MG, Callaini G, D'Avino PP. Citron kinase controls a molecular network required for midbody formation in cytokinesis. Proceedings of the National Academy of Sciences of the United States of America. 2013;**110**:9782-9787. DOI: 10.1073/pnas.1301328110

[48] Taira K, Umikawa M, Takei K, Myagmar BE, Shinzato M, Machida N, et al. The Traf2- and Nck-interacting kinase as a putative effector of Rap2 to regulate actin cytoskeleton. The Journal of Biological Chemistry. 2004;**279**:49488-49496. DOI: 10.1074/jbc.M406370200

[49] Chang EC, Philips MR. Spatial segregation of ras signaling: New evidence from fission yeast. Cell Cycle. 2006;**5**:1936-1939. DOI: 10.4161/cc.5.17.3187

[50] Cheffings TH, Burroughs NJ, Balasubramanian MK. Actomyosin ring formation and tension generation in eukaryotic cytokinesis. Current Biology. 2016;**26**:R719-RR37. DOI: 10.1016/j.cub.2016.06.071

[51] Garcia P, Garcia I, Marcos F, de Garibay GR, Sanchez Y. Fission yeast Rgf2p is a Rho1p guanine nucleotide exchange factor required for spore wall maturation and for the maintenance of cell integrity in the absence of Rgf1p. Genetics. 2009;**181**:1321-1334. DOI: 10.1534/genetics.108.094839

[52] McDonald NA, Lind AL, Smith SE, Li R, Gould KL. Nanoscale architecture of the *Schizosaccharomyces pombe* contractile ring. Elife. 15 Sep, 2017;**6**: pii: e28865. DOI: 10.7554/eLife.28865

[53] Ren L, Willet AH, Roberts-Galbraith RH, McDonald NA, Feoktistova A, Chen JS, et al. The Cdc15 and Imp2 SH3 domains cooperatively scaffold a network of proteins that redundantly ensure efficient cell division in fission yeast. Molecular Biology of the Cell. 2015;**26**:256-269. DOI: 10.1091/mbc.E14-10-1451

[54] Roberts-Galbraith RH, Chen JS, Wang J, Gould KL. The SH3 domains of two PCH family members cooperate in assembly of the *Schizosaccharomyces pombe* contractile ring. The Journal of Cell Biology. 2009;**184**:113-127. DOI: 10.1083/jcb.200806044

[55] Roberts-Galbraith RH, Ohi MD, Ballif BA, Chen JS, McLeod I, McDonald WH, et al. Dephosphorylation of F-BAR protein Cdc15 modulates its conformation and stimulates its scaffolding activity at the cell division site. Molecular Cell. 2010;**39**:86-99. DOI: 10.1016/j.molcel.2010.06.012

[56] Davidson R, Laporte D, Wu JQ. Regulation of rho-GEF Rgf3 by the arrestin Art1 in fission yeast cytokinesis. Molecular Biology of the Cell. 2015;**26**:453-466. DOI: 10.1091/mbc.E14-07-1252

[57] Manjon E, Edreira T, Munoz S, Sanchez Y. Rgf1p (Rho1p GEF) is required for double-strand break repair in fission yeast. Nucleic Acids Research. 2017;**45**:5269-5284. DOI: 10.1093/nar/gkx176

[58] Chang F, Martin SG. Shaping fission yeast with microtubules. Cold Spring Harbor Perspectives in Biology. 2009;**1**:a001347. DOI: 10.1101/cshperspect.a001347

[59] Huisman SM, Brunner D. Cell polarity in fission yeast: A matter of confining, positioning, and switching growth zones. Seminars in Cell & Developmental Biology. 2011;**22**:799-805. DOI: 10.1016/j.semcdb.2011.07.013

[60] Martin SG, Arkowitz RA. Cell polarization in budding and fission yeasts. FEMS Microbiology Reviews. 2014;**38**:228-253. DOI: 10.1111/1574-6976.12055

[61] Mitchison JM, Nurse P. Growth in cell length in the fission yeast *Schizosaccharomyces pombe*. Journal of Cell Science. 1985;**75**:357-376

[62] Grallert A, Patel A, Tallada VA, Chan KY, Bagley S, Krapp A, et al. Centrosomal MPF triggers the mitotic and morphogenetic switches of fission yeast. Nature Cell Biology. 2013;**15**:88-95. DOI: 10.1038/ncb2633

[63] Bohnert KA, Gould KL. Cytokinesis-based constraints on polarized cell growth in fission yeast. PLoS Genetics. 2012;**8**:e1003004. DOI: 10.1371/journal.pgen.1003004

[64] Rupes I, Jia Z, Young PG. Ssp1 promotes actin depolymerization and is involved in stress response and new end take-off control in fission yeast. Molecular Biology of the Cell. 1999;**10**:1495-1510. DOI: 10.1091/mbc.10.5.1495

[65] Martin SG, McDonald WH, Yates JR 3rd, Chang F. Tea4p links microtubule plus ends with the formin for3p in the establishment of cell polarity. Developmental Cell. 2005;**8**: 479-491. DOI: 10.1016/j.devcel.2005.02.008

[66] Mata J, Nurse P. Tea1 and the microtubular cytoskeleton are important for generating global spatial order within the fission yeast cell. Cell. 1997;**89**:939-949. DOI: 10.1016/S0092-8674(00)80279-2

[67] Tatebe H, Shimada K, Uzawa S, Morigasaki S, Shiozaki K. Wsh3/Tea4 is a novel cell-end factor essential for bipolar distribution of Tea1 and protects cell polarity under environmental stress in *S. pombe*. Current Biology. 2005;**15**:1006-1015. DOI: 10.1016/j.cub.2005.04.061

[68] Kokkoris K, Gallo Castro D, Martin SG. The Tea4-PP1 landmark promotes local growth by dual Cdc42 GEF recruitment and GAP exclusion. Journal of Cell Science. 2014;**127**: 2005-2016. DOI: 10.1242/jcs.142174

[69] Martin SG, Rincon SA, Basu R, Perez P, Chang F. Regulation of the formin for3p by cdc42p and bud6p. Molecular Biology of the Cell. 2007;**18**:4155-4167. DOI: 10.1091/mbc.E07-02-0094

[70] Tatebe H, Nakano K, Maximo R, Shiozaki K. Pom1 DYRK regulates localization of the Rga4 GAP to ensure bipolar activation of Cdc42 in fission yeast. Current Biology. 2008; **18**:322-330. DOI: 10.1016/j.cub.2008.02.005

[71] Lee ME, Rusin SF, Jenkins N, Kettenbach AN, Moseley JB. Mechanisms connecting the conserved protein kinases Ssp1, Kin1, and Pom1 in fission yeast cell polarity and division. Current Biology. 2018;**28**:84-92 e4. DOI: 10.1016/j.cub.2017.11.034

[72] Cadou A, Couturier A, Le Goff C, Soto T, Miklos I, Sipiczki M, et al. Kin1 is a plasma membrane-associated kinase that regulates the cell surface in fission yeast. Molecular Microbiology. 2010;**77**:1186-1202. DOI: 10.1111/j.1365-2958.2010.07281.x

[73] Drewes G, Nurse P. The protein kinase kin1, the fission yeast orthologue of mammalian MARK/PAR-1, localises to new cell ends after mitosis and is important for bipolar growth. FEBS Letters. 2003;**554**:45-49. DOI: 10.1016/S0014-5793(03)01080-9

[74] Koyano T, Kume K, Konishi M, Toda T, Hirata D. Search for kinases related to transition of growth polarity in fission yeast. Bioscience, Biotechnology, and Biochemistry. 2010;**74**:1129-1133. DOI: 10.1271/bbb.100223

[75] Matsusaka T, Hirata D, Yanagida M, Toda T. A novel protein kinase gene ssp1+ is required for alteration of growth polarity and actin localization in fission yeast. The EMBO Journal. 1995;**14**:3325-3338. DOI: 10.1002/j.1460-2075.1995.tb07339.x

[76] Pollard TD, Wu JQ. Understanding cytokinesis: Lessons from fission yeast. Nature Reviews Molecular Cell Biology. 2010;**11**:149-155. DOI: 10.1038/nrm2834

[77] Rincon SA, Paoletti A. Molecular control of fission yeast cytokinesis. Seminars in Cell & Developmental Biology. 2016;**53**:28-38. DOI: 10.1016/j.semcdb.2016.01.007

[78] Willet AH, McDonald NA, Gould KL. Regulation of contractile ring formation and septation in *Schizosaccharomyces pombe*. Current Opinion in Microbiology. 2015;**28**:46-52. DOI: 10.1016/j.mib.2015.08.001

[79] Garcia Cortes JC, Ramos M, Osumi M, Perez P, Ribas JC. The cell biology of fission yeast septation. Microbiology and Molecular Biology Reviews. 2016;**80**:779-791. DOI: 10.1128/MMBR.00013-16

[80] Humbel BM, Konomi M, Takagi T, Kamasawa N, Ishijima SA, Osumi M. In situ localization of beta-glucans in the cell wall of *Schizosaccharomyces pombe*. Yeast. 2001;**18**:433-444. DOI: 10.1002/yea.694

[81] Dekker N, Speijer D, Grun CH, van den Berg M, de Haan A, Hochstenbach F. Role of the alpha-glucanase Agn1p in fission-yeast cell separation. Molecular Biology of the Cell. 2004;**15**:3903-3914. DOI: 10.1091/mbc.E04-04-0319

[82] Martin-Cuadrado AB, Duenas E, Sipiczki M, Vazquez de Aldana CR, del Rey F. The endo-beta-1,3-glucanase eng1p is required for dissolution of the primary septum during cell separation in *Schizosaccharomyces pombe*. Journal of Cell Science. 2003;**116**:1689-1698. DOI: 10.1242/jcs.00377

[83] Arellano M, Duran A, Perez P. Rho 1 GTPase activates the (1-3)beta-D-glucan synthase and is involved in *Schizosaccharomyces pombe* morphogenesis. The EMBO Journal. 1996;**15**:4584-4591. DOI: 10.1002/j.1460-2075.1996.tb00836.x

[84] Alonso-Nunez ML, An H, Martin-Cuadrado AB, Mehta S, Petit C, Sipiczki M, et al. Ace2p controls the expression of genes required for cell separation in *Schizosaccharomyces pombe*. Molecular Biology of the Cell. 2005;**16**:2003-2017. DOI: 10.1091/mbc.E04-06-0442

[85] Wu JQ, Pollard TD. Counting cytokinesis proteins globally and locally in fission yeast. Science. 2005;**310**:310-314. DOI: 10.1126/science.1113230

[86] Arasada R, Pollard TD. Contractile ring stability in *S. pombe* depends on F-BAR protein Cdc15p and Bgs1p transport from the Golgi complex. Cell Reports. 2014;**8**:1533-1544. DOI: 10.1016/j.celrep.2014.07.048

[87] Arasada R, Pollard TD. A role for F-BAR protein Rga7p during cytokinesis in *S. pombe*. Journal of Cell Science. 2015;**128**:2259-2268. DOI: 10.1242/jcs.162974

[88] Goyal A, Takaine M, Simanis V, Nakano K. Dividing the spoils of growth and the cell cycle: The fission yeast as a model for the study of cytokinesis. Cytoskeleton (Hoboken). 2011;**68**:69-88. DOI: 10.1002/cm.20500

[89] Simanis V. Pombe's thirteen – control of fission yeast cell division by the septation initiation network. Journal of Cell Science. 2015;**128**:1465-1474. DOI: 10.1242/jcs.094821

[90] Alcaide-Gavilan M, Lahoz A, Daga RR, Jimenez J. Feedback regulation of SIN by Etd1 and Rho1 in fission yeast. Genetics. 2014;**196**:455-470. DOI: 10.1534/genetics.113.155218

[91] Jin QW, Zhou M, Bimbo A, Balasubramanian MK, McCollum D. A role for the septation initiation network in septum assembly revealed by genetic analysis of sid2-250 suppressors. Genetics. 2006;**172**:2101-2112. DOI: 10.1534/genetics.105.050955

[92] Mah AS, Elia AE, Devgan G, Ptacek J, Schutkowski M, Snyder M, et al. Substrate specificity analysis of protein kinase complex Dbf2-Mob1 by peptide library and proteome array screening. BMC Biochemistry. 2005;**6**:22. DOI: 10.1186/1471-2091-6-22

[93] Gupta S, Mana-Capelli S, McLean JR, Chen CT, Ray S, Gould KL, et al. Identification of SIN pathway targets reveals mechanisms of crosstalk between NDR kinase pathways. Current Biology. 2013;**23**:333-338. DOI: 10.1016/j.cub.2013.01.014

[94] Matthews HK, Delabre U, Rohn JL, Guck J, Kunda P, Baum B. Changes in Ect2 localization couple actomyosin-dependent cell shape changes to mitotic progression. Developmental Cell. 2012;**23**:371-383. DOI: 10.1016/j.devcel.2012.06.003

[95] Rosa A, Vlassaks E, Pichaud F, Baum B. Ect2/Pbl acts via Rho and polarity proteins to direct the assembly of an isotropic actomyosin cortex upon mitotic entry. Developmental Cell. 2015;**32**:604-616. DOI: 10.1016/j.devcel.2015.01.012

[96] Aoki T, Ueda S, Kataoka T, Satoh T. Regulation of mitotic spindle formation by the RhoA guanine nucleotide exchange factor ARHGEF10. BMC Cell Biology. 2009;**10**:56. DOI: 10.1186/1471-2121-10-56

[97] Menon S, Oh W, Carr HS, Frost JA. Rho GTPase-independent regulation of mitotic progression by the RhoGEF Net1. Molecular Biology of the Cell. 2013;**24**:2655-2667. DOI: 10.1091/mbc.E13-01-0061

[98] Yoshida S, Kono K, Lowery DM, Bartolini S, Yaffe MB, Ohya Y, et al. Polo-like kinase Cdc5 controls the local activation of Rho1 to promote cytokinesis. Science. 2006;**313**:108-111. DOI: 10.1126/science.1126747

[99] Tolliday N, VerPlank L, Li R. Rho1 directs formin-mediated actin ring assembly during budding yeast cytokinesis. Current Biology. 2002;**12**:1864-1870. DOI: 10.1016/S0960-9822(02)01238-1

[100] Rajakyla EK, Vartiainen MK. Rho, nuclear actin, and actin-binding proteins in the regulation of transcription and gene expression. Small GTPases. 2014;**5**:e27539. DOI: 10.4161/sgtp.27539

[101] Weston L, Coutts AS, La Thangue NB. Actin nucleators in the nucleus: An emerging theme. Journal of Cell Science. 2012;**125**:3519-3527. DOI: 10.1242/jcs.099523

[102] Guerra L, Carr HS, Richter-Dahlfors A, Masucci MG, Thelestam M, Frost JA, et al. A bacterial cytotoxin identifies the RhoA exchange factor Net1 as a key effector in the response to DNA damage. PLoS One. 2008;**3**:e2254. DOI: 10.1371/journal.pone.0002254

[103] Mamouni K, Cristini A, Guirouilh-Barbat J, Monferran S, Lemarie A, Faye JC, et al. RhoB promotes gammaH2AX dephosphorylation and DNA double-strand break repair. Molecular and Cellular Biology. 2014;**34**:3144-3155. DOI: 10.1128/MCB.01525-13

[104] Srougi MC, Burridge K. The nuclear guanine nucleotide exchange factors Ect2 and Net1 regulate RhoB-mediated cell death after DNA damage. PLoS One. 2011;**6**:e17108. DOI: 10.1371/journal.pone.0017108

[105] Dubash AD, Guilluy C, Srougi MC, Boulter E, Burridge K, Garcia-Mata R. The small GTPase RhoA localizes to the nucleus and is activated by Net1 and DNA damage signals. PLoS One. 2011;**6**:e17380. DOI: 10.1371/journal.pone.0017380

[106] Lagana A, Dorn JF, De Rop V, Ladouceur AM, Maddox AS, Maddox PS. A small GTPase molecular switch regulates epigenetic centromere maintenance by stabilizing newly incorporated CENP-A. Nature Cell Biology. 2010;**12**:1186-1193. DOI: 10.1038/ncb2129

[107] Boddy MN, Russell P. DNA replication checkpoint. Current Biology. 2001;**11**:R953-R956. DOI: 10.1016/S0960-9822(01)00572-3

[108] Lambert S, Carr AM. Replication stress and genome rearrangements: Lessons from yeast models. Current Opinion in Genetics & Development. 2013;**23**:132-139. DOI: 10.1016/j.gde.2012.11.009

[109] Langerak P, Russell P. Regulatory networks integrating cell cycle control with DNA damage checkpoints and double-strand break repair. Philosophical Transactions of the Royal Society of London. Series B, Biological Sciences. 2011;**366**:3562-3571. DOI: 10.1098/rstb.2011.0070

[110] Chen J, Stubbe J. Bleomycins: New methods will allow reinvestigation of old issues. Current Opinion in Chemical Biology. 2004;**8**:175-181. DOI: 10.1016/j.cbpa.2004.02.008

[111] Levin JD, Demple B. In vitro detection of endonuclease IV-specific DNA damage formed by bleomycin in vivo. Nucleic Acids Research. 1996;**24**:885-889. DOI: 10.1093/nar/24.5.885

[112] Pommier Y. Topoisomerase I inhibitors: Camptothecins and beyond. Nature Reviews Cancer. 2006;**6**:789-802. DOI: 10.1038/nrc1977

[113] Kim WJ, Lee S, Park MS, Jang YK, Kim JB, Park SD. Rad22 protein, a rad52 homologue in *Schizosaccharomyces pombe*, binds to DNA double-strand breaks. The Journal of Biological Chemistry. 2000;**275**:35607-35611. DOI: 10.1074/jbc.M007060200

[114] Meister P, Poidevin M, Francesconi S, Tratner I, Zarzov P, Baldacci G. Nuclear factories for signalling and repairing DNA double strand breaks in living fission yeast. Nucleic Acids Research. 2003;**31**:5064-5073. DOI: 10.1093/nar/gkg719

[115] Raji H, Hartsuiker E. Double-strand break repair and homologous recombination in *Schizosaccharomyces pombe*. Yeast. 2006;**23**:963-976. DOI: 10.1002/yea.1414

Chapter 3

Biosensing Techniques in Yeast: G-Protein Signaling and Protein-Protein Interaction Assays for Monitoring Ligand Stimulation and Oligomer Formation of

Yasuyuki Nakamura, Akihiko Kondo and Jun Ishii

Additional information is available at the end of the chapter

http://dx.doi.org/10.5772/intechopen.76330

Abstract

Guanine nucleotide-binding proteins (G-proteins) act as transducers of external stimuli for intracellular signaling, and control various cellular processes in cooperation with seven transmembrane G-protein-coupled receptors (GPCRs). Because GPCRs constitute the largest family of eukaryotic membrane proteins and enable the selective recognition of a diverse range of molecules (ligands), they are the major molecular targets in pharmaceutical and medicinal fields. In addition, GPCRs have been known to form heteromers as well as homomers, which may result in vast physiological diversity and provide opportunities for drug discovery. G-proteins and their signal transduction machinery are universally conserved in eukaryotes; thereby, the yeast *Saccharomyces cerevisiae* has been used to construct artificial *in vivo* GPCR biosensors. In this chapter, we focus on the yeast-based GPCR biosensors that can detect ligand stimulation and oligomer formation, and summarize their techniques using the G-protein signaling and protein-protein interaction assays.

Keywords: yeast, G-protein, G-protein-coupled receptor, signal transduction, oligomer formation, reporter gene assay, protein-protein interaction

1. Introduction

Guanine nucleotide-binding proteins (G-proteins) are highly conserved among various eukaryotes, and act as signal transduction molecules [1, 2]. In cooperation with seven

transmembrane G-protein-coupled receptors (GPCRs), G-proteins transduce external stimuli to intracellular signaling and control a wide variety of cellular processes. GPCRs, which represent the largest family of integral membrane proteins and present more than 800 genes in the human genome [3], engage a wide range of ligands. GPCR ligands range from small molecules to large proteins, such as hormones, neurotransmitters, ions, tastants, odor molecules and even light [4]. Thus, GPCRs are involved in various physiological processes, and are the targets of several prescribed drugs [5–8].

Agonist ligand binding to a GPCR causes ligand-specific active conformational changes, and allows the receptor to couple to G-proteins that are composed of Gα, Gβ and Gγ subunits [9]. Subsequently, heterotrimeric G-proteins dissociate from the receptor, and then G-protein signaling generates second messengers such as cyclic adenosine monophosphate (cAMP), inositol phosphates, and intracellular Ca^{2+}. These second messengers trigger different cellular and ultimately physiological responses [10]. During these processes, G-proteins switch from an inactive state to an active state by exchanging a guanosine diphosphate (GDP) molecule from the Gα subunit for guanosine triphosphate (GTP). To resume an inactive state, G-proteins hydrolyze GTP to GDP [11].

Historically, GPCRs transduce signals only as single monomeric entities (homomers) [12]. However, in the past two decades, several studies have shown that GPCRs also transduce signals as heteromers [13–18]. Heteromerization is involved in both the regulation and modulation of GPCR signaling, consequently increasing the potentially large functional and physiological diversity of various GPCR-mediated processes (e.g., ligand binding, receptor biosynthesis, cellular trafficking, maturation, G-protein activation, and internalization) [19–24]. Therefore, heteromerization among GPCRs may provide new opportunities for drug discovery [25, 26]. For example, GPCR heteromers may be new molecular targets for therapeutic treatments, or for developing more potent and selective compounds, such as bispecific or bivalent ligands, with reduced side effects [27–29]. The mechanism of GPCR heteromerization has been under debate, because the identification of individual heteromer pairs is ongoing and the *in vivo* physiological importance of heteromerization has not been well explored. Thus, the search for functional GPCR oligomer pairs is still a challenging task, due to the continued need for elucidation of their physiological roles.

Saccharomyces cerevisiae is an extremely simplistic unicellular eukaryote and an excellent host system for investigating both GPCR signaling and GPCR oligomerization, as the simplicity of this fungus allows for simplified analyses of the more complicated mammalian GPCR signaling [30]. For instance, since haploid yeast cells harbor a monopolistic G-protein (pheromone) signaling pathway, and experience a variety of heterologous GPCR expressions, yeast cells have often been utilized for studies of human and other mammalian GPCRs such as: identification of agonistic ligands, analysis of ligand-mediated signaling properties, and mutational analysis of critical amino acid residues [30–32]. Additionally, yeast two-hybrid (Y2H) techniques can be utilized to investigate exhaustive protein interaction pairs [30], in which the split-ubiquitin membrane Y2H (mY2H) system is suitable for screening membrane protein interaction partners [33] including GPCR heteromer pairs [34]. In this chapter, we focus on yeast-based biosensors that detect ligand stimulation and oligomer formation of GPCRs, and summarize their techniques using the G-protein signaling and protein-protein interaction assays.

http://dx.doi.org/10.5772/intechopen.76330

2. G-protein signaling

Heterotrimeric G-proteins, as peripheral membrane proteins, interact with the plasma membrane on the cytoplasmic side. G-proteins consist of three subunits, Gα, Gβ, and Gγ, which are widely conserved in eukaryotic species, and there are various subfamilies within each subunit, especially the Gα subunit. The heterotrimeric G-proteins transduce messages from GPCRs, which regulate important functions such as vision, taste, smell, heart rate, blood pressure, neurotransmission, cell growth, and numerous other processes [10, 35]. When, in response to extracellular stimuli, GPCRs transduce ligand-specific intracellular signaling cascades, they activate a GDP to GTP exchange on the Gα subunit, resulting in Gα dissociation from the Gβγ complex. Free Gα or Gβγ interacts with several downstream effectors including phospholipases, adenylyl cyclases, phosphodiesterases, tyrosine kinases, ion channels, and ion transporters in human and other mammalian cells [36, 37].

2.1. Heterotrimeric G-protein signaling in yeast

S. cerevisiae's pheromone-based mating response provides a valuable model system for characterization of G-protein-mediated GPCR signaling (**Figure 1**) [38], because it allows for simplified analyses of the more complicated signaling pathways employed by higher eukaryotic cells [30]. The yeast pheromone signaling pathway is non-competitive and monopolistic, unlike other higher eukaryotes, and is mediated by a sole heterotrimeric G-protein comprising three subunits, a Gα subunit (Gpa1p) and the Gβγ complex (Ste4p − Ste18p) [39]. Haploid yeast cells of mating type **a** (*MAT***a**) express Ste2p, which binds the peptide pheromone α-factor secreted by cells of the opposite mating type (*MAT*α). Upon pheromone binding, Ste2p undergoes a conformational change and induces a guanine-nucleotide exchange on Gpa1p [40]. Replacement of GDP with GTP on Gpa1p causes a dissociation of the Ste4p − Ste18p complex. Ste4p facilitates binding of the dissociated Ste4p − Ste18p complex to effectors, and results in activation of the mitogen-activated protein kinase (MAPK) cascade [41, 42]. Ste5p scaffold protein binds to the components of a MAPK cascade to bring them to the plasma membrane, and the concentrated kinases on the membrane may facilitate amplification of the signal [43, 44]. As a consequence, the activated yeast pheromone signaling leads to phosphorylation of the cyclin-dependent kinase inhibitor Far1p and the transcription factor Ste12p. These phosphorylated proteins induce G1 cell cycle arrest [45–47] and global changes in transcription [48, 49]. For example, *FUS1* gene expression experiences drastic transcriptional changes in response to yeast pheromone signaling [50, 51]. The *FIG1* gene is also a mating-specific Ste12p target gene [52, 53]. Sst2p is one of the main negative regulators of the yeast pheromone pathway [54] and acts as a GTPase-activating protein (GAP), enhancing the rate of Gα-catalyzed GTP hydrolysis [55–57]. GDP-bound Gα rapidly reassociates with the Gβγ complex, inactivating the pheromone response.

The yeast *S. cerevisiae* is amenable for reporter gene assays investigating agonist-stimulated G-protein signaling. Briefly, yeast cells become available to detect signaling through endogenous or heterologously expressed GPCRs by putting reporter genes, such as *HIS3* (detected by complementation of auxotrophy), *lacZ* (detected by colorimetry), *luc* (detected by luminometry)

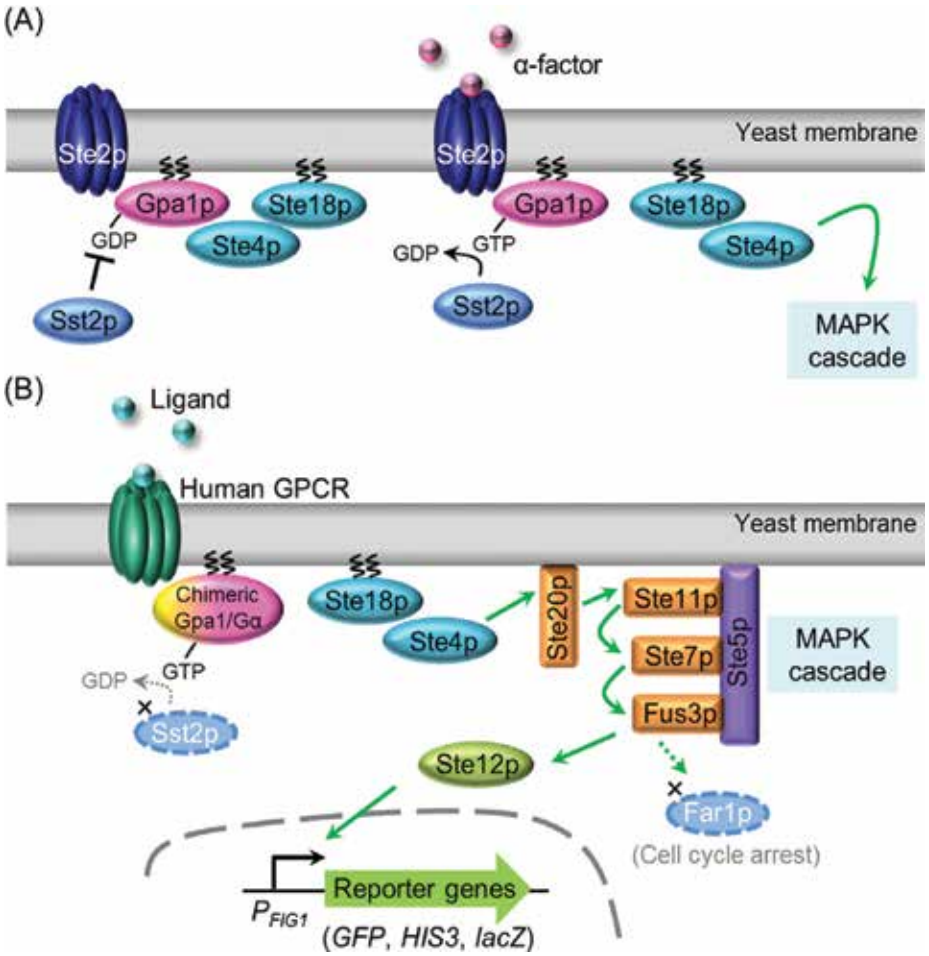

Figure 1. Overview of the yeast pheromone signaling pathway and the human GPCR-expressing yeast signaling biosensor. (A) Schematic illustration of the pheromone signaling pathway. The pheromone signaling pathway is activated, via the heterotrimeric G-protein, when α-factor binds to the Ste2p receptor. The effectors and kinases constitute that MAPK cascades are activated by sequestered Ste4p – Ste18p complex from Gpa1p. Sst2p stimulates hydrolysis of GTP to GDP on Gpa1p and helps to inactivate pheromone signaling. (B) Schematic illustration of typical genetic modifications enabling the pheromone signaling pathway to be used as a biosensor for GPCR activation. Chimeric Gpa1/Gα (transplant) can help to transduce the signal from human GPCRs expressed on the yeast plasma membrane. Transcription machineries, closely regulated by the phosphorylated transcription factor Ste12p, are used to detect activation of pheromone signaling with various reporter genes. *SST2*, *FAR1*, and *STE2* genes are often disrupted to improve ligand sensitivity, prevent growth arrest (cell cycle arrest), and avoid competitive expression of the yeast endogenous receptor.

and gene encoding green fluorescent protein (GFP) (detected via fluorescence), under the expression control of a pheromone-responsive promoter like *FUS1* or *FIG1* [58–60].

2.2. Improvement of the sensitivity of the yeast G-protein signaling

To increase the sensitivity of human GPCR expressing yeast cells, several modifications of yeast-based biosensors have been reported. The yeast's single GPCR (yeast pheromone receptor Ste2p) is often deleted to avoid competitive expression with heterologous GPCRs

[30]; therefore, expressing human GPCR on the plasma membrane of *ste2*Δ **a**-cells harboring reporter genes facilitates the monitoring of agonist-promoted signaling [30, 61]. The yeast G1-cyclin-dependent kinase inhibitor Far1p, which induces G1 cell cycle arrest in response to signaling, is usually disrupted in positive selection screening to avoid abnormal cell growth [30], because the *far1*Δ strain continues cell growth and improves plasmid retention rates [62]. Removing Sst2p facilitates experiments requiring high ligand binding sensitivity [30, 31, 63], as this removal results in a significant decrease in Gpa1p's GTPase activity by inhibiting the conversion of GTP to GDP.

Yeast Gpa1p is equivalent to mammalian Gα. Gpa1p shares particularly high homology with the human Gα_i classes, and GPCRs from a variety of species, including human, are able to both interact with Gpa1p and activate yeast pheromone signaling [32, 64, 65]. Various genetic modifications allow many other human GPCRs to function as yeast signaling modulators. In one such modification, a chimeric Gpa1p system, referred to 'as "transplants", has' been employed to substitute only five Gpa1p C-terminus amino acids for those of human Gα subunits, of which there are three key families: G$\alpha_{i/o}$, Gα_s, and Gα_q [66]. Indeed, these transplants have allowed functional coupling of various GPCRs (including serotonin, purinergic, muscarinic, and many other receptors) to the yeast pheromone pathway with greater coupling efficiency [32, 66–68].

The use of fluorescent reporter genes can provide the most simple and convenient procedure for comparative quantification of signaling levels, as this removed the need for laborious operations such as sample preparations and enzyme reactions. GFP is commonly chosen as the fluorescent reporter and enhanced green fluorescent protein (EGFP) is often utilized as the GFP. However, the *EGFP* gene was originally codon-optimized for mammalian cells, and it was not suitable for expression in yeast cells [69]. To increase the maximum expression level of GFP and decrease the detection limit of signaling, Nakamura et al. used the tetrameric *Zoanthus* sp. green fluorescent protein (ZsGreen) as a reporter [70]. The use of the *ZsGreen* reporter gene exhibited extremely bright fluorescence and a high signal-to-noise (S/N) ratio in yeast, showing a dramatic improvement in both brightness and sensitivity for GPCR signaling assays compared to a fluorescence reporter system using the *EGFP* reporter gene [70].

2.3. Detection of GPCR agonists by utilizing yeast G-protein signaling

Many heterologous GPCRs (including muscarinic, neurotensin, serotonin, somatostatin, adrenergic, olfactory, and many other receptors) have been functionally expressed in yeast, successfully demonstrating the feasibility of yeast-based GPCR biosensors [31, 32, 63–67, 71–73].

For example, the cyclic neuropeptide somatostatin, known to inhibit growth hormone release, regulates the human endocrine system through somatostatin receptor (SSTR) binding. There are five identified SSTR subtypes (SSTR1 − SSTR5) [74, 75]. SSTR2 and SSTR5 are known to regulate acromegaly patient growth hormone secretion, and are also expressed in most growth hormone secreting tumors [76]. Several researchers demonstrated functional expression of human SSTR2 and SSTR5 in yeasts, and SSTR5 has been often used for constructing yeast-based somatostatin-specific biosensors. To modify the functional expression of human

SSTR5 and somatostatin-specific signaling functions in yeasts, addition of signal sequences derived from secretion or membrane proteins (e.g., prepro- and pre-regions of α-factor, and a N-terminal 20 amino acids of yeast Ste2p; Ste2N) to the N-terminus of the receptor, and implementation of the chimeric Gpa1/Gα_{i3} transplant (see Section 2.2) were tested [77]. Additionally, the *GFP* reporter gene assay (see Section 2.1) was used for evaluating the functional expression of SSTR5 and the signaling response to somatostatin binding. Through these evaluations, yeast cells with improved capabilities as a biosensor capable of detecting somatostatin-promoted signaling (such as potency and efficacy) were successfully constructed. Using this yeast-based biosensor, Togawa et al. performed site-directed mutagenesis of human SSTR5, showing the importance of two asparagine residues (Asn13 and Asn26) on the *N*-linked glycosylation motifs for signaling activation [78]. Furthermore, the artificial signaling circuit formulated a positive feedback loop using Gβ (Ste4p; artificial signal activator, which was set downstream the pheromone-responsive promoter), and was demonstrated to enable highly sensitive agonist detection in SSTR5 expressing yeast [79].

Neurotensin receptor type-1 (NTSR1), a member of the GPCR family, is another example of site-directed mutagenesis of human SSTR5. Neurotensin is the natural ligand of NTSR1, as well as a central nervous system neuromodulator [80]. As neurotensin is also involved in many oncogenic events [81], NTSR1 is a significant therapeutic target. To monitor the activation of human NTSR1 signaling responding to its agonist, a fluorescence-based microbial *S. cerevisiae*-based biosensor was constructed [82]. Successful detection of NTSR1 signaling responding to agonistic ligands was achieved in the Gα-engineered yeast strains IMFD-72 and IMFD-74, which were generated by substituting the Gpa1/Gα_{i3} and Gpa1/Gα_q transplants for the intact Gpa1p in modified yeast IMFD-70 strain (*ste2*Δ, *sst2*Δ, *far1*Δ, P_{FIG1}-*EGFP* x2) [82]. *EGFP* genes on the genomes of IMFD-70 and IMFD-72 were replaced with *ZsGreen* genes to generate IMFD-70ZsD and IMFD-72ZsD strains, resulting in the drastic improvement in bright fluorescence and high S/N ratio in the NTSR1 signaling assay [70]. Recently, Hashi et al. modified the expression modes of the human NTSR1 receptor by altering the promoter, consensus Kozak-like sequence, and secretion signal sequences of the receptor-encoding gene [83]. The resulting yeast cells exhibited increased sensitivity to exogenously added neurotensin [83].

Angiotensin II (Ang II) type 1 receptor (AGTR1) is also a GPCR and its natural ligand, Ang II, is an important effector molecule for the renin-angiotensin system. Thus, AGTR1 controls blood pressure and volume in the cardiovascular system [84, 85]. Interaction of Asn295 with Asn111 may play a role in determining the ligand peptide binding selectivity of AGTR1 receptors [86, 87]. Therefore, a single alanine or serine mutation was introduced at Asn295 of human AGTR1, and the Asn295-mutated (N295A and N295S) AGTR1 was expressed in the IMFD-72ZsD yeast strain [88]. When exposed to Ang II and Ang II peptidic analogs, which differ in affinity toward AGTR1, these cells resulted in successful signal transmissions inside the yeast cells. Additionally, the secretory expression plasmids for angiotensin peptides (Ang II, Ang III, and Ang IV) were transformed into the yeasts expressing AGTR1-N295A or AGTR1-N295S, showing the ZsGreen fluorescence with different intensities according to the respective agonistic activities. In contrast, the monoamine neurotransmitter serotonin (5-HT) regulates a wide spectrum of human physiology through the 5-HT receptor family [89].

Nakamura et al. expressed the human HTR1A in the IMFD-72ZsD strain to enable improved detection of HTR1A signaling in response to the 5-HT [90]. The authors further validated the capability of this improved yeast biosensor for antagonistic ligand characterization and site-directed mutants of human HTR1A.

The rat M_3 muscarinic acetylcholine receptor (M3R) has been used for rapid identification of functionally critical amino acids with random mutagenesis [67]. In this system, the *CAN1* gene coding for arginine-canavanine permease was used as the reporter gene under the control of a pheromone responsive *FUS2* promoter, and in the endogenous *CAN1*-deleted yeast cells. Owing to the cytotoxicity of canavanine, caused by Can1p expression in response to promoted signaling, recombinant strains with inactivation mutations in the M3R receptor could survive on agar media containing canavanine and M3R-specific agonists. In another study, using this yeast platform, "antagonists" atropine and pirenzepine were found to be inverse agonists and low efficacy agonists when coupled to Gpa1/Gα_q and Gpa1/Gα_{12}, respectively [91]. In an extended study, the applicability of this yeast platform to identify allosteric ligand-mediated functional G-protein selectivity was also tested [92].

Human formyl peptide receptor-like 1, which was originally identified as an orphan GPCR, has been used to isolate agonists for functionally unknown GPCRs [93]. Both a library of secreted random tridecapeptides and a mammalian/yeast hybrid Gα subunit were employed for histidine prototrophic selection via the *FUS1 − HIS3* reporter gene. Subsequent peptidic candidate surrogate agonist screens have been successful.

In the case of olfactory receptors (ORs), Minic et al. optimized a yeast system for functional expression of rat I7 OR and subsequent characterization. In engineered yeasts lacking endogenous Gpa1p, the olfactory-specific Gα subunit (Gα_{olf}) was co-expressed. When the receptor was activated by its ligands, MAPK signaling was switched on and luciferase (as a functional reporter) synthesis was induced [71]. Marrakchi et al. successfully expressed human olfactory receptor OR17-40 in yeast based on Minic's biosensor system to detect the conductometric changes [94]. Fukutani et al. improved the firefly luciferase-based biomimetic odor-sensing system [60], and replaced the N-terminal region of mOR226 with the corresponding domain of the rat I7 receptor [95]. They further improved some ORs by the coexpression of either odorant accessory binding proteins or the receptor transporting protein 1 short (RTP1S) [96]. Tehseen et al. demonstrated that the *Caenorhabditis elegans* olfactory GPCR ODR-10 was functionally expressed in yeast by using chimeric Gpa1/*C. elegans* Gα [97]. Mukherjee et al. constructed a medium-chain fatty acid biosensor by using the olfactory receptor OR1G1 that functionally expressed in yeast [98].

2.4. Yeast cell-surface display technology for single-cell signaling assay of GPCR peptides

Yeast cell-surface display technology is a platform to tether functional proteins and peptides expressed in yeast to the cell surface [99–102]. Cell-surface display of peptides can be used as a powerful ligand screening based on the yeast GPCR signaling assay systems [70, 103]. Displaying peptidic ligands by fusing them to an anchor protein in the yeast can enable a series of biological processes within a single cell, from peptide synthesis to agonist detection

against an already expressing cognate GPCR. In such a system, a library of peptides is individually tethered to the plasma membrane on GPCR-producing yeast cells via attachment to a glycosyl-phosphatidylinositol (GPI) anchor. Upon phosphatidylinositol-specific phospholipase C (PI-PLC) cleavage of the GPI, the peptides, which are fused to the anchor protein, are released from the membrane and trapped in the cell wall [103]. In principle, the host cells unconsciously detect the binding of peptidic ligands to relevant receptors on the membrane and report the peptides resulting agonistic activation. Thus, this technique facilitates concomitant library synthesis and identification of peptide ligands at the single-cell level [104, 105].

Ishii et al. have developed a system for cell wall trapping of autocrine peptides (CWTrAP), which activates human SSTR5 signaling using short anchor proteins (e.g., 42 a.a. of Flo1p; Flo42) [103]. The engineered yeast strain concomitantly expressing human SSTR5 and somatostatin peptide successfully induced *GFP* reporter gene expression. Hara et al. demonstrated that the somatostatin displayed on the plasma membrane successfully activated human SSTR2 in yeast [106]. In this system, somatostatin was displayed on the yeast plasma membrane by linking it to the anchoring domain of the GPI-anchored plasma membrane protein Yps1p. Nakamura et al. drastically improved the sensitivity and output of this fluorescence reporter system using the ZsGreen reporter, which is applicable to CWTrAP technology [70].

3. Oligomerization among GPCRs

Many GPCRs have the capacity to form homomers or heteromers that show unique functional and biochemical characteristics including receptor pharmacology, regulation, and signaling [14, 107, 108]. Therefore, GPCR oligomers could be potential molecular targets for the development of new therapeutic agents. Yeast is a potential host for making cell-based biosensors for eukaryotic proteins and biological processes of interest [109], because varied reporting systems are available that can facilitate assays in yeast cells [110–112]. Notably, the "gold standard" for testing protein-protein interactions *in vivo*, Y2H systems, makes use of these reporters [113–115] and has also been used to identify membrane protein interaction partners [116].

3.1. Biophysical RET technologies to study GPCR oligomers in yeast cells

Varieties of resonance energy transfer (RET)-based techniques have promoted the visualization of GPCR oligomers in living cells. Fluorescence resonance energy transfer (FRET) is a strictly distance-dependent energy transfer technique using a cyan fluorescent protein (CFP) as energy donor and a yellow fluorescent protein (YFP) as energy acceptor, but other pairings are also possible [117]. Highly sensitive, bioluminescence resonance energy transfer (BRET) is based on the distance-dependent transfer of energy between a bioluminescent energy donor and a fluorescent acceptor molecule [118, 119].

Overton and Blumer [120] used subcellular fractionation and CFP/YFP FRET to demonstrate that oligomerization of the endogenous mating pheromone Ste2p receptors occurs via a stable association between protomers in yeast. Subsequently, the authors employed FRET in live yeast cells for detection of Ste2p oligomerization with its transmembrane domains [121–124].

Furthermore, FRET experiments with yeast cells demonstrated the oligomer formation of functional human complement factor 5a (C5a) receptors [125].

BRET was later used to increase the detection sensitivity for Ste2p oligomerization. Increased sensitivity was needed, because the C-terminal regions of full length Ste2p protomers did not reach a proximity sufficient for effective energy transfer [126]. With the BRET system, Gehret et al. [126] demonstrated that mutations previously reported as blocking Ste2p receptor oligomerization decreased but did not completely eliminate oligomerization. Previously, BRET has been employed in yeast to analyze the protein interactions involved with heterogeneous olfactory receptors [127, 128].

3.2. Membrane Y2H technology to study GPCR oligomers in yeast cells

In contrast to FRET and BRET technologies (see Section 3.1), mY2H method is based on transcription-dependent reporter gene assays, permitting colorimetric evaluations with *lacZ* and growth selections with *ADE2* and *HIS3* (detected by complementation of auxotrophies) [129]. Therefore, the split-ubiquitin mY2H approach can be employed both for quantitative assays and for comprehensive screening of protein-protein interactions of membrane proteins [129].

In the split-ubiquitin mY2H system, the N- and C-terminal halves (Nub*G* and Cub, respectively) of ubiquitin are fused to separate membrane proteins (**Figure 2A** and **B**). Nub*G* represent a mutant version of the N-terminal half of ubiquitin that harbors an Ile-13 to Gly substitution. This split-ubiquitin system functions when interaction between the membrane proteins results in ubiquitin reassembly. Notably, Cub is fused to a membrane protein along with an artificial transcription factor (LexA-VP16). Nub*G* has a very low intrinsic affinity for Cub, and therefore can interact with Cub only if the membrane proteins fused to both ubiquitin fragments have affinities for each other [130]. The reconstituted ubiquitin is recognized by ubiquitin-specific proteases, and cleavage liberates LexA-VP16. The released transcription factor then enters the nucleus and induces the transcription of reporter genes, permitting both screening (via *lacZ* expression) and selection (via *ADE2* and *HIS3* expression) based on interactions between membrane proteins.

Historically, the split-ubiquitin mY2H system was employed to screen interacting membrane-associated proteins (not GPCRs) for GPCRs, such as the μ-opioid receptor (MOR) [131, 132] and the M_3 muscarinic acetylcholine receptor (M3R) [133]. Jin et al. identified GPR177, the mammalian ortholog of *Drosophila melanogaster* Wntless, as a novel MOR-interacting protein using the split-ubiquitin mY2H system [131]. Further work showed both enhanced MOR/GPR177 complex formation at the cell periphery and inhibited Wnt secretion in response to morphine treatment, possibly causing decreased neurogenesis. Rosemond et al. investigated the predicted integral membrane protein Tmem147 and discovered that it functions as a novel M3R-associated protein [133]. Additional work also indicated that Tmem147 is as a potent M3R negative regulator, which may interfere with M3R trafficking to the cell surface.

The split-ubiquitin mY2H system has also been applied to identify GPCR heteromers [34]. Nakamura et al. developed a specialized method to screen candidate heteromer partners for target human GPCRs based on the split-ubiquitin mY2H method [34]. The authors noted that mating-associated induction of cell-cycle arrest, which causes robust growth inhibition in yeast, might impair the assessment of reporter gene activity. Therefore, the authors

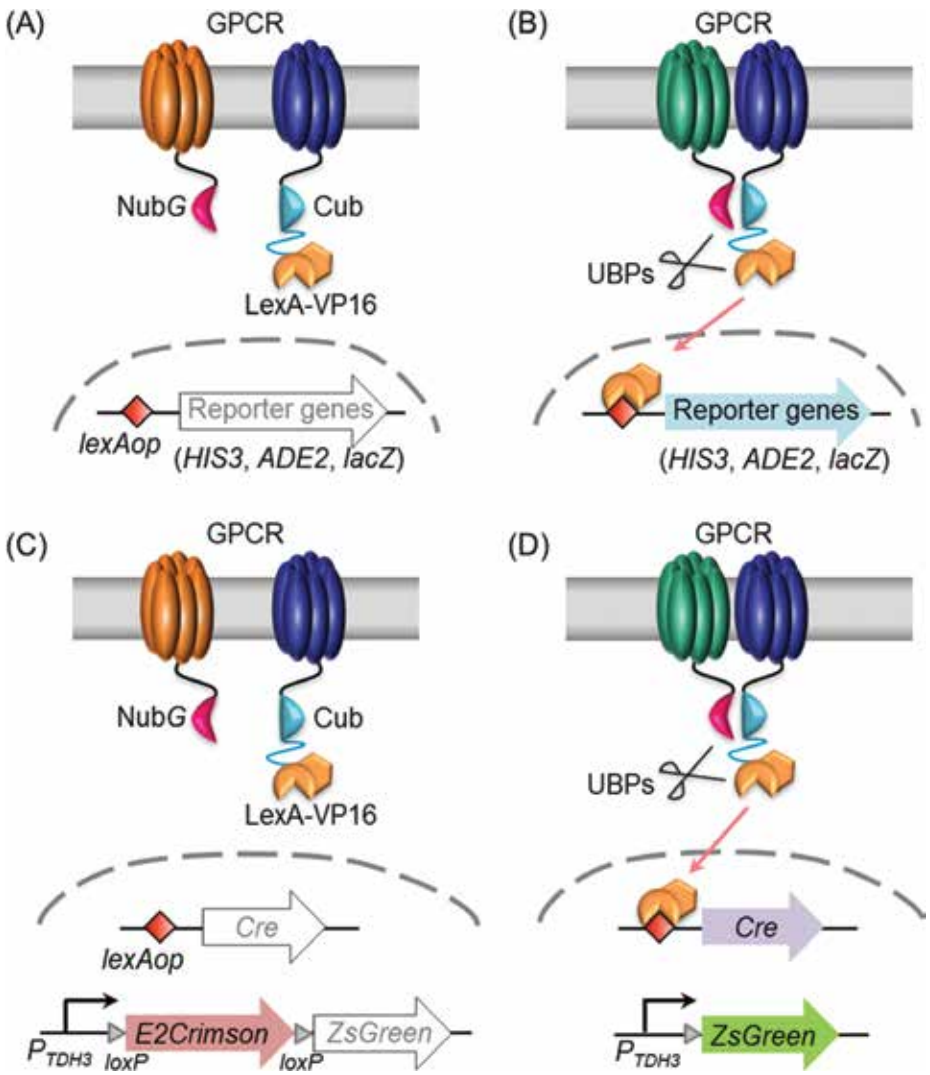

Figure 2. Schematic illustration of the yeast split-ubiquitin mY2H system to study GPCR oligomers. (A and C) No-oligomerization pairs. (B and D) Oligomerization pairs. The candidate GPCR oligomer pairs are fused to respective split-ubiquitin segments (NubG and Cub), and Cub is further fused to an artificial transcription factor (LexA-VP16). NubG and Cub become close in proximity only when the GPCRs form a dimer, leading to the reconstitution of the split-ubiquitin. Ubiquitin-specific proteases (UBPs) can recognize the reconstituted split-ubiquitin, resulting in LexA-VP16 transcription factor cleavage from the Cub-fused GPCRs. LexA-VP16 diffuses into the nucleus where it binds to *lexA*-binding sites on the *lexA* operator (*lexAop*). (A and B) Principal GPCR oligomer pair detection system: the reporter genes such as *HIS3*, *ADE2*, and *lacZ* are placed downstream of *lexAop*, and their expressions are induced when GPCR oligomer pairs interact with each other. (C and D) The reporter switching system for detecting GPCR oligomer pairs: the expressions of two reporter genes (*E2Crimson* and *ZsGreen*) are switched in response to the Y2H readout; one (*E2Crimson*) from ON to OFF and the other (*ZsGreen*) from OFF to ON. Briefly, after the release of the LexA-VP16 transcription factor, the *lexA* operator induces the expression of Cre recombinase, which causes a gene recombination that pops-out the *E2Crimson* gene and alternatively exposes the *ZsGreen* gene. Thus, the formation of GPCR oligomers can be discerned by monitoring the changes from far-red fluorescence to green fluorescence.

constructed a MAPK signal-defective yeast strain. This modified host permitted the rapid and facile detection, not only of target human GPCR heteromerization, but also of ligand-mediated conformational changes in living yeast cells [34]. Thus, the modified mY2H would be available to identify GPCR heteromer components and potential therapeutic targets for regulating physiological activities.

Furthermore, the authors subsequently designed a reporter switching system that can switch the expressions between two reporter genes (one from ON to OFF and the other from OFF to ON) in response to the Y2H readout (**Figure 2C** and **D**) [134]. Cre/*loxP* site-specific recombination was employed to induce reporter switching. The authors were able to utilize the split-ubiquitin mY2H system to optimize Cre-mediated reporter gene recombination and build a dual-color reporter switching system, which could discern GPCR dimer formation. To demonstrate reporter switching, the authors used a far-red derivative of the tetrameric fluorescent protein DsRed-Express2 (*E2Crimson*) and a tetrameric *ZsGreen* as the two reporter genes. Reporter gene expression was successfully switched in the engineered yeast cells and permitted the detection of the dimerized yeast endogenous pheromone receptor (Ste2p). The authors also validated the applicability of this system for monitoring the formation of human GPCRs homodimers and heterodimers, specifically human serotonin 1A receptor or β2-adrenergic receptor, and confirmed that this system had improved sensitivity when compared with the previous system [134].

Using a modified split-ubiquitin mY2H approach, Sokolina et al. reported the systematic interactome analysis of 48 clinically important human GPCRs in their ligand-unoccupied state [135]. The authors also carried out additional in-depth functional validation on selected GPCR protein-protein interactions using biochemical and cell-based assays as well as knock-out and knock-in animals. The authors found that a G-protein-regulated inducer of neurite outgrowth 2 (GPRIN2) and the GPR37 receptor, both physically and functionally, interact with the serotonin 5-HT4d receptor, a promising target for Alzheimer's disease [135].

3.3. GPCR oligomerization and G-protein signaling

GPCR oligomerization can increase the potential for diversity in the regulation and modulation of GPCR signaling, and thus the specific evaluation of signaling properties among various receptor oligomer pairs. This work has important implications, not only for the development of new drugs, but also for the understanding of signaling networks [22]. This unique system was developed for simultaneous detection of oligomer formation and GPCR signaling activation. This new methodology uses a combination of the split-ubiquitin mY2H assay and a G-protein signaling assay, and is expected to facilitate the identification of physiologically relevant GPCR oligomers [136]. Using this system, Nakamura et al. monitored the physiological relevance of yeast pheromone receptor Ste2p, in both native and mutated forms. In addition, the authors demonstrated the simultaneous detection of homo- and heteromerization, and somatostatin-induced signaling of the human SSTR5 somatostatin receptor [136]. In the future, this system will be useful for identifying agonists that bind to the heteromer, promising to serve as a powerful platform for uncovering the novel functions, modes of action, and potential molecular targets of GPCR heteromerization for the development of new therapeutic agents.

4. Conclusion

In summary, we focused on yeast-based biosensors employed for the detection of GPCR ligand stimulation and oligomer formation, and described yeast-based techniques using the G-protein signaling and protein-protein interaction assays. Due to their involvement in signal transduction machinery, GPCRs are excellent therapeutic targets for various diseases and clinical indications [137]. The identification of new physiologically relevant GPCR oligomers provides a promising opportunity for drug discovery, based on the effect of allosteric communication between GPCR protomers (each subunit within the oligomer complex) on known pharmacological properties. Thus, approaches for investigating the relationship between oligomerization and GPCR signaling are necessary for creating oligomer-specific bivalent ligands. Additionally, there is great potential for identifying previously undiscovered physiological diversities and therapeutic targets through the generation of comprehensive and interactive GPCR oligomer maps. It is also important to expand our knowledge of the molecular details of GPCR-mediated signal transduction, including the identification of all proteins that interact with clinically relevant GPCRs. Further development of various methods, including yeast-based approaches and the investigation of GPCR oligomers, are expected to facilitate these outcomes in the near future.

Acknowledgements

This work was supported in part by a Grant-in-Aid for Young Scientists (B) from the Japan Society for the Promotion of Science (JSPS), and a Special Coordination Funds for Promoting Science and Technology, Creation of Innovation Centers for Advanced Interdisciplinary Research Areas (Innovative Bioproduction Kobe; iBioK) from the Ministry of Education, Culture, Sports, Science and Technology (MEXT) of Japan.

Conflict of interest

The authors declare no commercial or financial conflict of interest.

Author details

Yasuyuki Nakamura[1], Akihiko Kondo[1,2] and Jun Ishii[1]*

*Address all correspondence to: junjun@port.kobe-u.ac.jp

1 Graduate School of Science, Technology and Innovation, Kobe University, Kobe, Japan

2 Department of Chemical Science and Engineering, Graduate School of Engineering, Kobe University, Kobe, Japan

References

[1] Wang Y, Dohlman HG. Regulation of G protein and mitogen-activated protein kinase signaling by ubiquitination: Insights from model organisms. Circulation Research. 2006;**99**:1305-1314. DOI: 10.1161/01.RES.0000251641.57410.81

[2] Vögler O, Barceló JM, Ribas C, Escribá PV. Membrane interactions of G proteins and other related proteins. Biochimica et Biophysica Acta (BBA)-Biomembranes. 2008;**1778**:1640-1652. DOI: 10.1016/j.bbamem.2008.03.008

[3] Fredriksson R, Lagerström MC, Lundin LG, Schiöth HB. The G-protein-coupled receptors in the human genome form five main families. Phylogenetic analysis, paralogon groups, and fingerprints. Molecular Pharmacology. 2003;**63**:1256-1272. DOI: 10.1124/mol.63.6.1256

[4] Kim TH, Chung KY, Manglik A, Hansen AL, Dror RO, Mildorf TJ, Shaw DE, Kobilka BK, Prosser RS. The role of ligands on the equilibria between functional states of a G protein-coupled receptor. Journal of the American Chemical Society. 2013;**135**:9465-9474. DOI: 10.1021/ja404305k

[5] Nieto Gutierrez A, McDonald PH. GPCRs: Emerging anti-cancer drug targets. Cellular Signalling. 2018;**41**:65-74. DOI: 10.1016/j.cellsig.2017.09.005

[6] Venkatakrishnan AJ, Deupi X, Lebon G, Tate CG, Schertler GF, Babu MM. Molecular signatures of G-protein-coupled receptors. Nature. 2013;**494**:185-194. DOI: 10.1038/nature11896

[7] Katritch V, Cherezov V, Stevens RC. Diversity and modularity of G protein-coupled receptor structures. Trends in Pharmacological Sciences. 2012;**33**:17-27. DOI: 10.1016/j.tips.2011.09.003

[8] Wise A, Gearing K, Rees S. Target validation of G-protein coupled receptors. Drug Discovery Today. 2002;**7**:235-246. DOI: 10.1016/S1359-6446(01)02131-6

[9] Ghosh E, Kumari P, Jaiman D, Shukla AK. Methodological advances: The unsung heroes of the GPCR structural revolution. Nature Reviews Molecular Cell Biology. 2015;**16**:69-81. DOI: 10.1038/nrm3933

[10] Rosenbaum DM, Rasmussen SG, Kobilka BK. The structure and function of G-protein-coupled receptors. Nature. 2009;**459**:356-363. DOI: 10.1038/nature08144

[11] Karnik SS, Gogonea C, Patil S, Saad Y, Takezako T. Activation of G-protein-coupled receptors: A common molecular mechanism. Trends in Endocrinology & Metabolism. 2003;**14**:431-437. DOI: 10.1016/j.tem.2003.09.007

[12] Park PS, Filipek S, Wells JW, Palczewski K. Oligomerization of G protein-coupled receptors: Past, present, and future. Biochemistry. 2004;**43**:15643-15656. DOI: 10.1021/bi047907k

[13] Devi LA. G-protein-coupled receptor dimers in the lime light. Trends in Pharmacological Sciences. 2000;**21**:324-326. DOI: 10.1016/S0165-6147(00)01519-4

[14] Ferré S, Casadó V, Devi LA, Filizola M, Jockers R, Lohse MJ, Milligan G, Pin JP, Guitart X. G protein-coupled receptor oligomerization revisited: Functional and pharmacological perspectives. Pharmacological Reviews. 2014;**66**:413-434. DOI: 10.1124/pr.113.008052

[15] Milligan G. G protein-coupled receptor dimerization: Function and ligand pharmacology. Molecular Pharmacology. 2004;**66**:1-7. DOI: 10.1124/mol.104.000497

[16] White JH, Wise A, Main MJ, Green A, Fraser NJ, Disney GH, Barnes AA, Emson P, Foord SM, Marshall FH. Heterodimerization is required for the formation of a functional GABA(B) receptor. Nature. 1998;**396**:679-682. DOI: 10.1038/25354

[17] Smith NJ, Milligan G. Allostery at G protein-coupled receptor homo- and heteromers: Uncharted pharmacological landscapes. Pharmacological Reviews. 2010;**62**:701-725. DOI: 10.1124/pr.110.002667

[18] Xue L, Rovira X, Scholler P, Zhao H, Liu J, Pin JP, Rondard P. Major ligand-induced rearrangement of the heptahelical domain interface in a GPCR dimer. Nature Chemical Biology. 2015;**11**:134-140. DOI: 10.1038/nchembio.1711

[19] Bouvier M. Oligomerization of G-protein-coupled transmitter receptors. Nature Reviews Neuroscience. 2001;**2**:274-286. DOI: 10.1038/35067575

[20] Bulenger S, Marullo S, Bouvier M. Emerging role of homo- and heterodimerization in G-protein-coupled receptor biosynthesis and maturation. Trends in Pharmacological Sciences. 2005;**26**:131-137. DOI: 10.1016/j.tips.2005.01.004

[21] Devi LA. Heterodimerization of G-protein-coupled receptors: Pharmacology, signaling and trafficking. Trends in Pharmacological Sciences. 2001;**22**:532-537. DOI: 10.1016/S0165-6147(00)01799-5

[22] Jordan BA, Devi LA. G-protein-coupled receptor heterodimerization modulates receptor function. Nature. 1999;**399**:697-700. DOI: 10.1038/21441

[23] Jordan BA, Trapaidze N, Gomes I, Nivarthi R, Devi LA. Oligomerization of opioid receptors with beta 2-adrenergic receptors: A role in trafficking and mitogen-activated protein kinase activation. Proceedings of the National Academy of Sciences of the United States of America. 2001;**98**:343-348. DOI: 10.1073/pnas.011384898

[24] Terrillon S, Bouvier M. Roles of G-protein-coupled receptor dimerization. EMBO Reports. 2004;**5**:30-34. DOI: 10.1038/sj.embor.7400052

[25] Lane JR, Donthamsetti P, Shonberg J, Draper-Joyce CJ, Dentry S, Michino M, Shi L, López L, Scammells PJ, Capuano B, Sexton PM, Javitch JA, Christopoulos A. A new mechanism of allostery in a G protein-coupled receptor dimer. Nature Chemical Biology. 2014;**10**:745-752. DOI: 10.1038/nchembio.1593

[26] Teitler M, Klein MT. A new approach for studying GPCR dimers: Drug-induced inactivation and reactivation to reveal GPCR dimer function in vitro, in primary culture, and in vivo. Pharmacology & Therapeutics. 2012;**133**:205-217. DOI: 10.1016/j.pharmthera.2011.10.007

[27] George SR, O'Dowd BF, Lee SP. G-protein-coupled receptor oligomerization and its potential for drug discovery. Nature Reviews Drug Discovery. 2002;**1**:808-820. DOI: 10.1038/nrd913

[28] Hiller C, Kühhorn J, Gmeiner P. Class A G-protein-coupled receptor (GPCR) dimers and bivalent ligands. Journal of Medicinal Chemistry. 2013;**56**:6542-6559. DOI: 10.1021/jm4004335

[29] Le Naour M, Lunzer MM, Powers MD, Kalyuzhny AE, Benneyworth MA, Thomas MJ, Portoghese PS. Putative kappa opioid heteromers as targets for developing analgesics free of adverse effects. Journal of Medicinal Chemistry. 2014;**57**:6383-6392. DOI: 10.1021/jm500159d

[30] Ishii J, Fukuda N, Tanaka T, Ogino C, Kondo A. Protein-protein interactions and selection: Yeast-based approaches that exploit guanine nucleotide-binding protein signaling. FEBS Journal. 2010;**277**:1982-1995. DOI: 10.1111/j.1742-4658.2010.07625.x

[31] Minic J, Sautel M, Salesse R, Pajot-Augy E. Yeast system as a screening tool for pharmacological assessment of G protein coupled receptors. Current Medicinal Chemistry. 2005;**12**:961-969. DOI: 10.2174/0929867053507261

[32] Brown AJ, Dyos SL, Whiteway MS, White JH, Watson MA, Marzioch M, Clare JJ, Cousens DJ, Paddon C, Plumpton C, Romanos MA, Dowell SJ. Functional coupling of mammalian receptors to the yeast mating pathway using novel yeast/mammalian G protein α-subunit chimeras. Yeast. 2000;**16**:11-22. DOI: 10.1002/(SICI)1097-0061(20000115)16:1<11::AID-YEA502>3.0.CO;2-K

[33] Stagljar I, Korostensky C, Johnsson N, te Heesen S. A genetic system based on split-ubiquitin for the analysis of interactions between membrane proteins in vivo. Proceedings of the National Academy of Sciences of the United States of America. 1998;**95**:5187-5192

[34] Nakamura Y, Ishii J, Kondo A. Rapid, facile detection of heterodimer partners for target human G-protein-coupled receptors using a modified split-ubiquitin membrane yeast two-hybrid system. PLoS One. 2013;**8**:e66793. DOI: 10.1371/journal.pone.0066793

[35] Cotton M, Claing A. G protein-coupled receptors stimulation and the control of cell migration. Cellular Signalling. 2009;**21**:1045-1053. DOI: 10.1016/j.cellsig.2009.02.008

[36] Dupré DJ, Robitaille M, Rebois RV, Hébert TE. The role of Gbetagamma subunits in the organization, assembly, and function of GPCR signaling complexes. Annual Review of Pharmacology and Toxicology. 2009;**49**:31-56. DOI: 10.1146/annurev-pharmtox-061008-103038

[37] Ritter SL, Hall RA. Fine-tuning of GPCR activity by receptor-interacting proteins. Nature Reviews Molecular Cell Biology. 2009;**10**:819-830. DOI: 10.1038/nrm2803

[38] Bardwell L. A walk-through of the yeast mating pheromone response pathway. Peptides. 2005;**26**:339-350. DOI: 10.1016/j.peptides.2003.10.022

[39] Elion EA. Pheromone response, mating and cell biology. Current Opinion in Microbiology. 2000;**3**:573-581. DOI: 10.1016/S1369-5274(00)00143-0

[40] Alvaro CG, Thorner J. Heterotrimeric G protein-coupled receptor signaling in yeast mating pheromone response. Journal of Biological Chemistry. 2016;**291**:7788-7795. DOI: 10.1074/jbc.R116.714980

[41] Leberer E, Thomas DY, Whiteway M. Pheromone signalling and polarized morphogenesis in yeast. Current Opinion in Genetics & Development. 1997;**7**:59-66. DOI: 10.1016/S0959-437X(97)80110-4

[42] Leeuw T, Wu C, Schrag JD, Whiteway M, Thomas DY, Leberer E. Interaction of a G-protein beta-subunit with a conserved sequence in Ste20/PAK family protein kinases. Nature. 1998;**391**:191-195. DOI: 10.1038/34448

[43] Elion EA. The Ste5p scaffold. Journal of Cell Science. 2001;**114**:3967-3978

[44] Pryciak PM, Huntress FA. Membrane recruitment of the kinase cascade scaffold protein Ste5 by the Gβγ complex underlies activation of the yeast pheromone response pathway. Genes & Development. 1998;**12**:2684-2697. DOI: 10.1101/gad.12.17.2684

[45] Chang F, Herskowitz I. Identification of a gene necessary for cell cycle arrest by a negative growth factor of yeast: FAR1 is an inhibitor of a G1 cyclin, CLN2. Cell. 1990;**63**:999-1011. DOI: 10.1016/0092-8674(90)90503-7

[46] Chang F, Herskowitz I. Phosphorylation of FAR1 in response to alpha-factor: A possible requirement for cell-cycle arrest. Molecular Biology of the Cell. 1992;**3**:445-450. DOI: 10.1091/mbc.3.4.445

[47] McKinney JD, Cross FR. FAR1 and the G1 phase specificity of cell cycle arrest by mating factor in Saccharomyces cerevisiae. Molecular and Cellular Biology. 1995;**15**:2509-2516. DOI: 10.1128/MCB.15.5.2509

[48] Dolan JW, Kirkman C, Fields S. The yeast STE12 protein binds to the DNA sequence mediating pheromone induction. Proceedings of the National Academy of Sciences of the United States of America. 1989;**86**:5703-5707

[49] Song D, Dolan JW, Yuan YL, Fields S. Pheromone-dependent phosphorylation of the yeast STE12 protein correlates with transcriptional activation. Genes & Development. 1991;**5**:741-750. DOI: 10.1101/gad.5.5.741

[50] McCaffrey G, Clay FJ, Kelsay K, Sprague GF Jr. Identification and regulation of a gene required for cell fusion during mating of the yeast Saccharomyces cerevisiae. Molecular and Cellular Biology. 1987;**7**:2680-2690. DOI: 10.1128/MCB.7.8.2680

[51] Hagen DC, McCaffrey G, Sprague GF Jr. Pheromone response elements are necessary and sufficient for basal and pheromone-induced transcription of the FUS1 gene of Saccharomyces cerevisiae. Molecular and Cellular Biology. 1991;**11**:2952-2961. DOI: 10.1128/MCB.11.6.2952

[52] Zeitlinger J, Simon I, Harbison CT, Hannett NM, Volkert TL, Fink GR, Young RA. Program-specific distribution of a transcription factor dependent on partner transcription factor and MAPK signaling. Cell. 2003;**113**:395-404. DOI: 10.1016/S0092-8674(03)00301-5

[53] White JM, Rose MD. Yeast mating: Getting close to membrane merger. Current Biology. 2001;**11**:R16-R20. DOI: 10.1016/S0960-9822(00)00036-1

[54] Chasse SA, Flanary P, Parnell SC, Hao N, Cha JY, Siderovski DP, Dohlman HG. Genome-scale analysis reveals Sst2 as the principal regulator of mating pheromone signaling in the yeast Saccharomyces cerevisiae. Eukaryotic Cell. 2006;**5**:330-346. DOI: 10.1128/EC.5.2.330-346.2006

[55] Dohlman HG, Song J, Ma D, Courchesne WE, Thorner J. Sst2, a negative regulator of pheromone signaling in the yeast Saccharomyces cerevisiae: Expression, localization, and genetic interaction and physical association with Gpa1 (the G-protein alpha subunit). Molecular and Cellular Biology. 1996;**16**:5194-5209. DOI: 10.1128/MCB.16.9.5194

[56] Apanovitch DM, Slep KC, Sigler PB, Dohlman HG. Sst2 is a GTPase-activating protein for Gpa1: Purification and characterization of a cognate RGS-Gα protein pair in yeast. Biochemistry. 1998;**37**:4815-4822. DOI: 10.1021/bi9729965

[57] Dohlman HG, Apaniesk D, Chen Y, Song J, Nusskern D. Inhibition of G-protein signaling by dominant gain-of-function mutations in Sst2p, a pheromone desensitization factor in Saccharomyces cerevisiae. Molecular and Cellular Biology. 1995;**15**:3635-3643. DOI: 10.1128/MCB.15.7.3635

[58] Ishii J, Matsumura S, Kimura S, Tatematsu K, Kuroda S, Fukuda H, Kondo A. Quantitative and dynamic analyses of G protein-coupled receptor signaling in yeast using Fus1, enhanced green fluorescence protein (EGFP), and His3 fusion protein. Biotechnology Progress. 2006;**22**:954-960. DOI: 10.1021/bp0601387

[59] Evans BJ, Wang Z, Broach JR, Oishi S, Fujii N, Peiper SC. Expression of CXCR4, a G-protein-coupled receptor for CXCL12 in yeast. Identification of new-generation inverse agonists. Methods in Enzymology. 2009;**460**:399-412. DOI: 10.1016/S0076-6879(09)05220-3

[60] Fukutani Y, Ishii J, Noguchi K, Kondo A, Yohda M. An improved bioluminescence-based signaling assay for odor sensing with a yeast expressing a chimeric olfactory receptor. Biotechnology and Bioengineering. 2012;**109**:3143-3151. DOI: 10.1002/bit.24589

[61] Pausch MH. G-protein-coupled receptors in Saccharomyces cerevisiae: High-throughput screening assays for drug discovery. Trends in Biotechnology. 1997;**15**:487-494. DOI: 10.1016/S0167-7799(97)01119-0

[62] Ishii J, Tanaka T, Matsumura S, Tatematsu K, Kuroda S, Ogino C, Fukuda H, Kondo A. Yeast-based fluorescence reporter assay of G protein-coupled receptor signalling for flow cytometric screening: FAR1-disruption recovers loss of episomal plasmid caused by signalling in yeast. The Journal of Biochemistry. 2008;**143**:667-674. DOI: 10.1093/jb/mvn018

[63] Ladds G, Goddard A, Davey J. Functional analysis of heterologous GPCR signalling pathways in yeast. Trends in Biotechnology. 2005;**23**:367-373. DOI: 10.1016/j.tibtech.2005.05.007

[64] Leplatois P, Josse A, Guillemot M, Febvre M, Vita N, Ferrara P, Loison G. Neurotensin induces mating in *Saccharomyces cerevisiae* cells that express human neurotensin receptor type 1 in place of the endogenous pheromone receptor. European Journal of Biochemistry. 2001;**268**:4860-4867. DOI: 10.1046/j.0014-2956.2001.02407.x

[65] Price LA, Kajkowski EM, Hadcock JR, Ozenberger BA, Pausch MH. Functional coupling of a mammalian somatostatin receptor to the yeast pheromone response pathway. Molecular and Cellular Biology. 1995;**15**:6188-6195. DOI: 10.1128/MCB.15.11.6188

[66] Erlenbach I, Kostenis E, Schmidt C, Hamdan FF, Pausch MH, Wess J. Functional expression of M1, M3 and M5 muscarinic acetylcholine receptors in yeast. Journal of Neurochemistry. 2001;**77**:1327-1337. DOI: 10.1046/j.1471-4159.2001.00344.x

[67] Li B, Scarselli M, Knudsen CD, Kim SK, Jacobson KA, McMillin SM, Wess J. Rapid identification of functionally critical amino acids in a G protein-coupled receptor. Nature Methods. 2007;**4**:169-174. DOI: 10.1038/nmeth990

[68] Pausch MH, Lai M, Tseng E, Paulsen J, Bates B, Kwak S. Functional expression of human and mouse P2Y12 receptors in Saccharomyces cerevisiae. Biochemical and Biophysical Research Communications. 2004;**324**:171-177. DOI: 10.1016/j.bbrc.2004.09.034

[69] Kaishima M, Ishii J, Matsuno T, Fukuda N, Kondo A. Expression of varied GFPs in Saccharomyces cerevisiae: Codon optimization yields stronger than expected expression and fluorescence intensity. Scientific Reports. 2016;**6**:35932. DOI: 10.1038/srep35932

[70] Nakamura Y, Ishii J, Kondo A. Bright fluorescence monitoring system utilizing *Zoanthus* sp. green fluorescent protein (ZsGreen) for human G-protein-coupled receptor signaling in microbial yeast cells. PLoS One. 2013;**8**:e82237. DOI: 10.1371/journal.pone.0082237

[71] Minic J, Persuy MA, Godel E, Aioun J, Connerton I, Salesse R, Pajot-Augy E. Functional expression of olfactory receptors in yeast and development of a bioassay for odorant screening. The FEBS Journal. 2005;**272**:524-537. DOI: 10.1111/j.1742-4658.2004.04494.x

[72] King K, Dohlman HG, Thorner J, Caron MG, Lefkowitz RJ. Control of yeast mating signal transduction by a mammalian beta 2-adrenergic receptor and Gs alpha subunit. Science. 1990;**250**:121-123. DOI: 10.1126/science.2171146

[73] Liu R, Wong W, IJzerman AP. Human G protein-coupled receptor studies in *Saccharomyces cerevisiae*. Biochemical Pharmacology. 2016;**114**:103-115. DOI: 10.1016/j.bcp.2016.02.010

[74] Raynor K, Murphy WA, Coy DH, Taylor JE, Moreau JP, Yasuda K, Bell GI, Reisine T. Cloned somatostatin receptors: Identification of subtype-selective peptides and demonstration of high affinity binding of linear peptides. Molecular Pharmacology. 1993; **43**:838-844

[75] Raynor K, O'Carroll AM, Kong H, Yasuda K, Mahan LC, Bell GI, Reisine T. Characterization of cloned somatostatin receptors SSTR4 and SSTR5. Molecular Pharmacology. 1993;**44**: 385-392

[76] Jaquet P, Saveanu A, Gunz G, Fina F, Zamora AJ, Grino M, Culler MD, Moreau JP, Enjalbert A, Ouafik LH. Human somatostatin receptor subtypes in acromegaly: Distinct patterns of messenger ribonucleic acid expression and hormone suppression identify different tumoral phenotypes. The Journal of Clinical Endocrinology & Metabolism. 2000;**85**:781-792. DOI: 10.1210/jcem.85.2.6338

[77] Iguchi Y, Ishii J, Nakayama H, Ishikura A, Izawa K, Tanaka T, Ogino C, Kondo A. Control of signalling properties of human somatostatin receptor subtype-5 by additional signal sequences on its amino-terminus in yeast. The Journal of Biochemistry. 2010;**147**:875-884. DOI: 10.1093/jb/mvq023

[78] Togawa S, Ishii J, Ishikura A, Tanaka T, Ogino C, Kondo A. Importance of asparagine residues at positions 13 and 26 on the amino-terminal domain of human somatostatin receptor subtype-5 in signalling. The Journal of Biochemistry. 2010;**147**:867-873. DOI: 10.1093/jb/mvq022

[79] Fukuda N, Ishii J, Kaishima M, Kondo A. Amplification of agonist stimulation of human G-protein-coupled receptor signaling in yeast. Analytical Biochemistry. 2011;**417**:182-187. DOI: 10.1016/j.ab.2011.06.006

[80] White JF, Noinaj N, Shibata Y, Love J, Kloss B, Xu F, Gvozdenovic-Jeremic J, Shah P, Shiloach J, Tate CG, Grisshammer R. Structure of the agonist-bound neurotensin receptor. Nature. 2012;**490**:508-513. DOI: 10.1038/nature11558

[81] Dupouy S, Mourra N, Doan VK, Gompel A, Alifano M, Forgez P. The potential use of the neurotensin high affinity receptor 1 as a biomarker for cancer progression and as a component of personalized medicine in selective cancers. Biochimie. 2011;**93**:1369-1378. DOI: 10.1016/j.biochi.2011.04.024

[82] Ishii J, Oda A, Togawa S, Fukao A, Fujiwara T, Ogino C, Kondo A. Microbial fluorescence sensing for human neurotensin receptor type 1 using Gα-engineered yeast cells. Analytical Biochemistry. 2014;**446**:37-43. DOI: 10.1016/j.ab.2013.10.016

[83] Hashi H, Nakamura Y, Ishii J, Kondo A. Modifying expression modes of human neurotensin receptor type 1 alters sensing capabilities for agonists in yeast signaling biosensor. Biotechnology Journal. 2018;**13**:e1700522. DOI: 10.1002/biot.201700522

[84] Griendling KK, Lassègue B, Alexander RW. Angiotensin receptors and their therapeutic implications. Annual Review of Pharmacology and Toxicology. 1996;**36**:281-306. DOI: 10.1146/annurev.pa.36.040196.001433

[85] Mehta PK, Griendling KK. Angiotensin II cell signaling: Physiological and pathological effects in the cardiovascular system. American Journal of Physiology Cell Physiology. 2007;**292**:C82-C97. DOI: 10.1152/ajpcell.00287.2006

[86] Groblewski T, Maigret B, Larguier R, Lombard C, Bonnafous JC, Marie J. Mutation of Asn111 in the third transmembrane domain of the AT(1A) angiotensin II receptor induces its constitutive activation. Journal of Biological Chemistry. 1997;**272**:1822-1826. DOI: 10.1074/jbc.272.3.1822

[87] Balmforth AJ, Lee AJ, Warburton P, Donnelly D, Ball SG. The conformational change responsible for AT1receptor activation is dependent upon two juxtaposed asparagine residues on transmembrane helices III and VII. Journal of Biological Chemistry. 1997;**272**:4245-4251. DOI: 10.1074/jbc.272.7.4245

[88] Nakamura Y, Ishii J, Kondo A. Construction of a yeast-based signaling biosensor for human angiotensin II type 1 receptor via functional coupling between Asn295-mutated receptor and Gpa1/Gi3 chimeric Gα. Biotechnology and Bioengineering. 2014;**111**:2220-2228. DOI: 10.1002/bit.25278

[89] Hoyer D, Clarke DE, Fozard JR, Hartig PR, Martin GR, Mylecharane EJ, Saxena PR, Humphrey PP. International Union of Pharmacology Classification of receptors for 5-hydroxytryptamine (serotonin). Pharmacological Reviews. 1994;**46**:157-203

[90] Nakamura Y, Ishii J, Kondo A. Applications of yeast-based signaling sensor for characterization of antagonist and analysis of site-directed mutants of the human serotonin 1A receptor. Biotechnology and Bioengineering. 2015;**112**:1906-1915. DOI: 10.1002/bit.25597

[91] Stewart GD, Sexton PM, Christopoulos A. Detection of novel functional selectivity at M3 muscarinic acetylcholine receptors using a *Saccharomyces cerevisiae* platform. ACS Chemical Biology. 2010;**5**:365-375. DOI: 10.1021/cb900276p

[92] Stewart GD, Sexton PM, Christopoulos A. Prediction of functionally selective allosteric interactions at an M3 muscarinic acetylcholine receptor mutant using Saccharomyces cerevisiae. Molecular Pharmacology. 2010;**78**:205-214. DOI: 10.1124/mol.110.064253

[93] Klein C, Paul JI, Sauvé K, Schmidt MM, Arcangeli L, Ransom J, Trueheart J, Manfredi JP, Broach JR, Murphy AJ. Identification of surrogate agonists for the human FPRL-1 receptor by autocrine selection in yeast. Nature Biotechnology. 1998;**16**:1334-1337. DOI: 10.1038/4310

[94] Marrakchi M, Vidic J, Jaffrezic-Renault N, Martelet C, Pajot-Augy E. A new concept of olfactory biosensor based on interdigitated microelectrodes and immobilized yeasts expressing the human receptor OR17-40. European Biophysics Journal. 2007;**36**:1015-1018. DOI: 10.1007/s00249-007-0187-6

[95] Fukutani Y, Nakamura T, Yorozu M, Ishii J, Kondo A, Yohda M. The N-terminal replacement of an olfactory receptor for the development of a yeast-based biomimetic odor sensor. Biotechnology and Bioengineering. 2012;**109**:205-212. DOI: 10.1002/bit.23327

[96] Fukutani Y, Hori A, Tsukada S, Sato R, Ishii J, Kondo A, Matsunami H, Yohda M. Improving the odorant sensitivity of olfactory receptor-expressing yeast with accessory proteins. Analytical Biochemistry. 2015;**471**:1-8. DOI: 10.1016/j.ab.2014.10.012

[97] Tehseen M, Dumancic M, Briggs L, Wang J, Berna A, Anderson A, Trowell S. Functional coupling of a nematode chemoreceptor to the yeast pheromone response pathway. PLoS One. 2014;**9**:e111429. DOI: 10.1371/journal.pone.0111429

[98] Mukherjee K, Bhattacharyya S, Peralta-Yahya P. GPCR-based chemical biosensors for medium-chain fatty acids. ACS Synthetic Biology. 2015;**4**:1261-1269. DOI: 10.1021/sb500365m

[99] Ueda M, Tanaka A. Genetic immobilization of proteins on the yeast cell surface. Biotechnology Advances. 2000;**18**:121-140. DOI: 10.1016/S0734-9750(00)00031-8

[100] Kondo A, Ueda M. Yeast cell-surface display—Applications of molecular display. Applied Microbiology and Biotechnology. 2004;**64**:28-40. DOI: 10.1007/s00253-003-1492-3

[101] Gai SA, Wittrup KD. Yeast surface display for protein engineering and characterization. Current Opinion in Structural Biology. 2007;**17**:467-473. DOI: 10.1016/j.sbi.2007.08.012

[102] Pepper LR, Cho YK, Boder ET, Shusta EV. A decade of yeast surface display technology: Where are we now? Combinatorial Chemistry & High Throughput Screening. 2008;**11**:127-134. DOI: 10.2174/138620708783744516

[103] Ishii J, Yoshimoto N, Tatematsu K, Kuroda S, Ogino C, Fukuda H, Kondo A. Cell wall trapping of autocrine peptides for human G-protein-coupled receptors on the yeast cell surface. PLoS One. 2012;**7**:e37136. DOI: 10.1371/journal.pone.0037136

[104] Müller S, Nebe-von-Caron G. Functional single-cell analyses: Flow cytometry and cell sorting of microbial populations and communities. FEMS Microbiology Reviews. 2010;**34**:554-587. DOI: 10.1111/j.1574-6976.2010.00214.x

[105] Yoshimoto N, Tatematsu K, Iijima M, Niimi T, Maturana AD, Fujii I, Kondo A, Tanizawa K, Kuroda S. High-throughput de novo screening of receptor agonists with an automated single-cell analysis and isolation system. Scientific Reports. 2014;**4**:4242. DOI: 10.1038/srep04242

[106] Hara K, Shigemori T, Kuroda K, Ueda M. Membrane-displayed somatostatin activates somatostatin receptor subtype-2 heterologously produced in Saccharomyces cerevisiae. AMB Express. 2012;**2**:63. DOI: 10.1186/2191-0855-2-63

[107] Ferré S. The GPCR heterotetramer: Challenging classical pharmacology. Trends in Pharmacological Sciences. 2015;**36**:145-152. DOI: 10.1016/j.tips.2015.01.002

[108] Milligan G. The prevalence, maintenance, and relevance of G protein-coupled receptor oligomerization. Molecular Pharmacology. 2013;**84**:158-169. DOI: 10.1124/mol.113.084780

[109] Adeniran A, Sherer M, Tyo KE. Yeast-based biosensors: Design and applications. FEMS Yeast Research. 2015;**15**:1-15. DOI: 10.1111/1567-1364.12203

[110] Leskinen P, Virta M, Karp M. One-step measurement of firefly luciferase activity in yeast. Yeast. 2003;**20**:1109-1113. DOI: 10.1002/yea.1024

[111] Naylor LH. Reporter gene technology: The future looks bright. Biochemical Pharmacology. 1999;**58**:749-757. DOI: 10.1016/S0006-2952(99)00096-9

[112] Radhika V, Proikas-Cezanne T, Jayaraman M, Onesime D, Ha JH, Dhanasekaran DN. Chemical sensing of DNT by engineered olfactory yeast strain. Nature Chemical Biology. 2007;**3**:325-330. DOI: 10.1038/nchembio882

[113] Chen J, Zhou J, Bae W, Sanders CK, Nolan JP, Cai H. A yEGFP-based reporter system for high-throughput yeast two-hybrid assay by flow cytometry. Cytometry Part A. 2008;**73**:312-320. DOI: 10.1002/cyto.a.20525

[114] Ito T, Chiba T, Ozawa R, Yoshida M, Hattori M, Sakaki Y. A comprehensive two-hybrid analysis to explore the yeast protein interactome. Proceedings of the National Academy of Sciences of the United States of America. 2001;**98**:4569-4574. DOI: 10.1073/pnas.061034498

[115] Uetz P, Giot L, Cagney G, Mansfield TA, Judson RS, Knight JR, Lockshon D, Narayan V, Srinivasan M, Pochart P, Qureshi-Emili A, Li Y, Godwin B, Conover D, Kalbfleisch T, Vijayadamodar G, Yang M, Johnston M, Fields S, Rothberg JM. A comprehensive

analysis of protein-protein interactions in Saccharomyces cerevisiae. Nature. 2000;**403**:623-627. DOI: 10.1038/35001009

[116] Babu M, Vlasblom J, Pu S, Guo X, Graham C, Bean BD, Burston HE, Vizeacoumar FJ, Snider J, Phanse S, Fong V, Tam YY, Davey M, Hnatshak O, Bajaj N, Chandran S, Punna T, Christopolous C, Wong V, Yu A, Zhong G, Li J, Stagljar I, Conibear E, Wodak SJ, Emili A, Greenblatt JF. Interaction landscape of membrane-protein complexes in Saccharomyces cerevisiae. Nature. 2012;**489**:585-589. DOI: 10.1038/nature11354

[117] Milligan G, Bouvier M. Methods to monitor the quaternary structure of G protein-coupled receptors. The FEBS Journal. 2005;**272**:2914-2925. DOI: 10.1111/j.1742-4658.2005.04731.x

[118] Angers S, Salahpour A, Joly E, Hilairet S, Chelsky D, Dennis M, Bouvier M. Detection of beta 2-adrenergic receptor dimerization in living cells using bioluminescence resonance energy transfer (BRET). Proceedings of the National Academy of Sciences of the United States of America. 2000;**97**:3684-3689. DOI: 10.1073/pnas.060590697

[119] Issafras H, Angers S, Bulenger S, Blanpain C, Parmentier M, Labbé-Jullié C, Bouvier M, Marullo S. Constitutive agonist-independent CCR5 oligomerization and antibody-mediated clustering occurring at physiological levels of receptors. Journal of Biological Chemistry. 2002;**277**:34666-34673. DOI: 10.1074/jbc.M202386200

[120] Overton MC, Blumer KJ. G-protein-coupled receptors function as oligomers in vivo. Current Biology. 2000;**10**:341-344. DOI: 10.1016/S0960-9822(00)00386-9

[121] Overton MC, Blumer KJ. Use of fluorescence resonance energy transfer to analyze oligomerization of G-protein-coupled receptors expressed in yeast. Methods. 2002;**27**:324-332. DOI: 10.1016/S1046-2023(02)00090-7

[122] Overton MC, Blumer KJ. The extracellular N-terminal domain and transmembrane domains 1 and 2 mediate oligomerization of a yeast G protein-coupled receptor. Journal of Biological Chemistry. 2002;**277**:41463-41472. DOI: 10.1074/jbc.M205368200

[123] Overton MC, Chinault SL, Blumer KJ. Oligomerization, biogenesis, and signaling is promoted by a glycophorin A-like dimerization motif in transmembrane domain 1 of a yeast G protein-coupled receptor. Journal of Biological Chemistry. 2003;**278**:49369-49377. DOI: 10.1074/jbc.M308654200

[124] Overton MC, Chinault SL, Blumer KJ. Oligomerization of G-protein-coupled receptors: Lessons from the yeast Saccharomyces cerevisiae. Eukaryotic Cell. 2005;**4**:1963-1970. DOI: 10.1128/EC.4.12.1963-1970.2005

[125] Floyd DH, Geva A, Bruinsma SP, Overton MC, Blumer KJ, Baranski TJ. C5a receptor oligomerization. II. Fluorescence resonance energy transfer studies of a human G protein-coupled receptor expressed in yeast. Journal of Biological Chemistry. 2003;**278**:35354-35361. DOI: 10.1074/jbc.M305607200

[126] Gehret AU, Bajaj A, Naider F, Dumont ME. Oligomerization of the yeast α-factor receptor: Implications for dominant negative effects of mutant receptors. Journal of Biological Chemistry. 2006;**281**:20698-20714. DOI: 10.1074/jbc.M513642200

[127] Tehseen M, Liao C, Dacres H, Dumancic M, Trowell S, Anderson A. Oligomerisation of C. Elegans olfactory receptors, ODR-10 and STR-112, in yeast. PLoS One. 2014;**9**:e108680. DOI: 10.1371/journal.pone.0108680

[128] Wade F, Espagne A, Persuy MA, Vidic J, Monnerie R, Merola F, Pajot-Augy E, Sanz G. Relationship between homo-oligomerization of a mammalian olfactory receptor and its activation state demonstrated by bioluminescence resonance energy transfer. Journal of Biological Chemistry. 2011;**286**:15252-15259. DOI: 10.1074/jbc.M110.184580

[129] Nakamura Y, Ishii J, Kondo A. Current techniques for studying oligomer formations of G-protein-coupled receptors using mammalian and yeast cells. Current Medicinal Chemistry. 2016;**23**:1638-1656. DOI: 10.2174/0929867323666160407113353

[130] Johnsson N, Varshavsky A. Split ubiquitin as a sensor of protein interactions in vivo. Proceedings of the National Academy of Sciences of the United States of America. 1994;**91**:10340-10344

[131] Jin J, Kittanakom S, Wong V, Reyes BA, Van Bockstaele EJ, Stagljar I, Berrettini W, Levenson R. Interaction of the mu-opioid receptor with GPR177 (Wntless) inhibits Wnt secretion: Potential implications for opioid dependence. BMC Neuroscience. 2010;**11**:33. DOI: 10.1186/1471-2202-11-33

[132] Petko J, Justice-Bitner S, Jin J, Wong V, Kittanakom S, Ferraro TN, Stagljar I, Levenson R. MOR is not enough: Identification of novel mu-opioid receptor interacting proteins using traditional and modified membrane yeast two-hybrid screens. PLoS One. 2013;**8**:e67608. DOI: 10.1371/journal.pone.0067608

[133] Rosemond E, Rossi M, McMillin SM, Scarselli M, Donaldson JG, Wess J. Regulation of M_3 muscarinic receptor expression and function by transmembrane protein 147. Molecular Pharmacology. 2011;**79**:251-261. DOI: 10.1124/mol.110.067363

[134] Nakamura Y, Hashimoto T, Ishii J, Kondo A. Dual-color reporter switching system to discern dimer formations of G-protein-coupled receptors using Cre/loxP site-specific recombination in yeast. Biotechnology and Bioengineering. 2016;**113**:2178-2190. DOI: 10.1002/bit.25974

[135] Sokolina K, Kittanakom S, Snider J, Kotlyar M, Maurice P, Gandía J, Benleulmi-Chaachoua A, Tadagaki K, Oishi A, Wong V, Malty RH, Deineko V, Aoki H, Amin S, Yao Z, Morató X, Otasek D, Kobayashi H, Menendez J, Auerbach D, Angers S, Przulj N, Bouvier M, Babu M, Ciruela F, Jockers R, Jurisica I, Stagljar I. Systematic protein-protein interaction mapping for clinically relevant human GPCRs. Molecular Systems Biology. 2017;**13**:918. DOI: 10.15252/msb.20167430

[136] Nakamura Y, Takemoto N, Ishii J, Kondo A. Simultaneous method for analyzing dimerization and signaling of G-protein-coupled receptor in yeast by dual-color reporter system. Biotechnology and Bioengineering. 2014;**111**:586-596. DOI: 10.1002/bit.25125

[137] Lagerström MC, Schiöth HB. Structural diversity of G protein-coupled receptors and significance for drug discovery. Nature Reviews Drug Discovery. 2008;**7**:339-357. DOI: 10.1038/nrd2518

Chapter 4

The Function of Rab35 in Development and Disease

Jia L. Song and Michael Testa

Additional information is available at the end of the chapter

http://dx.doi.org/10.5772/intechopen.75168

Abstract

Rab35 mediates membrane trafficking between the plasma membrane and the early endosomes at the cell surface. Our understanding of the cellular function of Rab35 reveals its role in development and diseases. In the developmental context, Rab35 has been shown to play an important role in regulating epithelial polarity, lumen opening, myoblast fusion, intercalation of epithelium, myelination, neurite outgrowth, and oocyte meiotic maturation. Disruption of recycling endosome mediated by Rab35 has been linked to several neurological diseases, including Parkinson's disease and Down syndrome. In addition, because Rab35 modulates cell migration through its interaction with various effectors, Rab35 plays an important role in cancers. Lastly, the Rab35-mediated recycling endosomal pathway and exocytosis is utilized by pathogens or hijacked by pathogens to promote their infection and survival. This review summarizes the function of Rab35 in endocytosis and focuses on the role of Rab35 in the context of development and diseases.

Keywords: small G proteins, Arf6, development, cell migration, protein trafficking

1. Introduction

Rab proteins constitute the largest subset of Ras-family small guanosine triphosphates (GTPases). Over 60 mammalian Rab proteins have been identified [1]. Rab35 is an evolutionarily conserved unique Rab GTPase that mediates membrane trafficking between the plasma membrane and endosomes in eukaryotic cells [1]. Similar to all G proteins, Rab35 undergoes molecular switching from active GTP-bound state to inactive GDP-bound state. The activity of Rab35 is highly regulated with four different Rab35 guanine-nucleotide exchange factor (GEF) and five Rab35 GTPase-activating proteins (GAPs). Depending on which effector proteins are associated with Rab35-GTP, it can mediate many cellular functions, such as cytokinesis, phagocytosis, cell migration, and exosome release [2–7]. Most of its cellular functions

involve the regulation of Rab35 in actin polymerization, Arf6 inactivation, or phosphoinositides (PtdIns(4,5)P2) [2, 8–10]. This review briefly summarizes the regulation of Rab35 in endocytosis and focuses on Rab35 in the context of development and diseases.

2. Rab35 mediates protein trafficking

Small G proteins mediate endosomal trafficking and maintain cell surface homeostasis. Two major types of endocytosis are the clathrin-mediated endocytosis (CME) and clathrin-independent endocytosis (CIE) [11]. CME involves the selective uptake of plasma membrane that is dependent on dynamin for vesicle scission. CIE is dynamin-independent and depends on free cholesterol at the plasma membrane; CIE does not require specific endocytic sorting sequence and is known as the bulk endocytic process [12]. The homeostasis at the cell surface requires balanced CME and CIE and the coordinated regulation by Rab35 and Arf6 [9]. Rab35 and Arf6 work antagonistically at the plasma membrane where Arf6 recruits the Rab35 GAP to inactivate Rab35, and Rab35 recruits the Arf6 GAP to inactivate Arf6. Thus, Rab35 from CME and the Arf6 from CIE work together to balance the two branches of the endocytic pathway [11].

Following endocytosis, endocytic vesicles converge on early endosomes where the cargos are sorted to be recycled or transported to late endosomes before eventually fusing with lysosomes. Activated Rab35 recruits effectors that mediate the formation of recycling tubules or vesicles. A diverse array of cargoes have been reported to undergo Rab35-dependent endocytic recycling back to the plasma membrane [13]. Overall, Rab35 plays a conserved role in mediating endocytosis recycling after cargo internalization.

The function of Rab35 is dependent on the effector proteins that bind to the active Rab35-GTP. Several key effectors of Rab35 have been identified that reveal its cellular functions. The level of the PtdIns(4,5)P2 lipid on endosomes is mediated by Rab35, since it binds to PtdIns(4,5)P2 phosphatase, OCRL [2]. Depletion of either Rab35 or OCRL leads to accumulation of PtdIns(4,5)P2 and F-actin binding proteins in enlarged peripheral endosome. Thus, Rab35 functions with OCRL to hydrolyze PIdIns(4,5)P2 on new endosomes and help define the lipid identity of early endosomes.

Fascin is another Rab35 effector protein. It crosslinks actin and assembles F-actin filaments into parallel bundles. Rab35-GTP recruits fascin in regulating *Drosophila* bristle development (Section 3.3) [10]. The shape and growth of the bristles depend on actin bundles. Rab35 also induces actin-rich protrusions in PC12 cells and regulates lamellipodia and filopodia formation in *Drosophila* [4].

Rab35 and Arf6 have been found to function antagonistically in regulating membrane trafficking [14]. Two Rab35 effectors are MICAL-L1 and ACAP2 (Arf6 GAP) that are involved in neurite outgrowth (Section 3.9.3) [15]. Another effector protein that interacts with Rab35-GTP in regulating neurite outgrowth is RUSC2. The overexpression of the RUN domain of RUSC2 inhibits Rab35-iduced neurite outgrowth in PC12 cells [16]. The role of RUSC2 downstream of Rab35 is not known. It is likely that the Rab35 interactome is far from complete.

3. Rab35 in development

The function of Rab35 in development has been examined mainly in the fly and worm. Various cell type such as myoblasts, fly S2 cells, oocytes, osteoclasts, neurons and oligodendrocytes have been used to study specific developmental processes. This section summarizes our current understanding of the role of Rab35 in the context of development.

3.1. Rab35 polarizes the fly tracheal seamless tubes

Drosophila trachea consists of multicellular, autocellular, and seamless tubes [17]. How seamless tubes are constructed is not well known; however, vesicular transport of apical membrane is thought to play an important role in forming the seamless tubes. During tubulogenesis, tip cells undergo epithelial to mesenchymal transition and initiate branching morphogenesis. A subpopulation of tip cells then differentiate in to terminal cells. A single seamless tube forms within each branched extension of the terminal cell. Together with Rab35, Whacked (a Rab35-GAP) mediates polarization of the growth of seamless tubes. Constitutive activation of Rab35 resulted in overgrowth of tubes at the terminal cell branch tips [18]. Conversely, Rab35-S22N dominant negative (DN) leads to ectopic branching surrounding the terminal cell nucleus. The function of Whacked and Rab35 is not in actin regulation, but in transporting vesicles from a recycling endosome to the branch tips [18]. Further, the polarized vesicular trafficking mediated by Rab35 is dependent on dynein motor-mediated transport towards the apical membrane [18]. Thus, polarized growth of the seamless tubes involves coordination of Rab-GAP, Rab35, and dynein.

3.2. Rab35 regulates epithelial organ lumen opening formation

Epithelial organs such as the lungs and kidneys are composed of a polarized cell monolayer surrounding a lumen. Madin-Darby canine kidney (MDCK) cells have been used as a model to examine the establishment of epithelial polarity and lumen [19]. It is thought that new apico-basal polarity in cysts arises from divisions of a single cell where apical transmembrane proteins are transcytosed from the plasma membrane to the cell-cell contact site. A recent study using MDCK cells indicated that Rab35 was found to directly interact with Podocalyxin (PODXL), a classical apical marker that has anti-adhesive properties that promote cell-cell repulsion at the apical membrane [20]. Rab35 knockdown with RNAi resulted in a complete inversion of polarity so that the PODXL localizes on the membrane facing the extracellular matrix instead of the lumen [20]. Rab35 establishes the apico-basal polarity by transporting PODXL to the site of lumen formation [20].

3.3. Rab35 recruits fascin to form *Drosophila* bristles

The *Drosophila* bristle is a mechanosensory organ where their shape and growth depends on actin bundles as the important structural component. *Drosophila* Rab GTPases were systematically tested for their impact on development with the use of DN mutant proteins. Of these 31 fly Rab GTPases tested, Rab35-S22N DN and Rab35 RNAi in the peripheral nervous system resulted in bristle morphology defects [10]. Adult bristles in reduced Rab35 function

were structurally abnormal, with sharp bends and kinks. Rab35-GTP binds to fascin, an actin cross-linking protein that organizes F-actin into bundles. In Rab35 DN cells, actin is found to be loose and disconnected. Although Rab35 has no effect on actin bundling *in vitro*, its association with fascin allows it to control when or where actin is bundled *in vivo* [10]. It was proposed that Rab35 may recruit fascin to initiate the cytoplasmic extension required for bristle extension. Insufficient Rab35 function would lead to bends and kinks in the bristles. Thus, Rab35 recruits fascin to subcellular location to drive actin bundling at the leading edge of cell protrusions to form the *Drosophila* bristles.

3.4. Rab35 functions in *Drosophila* germband extension

During development, cell assemblies that involve coordination of cellular adhesion and shape changes are needed to form tissues and organs. Internal organs such as the palate cochlea, gut and the kidney all require tissue elongation to shape an elongated body axis of an developing animal [21]. Cellular reshaping during organ formation requires the function of apical and junctional cytoskeletal and adhesion proteins. During *Drosophila* germband extension (GBE), cells undergo coordinated planar contraction of interfaces between Anterior-Posterior (AP) of neighboring cells. In the fly epithelium, Rab35 is expressed at low levels in the plasma membrane at the AP interfaces during active interface contractions. During this time, Rab35 functions in a conserved cell-shaping mechanism in which Rab35 shrinks AP cell surfaces by feeding endocytosed membranes and protein components to early endosomes to decrease plasma membranes to shape the epithelial cells. Rab35 directs the progressive shortening of anterior interface in response to apical area oscillations [22]. In addition, another developmental context where Rab35 shapes the epithelium is during mesodermal invagination where a ventral furrow is formed. In Rab35 knockdown embryos, rates of apical construction are greatly reduced and the embryo failed to form a ventral furrow for mesodermal invagination [22]. Thus, Rab35 functions by shrinking cell surfaces in shaping epithelial cell behaviors during development.

3.5. Rab35 regulates mouse oocyte meiosis

During meiosis, the oocytes undergo nuclear and cytoplasmic maturation where the migration of intracellular components such as spindle, mitochondria, and cortical granules is important for subsequent embryonic development. Rab35 localizes in the ooplasm at the germinal vesicle (GV) stage [23]. After germinal vesicle breakdown (GVBD), Rab35 is distributed at the spindle and colocalizes with α-tubulin. Rab35 RNAi treated oocytes displayed abnormal spindle morphology with multiple poles of spindle components, indicating that Rab35 regulates mouse oocyte spindle formation [23]. In addition, Rab35 RNAi and antibody blocking experiments indicated that GVBD is not affected, but polar body extrusion defect was observed. Overall, Rab35 was found to be important for forming spindles of oocytes during oocyte meiotic maturation and activation [23].

3.6. Terminal steps of cytokinesis is regulated by Rab35

Intracellular transport is essential for animal cytokinesis, with both the secretory and the endocytic pathways being implicated in the late phase of cytokinesis. Previously Rabs important in cytokinesis was screened with RNAi in S2 cells, in search for binucleated cells that

failed to undergo cytokinesis [2]. Rab35 is found to be required for the stabilization of the cytokinesis bridge connecting the daughter cells after furrow ingression as well as the abscission [2]. The proposed mechanism of Rab35 here is that Rab35 controls the localization of phosphatidylinositol 4,5-bis phosphate (PIP2) and SEPT2 at the bridge which are required for the stability of cytokinesis completion [2, 24, 25]. Rab35-mediated endocytic recycling is important for the stabilization of the late stage cytokinesis and abscission.

3.7. Rab35 regulates endocytic recycling of yolk receptor

Previously genetic mutants of endocytosis were identified in *C. elegans*. In rme-4 and rme-5 (Rab35) mutants, yolk uptake was greatly reduced [26]. Yolk uptake is necessary to support early embryonic growth. Biochemical and genetic evidence indicate that RME-4 recruits or activates Rab35 on endocytic vesicles to recycle receptors to the plasma membrane. RME-4 contained DENN domain that interacts with Rab35-GDP form, not the Rab35-GTP or WT forms [26]. In rem-4 and rem-5 mutants, sorting and/or recycling of yolk receptor RME-2 was impaired. Interestingly, in *C. elegans*, rab35 null mutants are viable and fertile, so it is not essential for the abscission step of cytokinesis as previously reported [2]. RME-4 is generally required for endocytosis in multiple cell types, whereas Rab35 may be cell type or cargo-specific.

3.8. Rab35 mediates myoblast fusion

During embryonic development, assembly and disassembly of cadherins play an important role in morphogenesis, cell differentiation, growth and migration [27]. Rab35 regulates cadherin trafficking and stabilization at cell-to-cell contacts to mediate myoblast fusion [28]. Rab35-S22N DN and RNAi results indicated a reduction of N- and M-cadherin at cell-to-cell contacts and increased accumulation in intracellular vacuoles. Rab35 RNAi and DN inhibited myoblast differentiation by preventing myoblast fusion to form myoblasts [28]. Overexpression of Rab35-WT and constitutively active Rab35-Q67L indicated their colocalization at the plasma membrane with $PI(4,5)P_2$, but no perturbation of $PI(4,5)P_2$ was observed [28]. The proposed mechanism is that Rab35 function is required for $PI(4,5)P_2$ production which stabilizes cadherin at cell-cell contact sites. Taken together, these results indicate that Rab35 regulates cadherin-dependent adherens junction formation and myoblast fusion [28].

3.9. Rab35 in the nervous system

3.9.1. Rab35 suppresses oligodendrocyte differentiation

During development of the central nervous system, oligodendrocytes precursor cells undergo cell division and migrate along axons where oligodendrocytes differentiate to wrap axons with myelin sheaths [29]. The dynamic morphological changes are in part mediated by small GTPase signaling. The regulatory role of Rab35 in oligodendrocyte differentiation was examined in FBD-102b (mouse oligodendroglial cells) cells [30]. Rab35 activates its effector protein ACAP2 (a Arf6-GAP) to deactivate Arf6, which inhibits FBD-102b differentiation [30]. Consistent with this result, knockdown of Arf6 with RNAi inhibits oligodendrocyte differentiation. In oligodendrocyte and neuronal cocultures, knockdown of Rab35 or ACAP2 promotes myelination, and inhibition of cytohesin-2 (Arf6-GAP) or Arf6 knockdown inhibits myelination [30]. These

studies revealed that Rab35 and Arf6 function antagonistically in regulating the differentiation of oligodendrocyte and myelination.

3.9.2. Rab35 coordinates synaptic vesicle trafficking and turnover

At least 30 out of the 60 mammalian Rab GTPases are associated with synaptic vesicle (SV) pools [31]. Antagonistic and synergistic functions of molecules within the Rab35 and Arf6 signaling network are necessary for regulating SV protein trafficking, degradation, and neurotransmitter release. Depending on neuronal activity, SVs may either get exocytosed when Arf6 is activated, or SVs can get recruited to presynaptic endosomes when Rab35 is activated [32]. Dysfunction of this signaling network may induce neurologic and neurodegenerative diseases. The molecular mechanism of SV protein turnover was further defined by using the rat hippocampal neurons [33]. Rab35 degrades SV proteins via the endosomal sorting complex required for transport (ESCRT) pathway, by recruiting Rab35 effector and ESCRT protein, Hrs. Upon neuronal stimulation, ESCRT proteins are recruited to SV pools to degrade specific SV proteins [33].

In addition, Rab35 and its GAP, Skywalker (Sky), were found to be key players in the endosomal sorting/recycling of SV proteins [34]. Sky was identified to facilitate endosomal trafficking of synaptic vesicles at *Drosophila* neuromuscular junction boutons, by controlling Rab35 GTPase activity. *Sky* mutants harbor a larger releasable pool of synaptic vesicles and led to increased basal neurotransmitter release. Rab35 DN rescues Rab35 GAP *sky* mutant phenotypes [33]. Consistent with the antagonistic function of Rab35 and Arf6, Arf6 loss-of-function is similar to that observed in *sky* mutants (result in accumulation of Rab35-GTP). Thus, Rab35 and Arf6 antagonistic regulation of synaptic endosomal trafficking maintains the SV protein homeostasis.

3.9.3. Rab35 mediates neurite outgrowth

Rab35 has been shown to promote neurite outgrowth of PC12 cells in response to nerve growth factor (NGF) stimulation [35, 36]. Upon nerve growth factor (NGF) stimulation, Rab35 accumulates in Arf6-positive endosomes [36]. Both Rab35 and Arf6 work antagonistically to regulate neurite outgrowth. The same Rab35 effector, ACAP2 (or centaurin-β2) that regulates the differentiation of oligodendrocytes (Section 3.9.1), is recruited to the Arf6-positive endosomes in a Rab-35-dependent manner upon NGF stimulation. The Arf6-GAP activity of ACAP2, leading to Arf6 inactivation, was required for NGF-induced neurite outgrowth [36]. In addition, Rab35 was found to form a tripartite structure with MICAL-L1 and ACAP2 and recruit them to Arf6-positive endosomes in response to NGF. MICAL-L1 and ACAP2 cooperatively recruit EHD1, which belongs to the dynamin-like C-terminal Eps15 homology domain protein family [37]. EHD1 promotes membrane trafficking of various receptors, mainly from recycling endosomes to the plasma membrane. EHD1 functions as molecular scissors that facilitate fission of vesicles from recycling endosomes via its ATPase activity. Knockdown of Rab35, MICAL-L1, ACAP2, and EHD1 all resulted in shortened neurite outgrowth, indicating the importance of each of these components [36, 38]. In summary, Rab35 recruits and coordinates MICAL-L1 and ACAP2 to Arf6-positive endosomes. At the same time, EHD1 is recruited by binding to MICAL-L1 where it may facilitate neurite tip outward growth by mediating fission of vesicles that target to neurite tips from recycling endosomes during neurite outgrowth.

Rab35 has been proposed to act as a master Rab that determines the intracellular localization of MICAL-L1, which functions as a scaffold for other recruited Rabs [15]. Upon NGF stimulation, Rab35 localizes to Arf6-positive recycling endosomes and recruits MICAL-L1, which interacts with Rabs 8, 13, and 36 [15]. Each of these recruited Rabs functions in a non-redundant manner downstream of Rab35 and MICAL-L1 in regulating neurite outgrowth [15]. Knockdown of individual MICAL-L1 interacting Rabs did not alter MICAL-L1 localization but inhibited NGF-induced neurite outgrowth. Overall, the NGF stimulation activates Rab35 which recruits several other Rabs at recycling endosomes that supply membranes and proteins to enable neurite outgrowth.

3.9.4. Rab35 functions in axon elongation

Neurons acquire an asymmetric morphology during embryonic development to establish neuronal polarization, where a single axon and several dendrites are formed [39]. Neuronal polarized trafficking is dependent on the supply of membrane needed to cell expansion and the differential distribution of proteins. This process involves Rab35 and its regulators. Rab35 was found to function in axon elongation that is regulated by p53-related protein kinase, or PRPK [40]. PRPK is a negative regulator of Rab35 that promotes the degradation of Rab35 via the ubiquitin proteasome degradation pathway. Another protein, microtubule-associated protein 1B (MAP1B), interacts with PRPK to inhibit its degradation of Rab35 [40]. MAP1B is necessary for proper axon outgrowth, as decreased MAP1B expression reduces axon length. MAP1B knock out is rescued by Rab35 overexpression or PRPK inactivation. Neurons overexpressing Rab35 WT and active Rab35-Q67L exhibited a significant increase in exon length. In contrast, Rab35-S22N DN transfected neurons had reduced axon length. In addition, Rab35 activates Cdc42 by either direct activation of Cdc42 or transporting vesicles containing polarity determinants to the elongating exons [40]. Overall, these results indicate that Rab35 is critical for mediating neuronal polarization trafficking to elongate axons.

4. Rab35 in diseases

Disruption of recycling endosome mediated by Rab35 has been linked to several neurological diseases, including Parkinson's disease and Down syndrome [41, 42]. In addition, because Rab35 modulates cell migration through its interaction with Wnt/Dvl signaling pathway and F-actin modulators, Rab35 plays an important role in cancers (see Section 4.3). Lastly, the Rab35-mediated recycling endosomal and exocytosis pathways are used by pathogens to promote their infections and survival (see Section 4.4). This section summarizes the role of Rab35 in various diseases (**Table 1**).

4.1. Rab35 may be involved in Parkinson's disease

Parkinson's disease (PD) is a neurodegenerative disease in which the patient's dopaminergic neurons in the substantia nigra are impaired [43]. Lewy bodies composed of abnormal α-synuclein accumulate in substantia nigra neurons of PD patients [44]. The serum levels of Rab35 was high in PD patients and in the substantia nigra of mice models for PD [41]. Overexpression

Disease	Function	Potential molecular mechanism	Ref
Parkinson's disease	Endocyclic recycling of α-synuclein	Unknown	[41]
Down syndrome	Exosome release	Unknown	[42]
Breast cancer	Promotes cell migration	Activation of Rac1 via Wnt5a/Dvl2.	[5, 43]
		Active Rab35 and MICAL1 generate ROS and activate Akt pathway	
Lung cancer	Enhance cell polarization and migration	Rab35 mediates interaction of RUSC2 and GIT2; mediate GIT2 phosphorylation	[44]
Allergy-induced asthma	Delayed TCR recycling; increase cytokines	DENND1B interacts with AP-2 to mediate Rab35 GTP exchange	[45]
Amoebic colitis *Entamoeba histolytica*	Uses Rab35 to phagocytose RBCs	Unknown	[46]
Uropathogenic *E. coli*	Iron acquisition; lysosome evasion	Exploits host TfR1 to acquire iron	[47]
Enterohemorrhagic *E. coli*	Inhibit host endocyclic recycling pathway	Bacteria EspG interacts with Arf6-GTP	[48]
Legionnaires disease	Evade fusion with host lysosomes	LepB stimulates GTP hydrolysis on Rab35	[49, 50]
		AnkX modifies Rab35 with phosphocholine	[51]
Antrax *Bacillus anthracis*	Endocytosis and release anthrax lethal toxin	Rab35 mediates MAPKK cleavage and exosome formation	[7]

Table 1. Summary of Rab35 in diseases.

of Rab35 in SH-SY5Y cells (cell line model to study neuronal function) resulted in increased aggregation and secretion of α-synuclein [41]. Although no detailed mechanism of Rab35 in the pathogenesis of PD is known, Rab35 may participate in the processing and endocyclic recycling of α-synuclein [43]. This proposed role of Rab35 in PD is in part supported by several studies that have shown α-synuclein to interact with other Rab proteins [45, 46]. The level of Rab35 in patient serum may be useful in the diagnoses of different Parkinsonian disorders.

In addition, activation of leucine-rich repeat protein kinase 2 (LRRK2), caused by autosomal dominant missense mutation, predisposes patients to PD [47]. LRRK2 is a Rab GTPase that has been found to phosphorylate 14 Rab proteins, including Rab35 [48]. Specific LRRK2 antibodies that recognize phosphorylated forms of Rab proteins have been developed to examine how LRRK2 and Rab proteins contribute to PD and may serve as a potential therapeutic tool [49, 50].

4.2. Rab35 controls exosome secretion in Down syndrome patients

Early endosomal abnormalities have been correlated to developmental brain defects in Alzheimer's disease (AD) and Down syndrome patients (DS) [51]. In the neurons of these patients, their endosomes are aberrantly numerous and enlarged with accumulated materials that lead to neuronal vulnerability and degeneration [52]. Early endosomes are the first

vesicular compartment along the endocytic pathway where internalized cargos are delivered to late endosomes or multivesicular bodies (MVBs) for sorting to either lysosomes for degradation or to the extracellular space via exosomes release (EVs). The docking of MVBs to the plasma membrane is regulated by Rab35 [6]. In human brain homogenates, Rab35 proteins were at a higher level in DS patients compared to controls using western blotting detection [42]. In addition, DS patients and Ts2 mice (murine model for DS) have higher levels of exosome-enriched EVs and Rab35 in the brain extracellular space [42]. Rab35 is proposed to play a protective role in mediating exosome release to relieve neurons of the toxic materials in neuronal endosomes in DS and AD patients [42].

4.3. Rab35 functions in cell migration and cancers

Rab35 has been shown to interact with effector proteins that are involved in cell adhesion and cell migration which are key processes that are disrupted in cancer. Rab35 is required for Wnt5a/Dvl2-induced Rac1 activation and cell migration in MCF-7 breast cancer cells [5]. Upon *in vitro* Wnt5a stimulation, Dvl2, Rab35 and Rac1 are activated to promote cell migration in MCF-7 breast cancer cells. Conversely, a knockdown of Wnt5a using siRNA resulted in significantly lowered expression of Rab35 and decreased MCF-7 cell migration [5]. Knockdown of Dvl2 also blocked Wnt5a-induced Rab35 and Rac1 activation, supporting that Rab35 was the downstream target of Wnt5a/Dvl2 signaling in MCF-7 breast cancer cells. Rab35 knockdown also resulted in decreased Rac1 activation and cell migration. Further, Rab35 was found to physically associate with Dvl2 in MCF-7 cells using immunofluorescence and co-immunoprecipitation assays. Thus, Wnt5 signaling results in activation of Dvl/Rab35/Rac1 activity that promotes breast cancer cell migration.

In another study, active Rab35 and its effector protein, MICAL1, control cell invasive phenotype in breast cancer cells [53]. MICAL1 has been shown to upregulate reactive oxygen species (ROS) in HeLa cells and phosphorylate proteins leading to malignancies and metastasis. Breast cancer cells receive signals from their microenvironment, such as epidermal growth factor (EGF), LPA and hypoxia, ROS level in cells may increase and functions as second messengers in intracellular signaling cascades to induce their metastasis [54]. Upon stimulation of EGF, Rab35 levels increased in MCF-7 cells [53]. Rab35 knockdown using siRNA in MCF-7 cells showed a dramatic decrease in cell invasion, demonstrating that Rab35 was required for EGF-induced invasion in breast cancer cells [53]. Transfection of cells with siRab35 or siMICAL1 led to decreased ROS, indicating that both Rab35 and MICAL1 are required for ROS generation. Further, the generated ROS was found to activate the PI3K/Akt pathway which also plays a key role in migratory potential regulation. Consistent with this result, knockdown of Rab35 or MICAL1 by RNAi resulted in decreased phosphorylated Akt (P-Akt) [53]. Similarly, P-Akt was higher when MICAL1 or Rab35-GTP (active) were overexpressed in MCF-7 cells. Together, these results revealed that Rab35 and MICAL1 promote ROS production which leads to PI3K/Akt signaling activation, resulting in increased breast cancer cell migration and invasion [53].

Consistent with the role of Rab35 in activating the Akt signaling pathway, an earlier study identified that Rab35 functions downstream of growth factor receptors and upstream of the Akt signaling pathway [55]. Using lentiviruses that express short hairpin RNAs (shRNAs) targeting genes coding for all known G-proteins and lipid/protein, Rab35 knockdown was found

to downregulate Akt phosphorylation [55]. Furthermore, the PI3K-dependent phosphorylation of FOXO1/3A was also decreased in cells depleted of Rab35. Wild type, constitutively active Rab35-Q67L and DN Rab35-S22N was each expressed in cell lines and only the Rab35-Q67L active form bound to and activate FOX01/3A and the P13K/AKT signaling pathway [55]. Based on missense mutations previously identified in the proto-oncogene KRAS in myeloid leukemia patients and colorectal tumors, Rab35 with A151T and F161L mutations were tested for their effect on AKT signaling [56, 57]. Interestingly, Rab35-A151T and Rab35-F161L mutants expressed stably in NIH-3T3 cells also resulted in elevated AKT phosphorylation levels, indicating that these gain-of-function alleles are sufficient to activate PI3K/AKT signaling [55]. Therefore, these studies demonstrated that Rab35 activates AKT signaling in cancer cells to suppress apoptosis and aid in cell transformation.

Rab35 plays an important role in non-small cell lung cancer (NSCLC) cell migration by regulating the interaction of RUSC2 (Rab35 effector protein) and GIT2 (Arf6-GAP) [58]. Both RUSC2 and GITS2 have been found to regulate cell polarity and directional cell migration [16, 59]. The function of RUSC2 is not well characterized and may participate in vesicle-mediated transport and secretory pathway to regulate directional migration [60]. GIT2 interacts with paxillin to mediate normal cell spreading and lamellipodia formation [61]. Upon EGF stimulation, Rab35 is activated and promotes the binding of RUSC2 to the non-phosphorylated form of GIT2 [58]. Knockdown of Rab35 or RUSC2 by RNAi resulted in decreased GIT2 phosphorylation and its half-life, indicating that Rab35 and RUSC2 are each essential for GIT2 phosphorylation and stability [58]. The phosphorylated form of GIT2 is released from RUSC2 and localizes to the plasma membrane to mediate cell migration [58]. Collectively, these data indicate that upon EGF stimulation, active Rab35 promotes the interaction of RUSC2 and GIT2, the intracellular stabilization and phosphorylation of GIT2, and lung cancer cell polarization and cell migration [58].

4.4. Rab35 may regulate T-cell receptor signaling

Upon receptor complex activation, the duration of signaling is affected by alterations in receptor internalization, recycling, and degradation [62]. The prolonged activation of T-cell receptor (TCR) on immune T_H2 cells promotes allergic asthma [63]. TCRs within the plasma membrane of T_H2 cells are dynamically regulated through endocytosis and recycling [64, 65]. The role of Rab35-GEF, DENND1B, in allergic asthma was investigated in mice [63]. The independent knockdown of DENN1B, Rab35, or clathrin adaptor AP-2 resulted in delayed TCR downmodulation after its activation [63]. This in turn resulted in aberrant, prolonged TCR signaling and increased cytokine secretion of IL-4, IL-5, and IL-13 in T_H2 cells. The ability of DENND1B to interact with AP-2 and mediate Rab35 GTP exchange is required for optimal regulation of surface TCR signaling in T_H2 cells [63]. These findings were consistent with enhanced *in vivo* T_H2-mediated inflammation in Dennd1b−/− mice when challenged with aerosolized antigen [63]. The regulation of DENND1B of T_H2 cells provides a potential mechanistic basis to explain the genetic association observe with DENND1B gene variants in early childhood asthma [66, 67].

4.5. Pathogens use the Rab35 pathway during infections

Rab35 has been demonstrated to be involved in the process of erythrophagocytosis of *Entamoeba histolytica* trophozoites, leading to amoebic colitis [68]. *E. histolytica* infect around 50 million people worldwide, and around 100,000 people die annually from this infection [69]. The ability

of *E. histolytica* trophozoites to phagocytose host red blood cells (RBCs), immune cells, apoptotic cells, and microbiota during infection is critical for their pathogenicity [70]. Using an amoebic expression plasmid for *E. histolytica* Rab35 (EhRab35), a previous study found that EhRab35 is mainly localized to both large vacuolar and smaller punctate structures that are distinct from giant early endocytic vacuoles in the cytoplasm [68]. Infection of human RBCs with a stable transgenic line of trophozoites expressing either active Rab35-Q67L or the inactive Rab35-S22N, EhRab35 was found to be involved in the early phase of erythrophagocytosis [68]. Specifically, the active Rab35-Q67L localized to the site of the phagocytic cups during erythrophagocytosis. In addition, live cell imaging data revealed that GFP-EhRab35 translocated to the newly formed actin-based phagocytic cup rapidly from the attachment of RBCs [68]. The number of phagocytic cups decreased when RBCs were incubated with the inactive form of Rab35-S22N trophozoites. Collectively, these results indicate that EhRab35 mediates phagocytosis of RBCs during infection and is involved in phagosome maturation and degradation of RBCs [68].

Uropathogenic *Escherichia coli* (UPEC) are the causative agent of 80% of the urinary tract injections (UTIs) [71]. UPEC hijacks the vesicular trafficking proteins of host bladder epithelial cells (BECs) to facilitate its survival [72]. In comparison to other tested Rab proteins, Rab35 showed a rather striking degree of localization to UPEC-enriched vesicular structures, termed UPEC-containing vacuoles (UCVs) [72]. BECs over-expressing GFP-tagged Rab35 protein were infected with UPEC. Results indicated that Rab35 is recruited to the UPEC-containing vacuoles during intracellular infection of BECs, and Rab35 protein is also increased during UPEC infection [72]. Rab35 knockdown with RNAi in BECs led to a significant reduction in the intracellular bacterial load, demonstrating that Rab35 plays an important role in the intracellular survival of UPEC in bladder epithelial cells. Mechanistically, UPECs usurp the host membrane trafficking system to facilitate trafficking of iron containing (transferrin) vesicles to their residing vacuoles [72]. This is supported by confocal microscopy analysis that showed colocalization of transferrin receptor 1 (TfR1) and Rab35 at the cell surface of BECs during UPEC infection. Both Rab35 and TfR1 knockdown BECs led to reduced iron pool and reduced survival of UPEC. Interestingly, iron supplementation in BECs during UPEC is not able to support intracellular UPEC survival in the absence of host Rab35 or TfR, indicating that the Rab35 pathway is critical for iron acquisition and survival during intracellular UPEC infection [72].

An additional function of the Rab35 recruitment from the host is to promote UPEC survival by preventing the fusion of UPEC-containing vesicles with the hosts' degradative lysosomes [72]. UPECs colocalized with lysosomes in normal and Rab35-deleted cells in late endosomes and lysosomes. In Rab35 knockdown BECs, a significantly higher number of intracellular UPECs colocalized with the lysosomal marker where UPECs are destroyed. Thus, UPECs utilize the host Rab35 mediated vesicular trafficking pathways to enhance its iron acquisition and prevent lysosomal degradation within the bladder epithelial cells during infection [72].

Enterohemorrhagic *E. coli* (EHEC) and enteropathogenic *E. coli* (EPEC) cause food-poisoning outbreaks, in which patients suffer from diarrhea, hemorrhagic colitis and hemolytic uremic syndrome (HUS) [73]. EHEC is common as a food or water-borne pathogen in industrialized countries, while EPEC remains a significant cause of diarrhea in low-income countries. Another characteristic of EHEC but not EPEC is the production of Shiga toxins, which are associated with the more severe hemorrhagic colitis and HUS [74]. During infections, both EHEC and EPEC deliver bacterial effector proteins into host gut epithelial cells to facilitate

their colonization [75]. One of these bacterial effector protein is EspG, which is critical for EHEC to deplete cell surface receptors from the plasma membrane during infections [76]. EspG may reorganize multiple host signaling networks during infection by binding to Arfs and Rab GTPases [77]. Recently, EHEC EspG during infection was found to modulate an ARF6:Rab35 signaling axis to prevent the host cell's recycling endosome function [78]. EspG binds with Arf6-GTP and not Arf6-GDP in a co-immunoprecipitation study [78]. Interestingly, EspG also acts as a Rab-GAP for Rab35 and other Rabs where it inactivates Rab35. During infections, EspG preferentially interacts with Arf6-GTP upstream of Rab35 binding to transport itself to endosomal structures and prevent Rab35 in mediating recycling of cargo to the host cell surface. Thus, the EHEC secretes its effector protein EspG to shut down the recycling endosomal trafficking in the host cell.

Legionella pneumophila is the causative agent for Legionnaires disease, a community or hospital-acquired pneumonia [79]. *L. pneumophila* proliferates within amoebae in nature and infects human alveolar macrophages. Alveolar macrophages engulf *L. pneumophila* through phagocytosis; however, by secreting over 250 effector proteins that modify the host signaling networks and cell membrane trafficking machineries, this intracellular pathogen converts the macrophage phagosomes into the *Legionella*-containing vacuoles (LCV) where *Legionella* survive and replicate. One of the *L. pneumophila* effector proteins is LepB, which is secreted by *Legionella* at later stages of infection and accumulates in the host cell [80]. In biochemical enzyme kinetic studies, LepB was identified to act as a Rab-GAP to inactivate multiple Rab proteins [80]. LepB can stimulate GTP hydrolysis on Rab35, although with 10–100 times decreased catalytic efficiency than Rab1b [81]. The proposed function of LepB is that it may target multiple Rab proteins that are involved in the biogenesis or maintenance of the LCVs to promote *Legionella* survival.

Another *L. pneumophila* effector protein is AnkX, a phosphocholine transferase that covalently links a phosphocholine moiety to Rab35 [82]. Fluorescent protein-tagged AnkX introduced to mammalian cells was found to localize at the plasma membrane and tubular membrane compartments by transmission electron microscopy [83]. Consistent with its targeting of the endocytic recycling pathway, AnkX co-localized with Rab35 and a Rab35 cargo, the major histocompatibility class I protein (MHCI) [83]. AnkX mediated phosphocholination of Rab35 has been found to stabilize phosphocholinated Rab35-GDP in the membranes [84]. These sequestered membrane-bound phosphocholinated Rab-GDP proteins cannot be converted to the Rab35-GTP form, because they cannot interact with cellular Rab35-GEFs [84]. The phosphocholine modification of Rab35 by AnkX was found to be critical for preventing the activation of Rab35 and prevent the fusion of LCV with phagosomes [83, 85]. Thus, AnkX mediates post-translational modification to Rab35 to manipulate the host endocytic recycling trafficking to evade the immune system.

Rab35 may play a role in the pathogenesis of *Bacillus anthracis* infection. The lethal toxin (LT) is made of protein subunits lethal factor (LF) and protective antigen (PA). PA oligomerizes into ring-shaped structure that bind to four LF subunits that then gets taken up by host cells via clathrin-mediated, dynamin-dependent endocytosis to the early endosomes [86]. The anthrax PA forms a pore into the membrane of the intraluminal vesicles (ILV) that can be delivered to the cytosol or released into the extracellular medium as exosomes which can be taken up by naive recipient cells to propagate infection [87]. Rab11 and Rab35 knockdown in RPE cells failed to trigger MAPKK cleavage in naive RPE-1 cells [7]. Furthermore, Rab35

knockdown prevented exosome formation, indicating that Rab35 is required for the delivery of LF-containing exosomes to extracellular medium in RPE1 cells where these LF-containing exosomes can be taken up by additional cells [7].

5. Conclusions

Rab35 is a highly conserved small GTPase that is the only Rab that mediates endosomal recycling of target proteins between the plasma membrane and the early endosomes. Further understanding of the interactome of Rab35 will elucidate additional functions of Rab35 in the context of development and disease.

Conflict of interest

The authors declare no conflict of interest.

Author details

Jia L. Song* and Michael Testa

*Address all correspondence to: jsong@udel.edu

University of Delaware, Newark, Delaware, USA

References

[1] Hutagalung AH, Novick PJ. Role of Rab GTPases in membrane traffic and cell physiology. Physiological Reviews. 2011;**91**(1):119-149. DOI: 10.1152/physrev.00059.2009

[2] Kouranti I, Sachse M, Arouche N, Goud B, Echard A. Rab35 regulates an endocytic recycling pathway essential for the terminal steps of cytokinesis. Current Biology. 2006;**16**(17):1719-1725. DOI: 10.1016/j.cub.2006.07.020

[3] Egami Y, Fujii M, Kawai K, Ishikawa Y, Fukuda M, Araki N. Activation-inactivation cycling of Rab35 and ARF6 is required for phagocytosis of Zymosan in RAW264 macrophages. Journal of Immunology Research. 2015;**2015**:429-439. DOI: 10.1155/2015/429439

[4] Shim J, Lee SM, Lee MS, Yoon J, Kweon HS, Kim YJ. Rab35 mediates transport of Cdc42 and Rac1 to the plasma membrane during phagocytosis. Molecular and Cellular Biology. 2010;**30**(6):1421-1433. DOI: 10.1128/MCB.01463-09

[5] Zhu Y, Shen T, Liu J, Zheng J, Zhang Y, Xu R, et al. Rab35 is required for Wnt5a/Dvl2-induced Rac1 activation and cell migration in MCF-7 breast cancer cells. Cellular Signalling. 2013;**25**(5):1075-1085. DOI: 10.1016/j.cellsig.2013.01.015

[6] Hsu C, Morohashi Y, Yoshimura S, Manrique-Hoyos N, Jung S, Lauterbach MA, et al. Regulation of exosome secretion by Rab35 and its GTPase-activating proteins TBC1D 10A-C. The Journal of Cell Biology. 2010;**189**(2):223-232. DOI: 10.1083/jcb.200911018

[7] Abrami L, Brandi L, Moayeri M, Brown MJ, Krantz BA, Leppla SH, et al. Hijacking multivesicular bodies enables long-term and exosome-mediated long-distance action of anthrax toxin. Cell Reports. 2013;**5**(4):986-996. DOI: 10.1016/j.celrep.2013.10.019

[8] Egami Y, Fukuda M, Araki N. Rab35 regulates phagosome formation through recruitment of ACAP2 in macrophages during FcgammaR-mediated phagocytosis. Journal of Cell Science. 2011;**124**(Pt 21):3557-3567. DOI: 10.1242/jcs.083881

[9] Dutta D, Donaldson JG. Sorting of clathrin-independent cargo proteins depends on Rab35 delivered by clathrin-mediated endocytosis. Traffic. 2015;**16**(9):994-1009. DOI: 10.1111/tra.12302

[10] Zhang J, Fonovic M, Suyama K, Bogyo M, Scott MP. Rab35 controls actin bundling by recruiting fascin as an effector protein. Science. 2009;**325**(5945):1250-1254. DOI: 10.1126/science.1174921

[11] Donaldson JG, Johnson DL, Dutta D. Rab and Arf G proteins in endosomal trafficking and cell surface homeostasis. Small GTPases. 2016;**7**(4):247-251. DOI: 10.1080/21541248.2016.1212687

[12] Mayor S, Parton RG, Donaldson JG. Clathrin-independent pathways of endocytosis. Cold Spring Harbor Perspectives in Biology. 2014;**6**(6):1-20. DOI: 10.1101/cshperspect.a016758

[13] Klinkert K, Echard A. Rab35 GTPase: A central regulator of phosphoinositides and F-actin in endocytic recycling and beyond. Traffic. 2016;**17**(10):1063-1077. DOI: 10.1111/tra.12422

[14] Dutta D, Donaldson JG. Rab and Arf G proteins in endosomal trafficking. Methods in Cell Biology. 2015;**130**:127-138. DOI: 10.1016/bs.mcb.2015.04.004

[15] Kobayashi H, Etoh K, Ohbayashi N, Fukuda M. Rab35 promotes the recruitment of Rab8, Rab13 and Rab36 to recycling endosomes through MICAL-L1 during neurite outgrowth. Biology Open. 2014;**3**(9):803-814. DOI: 10.1242/bio.20148771

[16] Fukuda M, Kobayashi H, Ishibashi K, Ohbayashi N. Genome-wide investigation of the Rab binding activity of RUN domains: Development of a novel tool that specifically traps GTP-Rab35. Cell Structure and Function. 2011;**36**(2):155-170

[17] Samakovlis C, Hacohen N, Manning G, Sutherland DC, Guillemin K, Krasnow MA. Development of the *Drosophila* tracheal system occurs by a series of morphologically distinct but genetically coupled branching events. Development. 1996;**122**(5):1395-1407

[18] Schottenfeld-Roames J, Ghabrial AS. Whacked and Rab35 polarize dynein-motor-complex-dependent seamless tube growth. Nature Cell Biology. 2012;**14**(4):386-393. DOI: 10.1038/ncb2454

[19] Sigurbjornsdottir S, Mathew R, Leptin M. Molecular mechanisms of de novo lumen formation. Nature Reviews. Molecular Cell Biology. 2014;**15**(10):665-676. DOI: 10.1038/nrm3871

[20] Klinkert K, Rocancourt M, Houdusse A, Echard A. Rab35 GTPase couples cell division with initiation of epithelial apico-basal polarity and lumen opening. Nature Communications. 2016;**7**:11166. DOI: 10.1038/ncomms11166

[21] Irvine KD, Wieschaus E. Cell intercalation during *Drosophila* germband extension and its regulation by pair-rule segmentation genes. Development. 1994;**120**(4):827-841

[22] Jewett CE, Vanderleest TE, Miao H, Xie Y, Madhu R, Loerke D, et al. Planar polarized Rab35 functions as an oscillatory ratchet during cell intercalation in the *Drosophila* epithelium. Nature Communications. 2017;**8**(1):476. DOI: 10.1038/s41467-017-00553-0

[23] Wang HH, Cui Q, Zhang T, Wang ZB, Ouyang YC, Shen W, et al. Rab3A, Rab27A, and Rab35 regulate different events during mouse oocyte meiotic maturation and activation. Histochemistry and Cell Biology. 2016;**145**(6):647-657. DOI: 10.1007/s00418-015-1404-5

[24] Emoto K, Inadome H, Kanaho Y, Narumiya S, Umeda M. Local change in phospholipid composition at the cleavage furrow is essential for completion of cytokinesis. The Journal of Biological Chemistry. 2005;**280**(45):37901-37907. DOI: 10.1074/jbc.M504282200

[25] Kinoshita M, Kumar S, Mizoguchi A, Ide C, Kinoshita A, Haraguchi T, et al. Nedd5, a mammalian septin, is a novel cytoskeletal component interacting with actin-based structures. Genes & Development. 1997;**11**(12):1535-1547

[26] Sato M, Sato K, Liou W, Pant S, Harada A, Grant BD. Regulation of endocytic recycling by *C. elegans* Rab35 and its regulator RME-4, a coated-pit protein. The EMBO Journal. 2008;**27**(8):1183-1196. DOI: 10.1038/emboj.2008.54

[27] Halbleib JM, Nelson WJ. Cadherins in development: Cell adhesion, sorting, and tissue morphogenesis. Genes & Development. 2006;**20**(23):3199-3214. DOI: 10.1101/gad.1486806

[28] Charrasse S, Comunale F, De Rossi S, Echard A, Gauthier-Rouviere C. Rab35 regulates cadherin-mediated adherens junction formation and myoblast fusion. Molecular Biology of the Cell. 2013;**24**(3):234-245. DOI: 10.1091/mbc.E12-02-0167

[29] Simons M, Lyons DA. Axonal selection and myelin sheath generation in the central nervous system. Current Opinion in Cell Biology. 2013;**25**(4):512-519. DOI: 10.1016/j.ceb.2013.04.007

[30] Miyamoto Y, Yamamori N, Torii T, Tanoue A, Yamauchi J. Rab35, acting through ACAP2 switching off Arf6, negatively regulates oligodendrocyte differentiation and myelination. Molecular Biology of the Cell. 2014;**25**(9):1532-1542. DOI: 10.1091/mbc.E13-10-0600

[31] Pavlos NJ, Jahn R. Distinct yet overlapping roles of Rab GTPases on synaptic vesicles. Small GTPases. 2011;**2**(2):77-81. DOI: 10.4161/sgtp.2.2.15201

[32] Sheehan P, Waites CL. Coordination of synaptic vesicle trafficking and turnover by the Rab35 signaling network. Small GTPases. 2017;**8**:1-10. DOI: 10.1080/21541248.2016.1270392

[33] Sheehan P, Zhu M, Beskow A, Vollmer C, Waites CL. Activity-dependent degradation of synaptic vesicle proteins requires Rab35 and the ESCRT pathway. The Journal of Neuroscience. 2016;**36**(33):8668-8686. DOI: 10.1523/JNEUROSCI.0725-16.2016

[34] Uytterhoeven V, Kuenen S, Kasprowicz J, Miskiewicz K, Verstreken P. Loss of skywalker reveals synaptic endosomes as sorting stations for synaptic vesicle proteins. Cell. 2011;**145**(1):117-132. DOI: 10.1016/j.cell.2011.02.039

[35] Chevallier J, Koop C, Srivastava A, Petrie RJ, Lamarche-Vane N, Presley JF. Rab35 regulates neurite outgrowth and cell shape. FEBS Letters. 2009;**583**(7):1096-1101. DOI: 10.1016/j.febslet.2009.03.012

[36] Kobayashi H, Fukuda M. Rab35 regulates Arf6 activity through centaurin-beta2 (ACAP2) during neurite outgrowth. Journal of Cell Science. 2012;**125**(Pt 9):2235-2243. DOI: 10.1242/jcs.098657

[37] Naslavsky N, Caplan S. EHD proteins: Key conductors of endocytic transport. Trends in Cell Biology. 2011;**21**(2):122-131. DOI: 10.1016/j.tcb.2010.10.003

[38] Kobayashi H, Fukuda M. Rab35 establishes the EHD1-association site by coordinating two distinct effectors during neurite outgrowth. Journal of Cell Science. 2013;**126**(Pt11):2424-2435. DOI: 10.1242/jcs.117846

[39] Lalli G. Crucial polarity regulators in axon specification. Essays in Biochemistry. 2012; **53**:55-68. DOI: 10.1042/bse0530055

[40] Villarroel-Campos D, Henriquez DR, Bodaleo FJ, Oguchi ME, Bronfman FC, Fukuda M, et al. Rab35 functions in axon elongation are regulated by P53-related protein kinase in a mechanism that involves Rab35 protein degradation and the microtubule-associated protein 1B. The Journal of Neuroscience. 2016;**36**(27):7298-7313. DOI: 10.1523/JNEUROSCI.4064-15.2016

[41] Chiu CC, Yeh TH, Lai SC, Weng YH, Huang YC, Cheng YC, et al. Increased Rab35 expression is a potential biomarker and implicated in the pathogenesis of Parkinson's disease. Oncotarget. 2016;**7**(34):54215-54227. DOI: 10.18632/oncotarget.11090

[42] Gauthier SA, Perez-Gonzalez R, Sharma A, Huang FK, Alldred MJ, Pawlik M, et al. Enhanced exosome secretion in down syndrome brain—A protective mechanism to alleviate neuronal endosomal abnormalities. Acta Neuropathologica Communications. 2017;**5**(1):65. DOI: 10.1186/s40478-017-0466-0

[43] Gao Y, Wilson GR, Stephenson SEM, Bozaoglu K, Farrer MJ, Lockhart PJ. The emerging role of Rab GTPases in the pathogenesis of Parkinson's disease. Movement Disorders. 2018;**33**(2): 196-207. DOI: 10.1002/mds.27270

[44] Baba M, Nakajo S, Tu PH, Tomita T, Nakaya K, Lee VM, et al. Aggregation of alpha-synuclein in Lewy bodies of sporadic Parkinson's disease and dementia with Lewy bodies. The American Journal of Pathology. 1998;**152**(4):879-884

[45] Chutna O, Goncalves S, Villar-Pique A, Guerreiro P, Marijanovic Z, Mendes T, et al. The small GTPase Rab11 co-localizes with alpha-synuclein in intracellular inclusions and modulates its aggregation, secretion and toxicity. Human Molecular Genetics. 2014;**23**(25):6732-6745. DOI: 10.1093/hmg/ddu391

[46] Yin G, Lopes da Fonseca T, Eisbach SE, Anduaga AM, Breda C, Orcellet ML, et al. alpha-Synuclein interacts with the switch region of Rab8a in a Ser129 phosphorylation-dependent manner. Neurobiology of Disease. 2014;**70**:149-161. DOI: 10.1016/j.nbd.2014.06.018

[47] Zimprich A, Biskup S, Leitner P, Lichtner P, Farrer M, Lincoln S, et al. Mutations in LRRK2 cause autosomal-dominant parkinsonism with pleomorphic pathology. Neuron. 2004; **44**(4):601-607. DOI: 10.1016/j.neuron.2004.11.005

[48] Steger M, Diez F, Dhekne HS, Lis P, Nirujogi RS, Karayel O, et al. Systematic proteomic analysis of LRRK2-mediated Rab GTPase phosphorylation establishes a connection to ciliogenesis. eLife. 2017;**6**:1-22. DOI: 10.7554/eLife.31012

[49] Lis P, Burel S, Steger M, Mann M, Brown F, Diez F, et al. Development of phospho-specific Rab protein antibodies to monitor in vivo activity of the LRRK2 Parkinson's disease kinase. The Biochemical Journal. 2018;**475**(1):1-22. DOI: 10.1042/BCJ20170802

[50] Fan Y, Howden AJM, Sarhan AR, Lis P, Ito G, Martinez TN, et al. Interrogating Parkinson's disease LRRK2 kinase pathway activity by assessing Rab10 phosphorylation in human neutrophils. The Biochemical Journal. 2018;**475**(1):23-44. DOI: 10.1042/BCJ20170803

[51] Wisniewski KE, Wisniewski HM, Wen GY. Occurrence of neuropathological changes and dementia of Alzheimer's disease in Down's syndrome. Annals of Neurology. 1985;**17**(3):278-282. DOI: 10.1002/ana.410170310

[52] Nixon RA. Niemann-Pick type C disease and Alzheimer's disease: The APP-endosome connection fattens up. American Journal of Pathology. 2004;**164**(3):757-761. DOI: 10.1016/S0002-9440(10)63163-X

[53] Deng W, Wang Y, Gu L, Duan B, Cui J, Zhang Y, et al. MICAL1 controls cell invasive phenotype via regulating oxidative stress in breast cancer cells. BMC Cancer. 2016;**16**:489. DOI: 10.1186/s12885-016-2553-1

[54] Du J, Xu R, Hu Z, Tian Y, Zhu Y, Gu L, et al. PI3K and ERK-induced Rac1 activation mediates hypoxia-induced HIF-1alpha expression in MCF-7 breast cancer cells. PLoS One. 2011;**6**(9):e25213. DOI: 10.1371/journal.pone.0025213

[55] Wheeler DB, Zoncu R, Root DE, Sabatini DM, Sawyers CL. Identification of an oncogenic RAB protein. Science. 2015;**350**(6257):211-217. DOI: 10.1126/science.aaa4903

[56] Tyner JW, Erickson H, Deininger MW, Willis SG, Eide CA, Levine RL, et al. High-throughput sequencing screen reveals novel, transforming RAS mutations in myeloid leukemia patients. Blood. 2009;**113**(8):1749-1755. DOI: 10.1182/blood-2008-04-152157

[57] Janakiraman M, Vakiani E, Zeng Z, Pratilas CA, Taylor BS, Chitale D, et al. Genomic and biological characterization of exon 4 KRAS mutations in human cancer. Cancer Research. 2010;**70**(14):5901-5911. DOI: 10.1158/0008-5472.CAN-10-0192

[58] Duan B, Cui J, Sun S, Zheng J, Zhang Y, Ye B, et al. EGF-stimulated activation of Rab35 regulates RUSC2-GIT2 complex formation to stabilize GIT2 during directional lung cancer cell migration. Cancer Letters. 2016;**379**(1):70-83. DOI: 10.1016/j.canlet.2016.05.027

[59] Yu JA, Deakin NO, Turner CE. Paxillin-kinase-linker tyrosine phosphorylation regulates directional cell migration. Molecular Biology of the Cell. 2009;**20**(22):4706-4719. DOI: 10.1091/mbc.E09-07-0548

[60] Brass AL, Dykxhoorn DM, Benita Y, Yan N, Engelman A, Xavier RJ, et al. Identification of host proteins required for HIV infection through a functional genomic screen. Science. 2008;**319**(5865):921-926. DOI: 10.1126/science.1152725

[61] West KA, Zhang H, Brown MC, Nikolopoulos SN, Riedy MC, Horwitz AF, et al. The LD4 motif of paxillin regulates cell spreading and motility through an interaction with paxillin kinase linker (PKL). The Journal of Cell Biology. 2001;**154**(1):161-176

[62] Brodsky FM. Diversity of clathrin function: New tricks for an old protein. Annual Review of Cell and Developmental Biology. 2012;**28**:309-336. DOI: 10.1146/annurev-cellbio-101011-155716

[63] Yang CW, Hojer CD, Zhou M, Wu X, Wuster A, Lee WP, et al. Regulation of T cell receptor signaling by DENND1B in TH2 cells and allergic disease. Cell. 2016;**164**(1-2):141-155. DOI: 10.1016/j.cell.2015.11.052

[64] Valitutti S, Muller S, Cella M, Padovan E, Lanzavecchia A. Serial triggering of many T-cell receptors by a few peptide-MHC complexes. Nature. 1995;**375**(6527):148-151. DOI: 10.1038/375148a0

[65] Valitutti S, Muller S, Dessing M, Lanzavecchia A. Signal extinction and T cell repolarization in T helper cell-antigen-presenting cell conjugates. European Journal of Immunology. 1996;**26**(9):2012-2016. DOI: 10.1002/eji.1830260907

[66] Sleiman PM, Flory J, Imielinski M, Bradfield JP, Annaiah K, Willis-Owen SA, et al. Variants of DENND1B associated with asthma in children. The New England Journal of Medicine. 2010;**362**(1):36-44. DOI: 10.1056/NEJMoa0901867

[67] Chawes BL, Bischoff AL, Kreiner-Moller E, Buchvald F, Hakonarson H, Bisgaard H. DENND1B gene variants associate with elevated exhaled nitric oxide in healthy high-risk neonates. Pediatric Pulmonology. 2015;**50**(2):109-117. DOI: 10.1002/ppul.22958

[68] Verma K, Datta S. The monomeric GTPase Rab35 regulates phagocytic cup formation and phagosomal maturation in *Entamoeba histolytica*. The Journal of Biological Chemistry. 2017;**292**(12):4960-4975. DOI: 10.1074/jbc.M117.775007

[69] Gunther J, Shafir S, Bristow B, Sorvillo F. Short report: Amebiasis-related mortality among United States residents, 1990-2007. The American Journal of Tropical Medicine and Hygiene. 2011;**85**(6):1038-1040. DOI: 10.4269/ajtmh.2011.11-0288

[70] Orozco E, Guarneros G, Martinez-Palomo A, Sanchez T. *Entamoeba histolytica*. Phagocytosis as a virulence factor. The Journal of Experimental Medicine. 1983;**158**(5):1511-1521

[71] Ronald A. The etiology of urinary tract infection: Traditional and emerging pathogens. Disease-a-Month. 2003;**49**(2):71-82. DOI: 10.1067/mda.2003.8

[72] Dikshit N, Bist P, Fenlon SN, Pulloor NK, Chua CE, Scidmore MA, et al. Intracellular uropathogenic *E. coli* exploits host Rab35 for iron acquisition and survival within urinary bladder cells. PLoS Pathogens. 2015;**11**(8):e1005083. DOI: 10.1371/journal.ppat.1005083

[73] Trachtman H. HUS and TTP in children. Pediatric Clinics of North America. 2013;**60**(6):1513-1526. DOI: 10.1016/j.pcl.2013.08.007

[74] Hartland EL, Leong JM. Enteropathogenic and enterohemorrhagic *E. coli*: Ecology, pathogenesis, and evolution. Frontiers in Cellular and Infection Microbiology. 2013;**3**:15. DOI: 10.3389/fcimb.2013.00015

[75] Wong AR, Pearson JS, Bright MD, Munera D, Robinson KS, Lee SF, et al. Enteropathogenic and enterohaemorrhagic *Escherichia coli*: Even more subversive elements. Molecular Microbiology. 2011;**80**(6):1420-1438. DOI: 10.1111/j.1365-2958.2011.07661.x

[76] Clements A, Stoneham CA, Furniss RC, Frankel G. Enterohaemorrhagic *Escherichia coli* inhibits recycling endosome function and trafficking of surface receptors. Cellular Microbiology. 2014;**16**(11):1693-1705. DOI: 10.1111/cmi.12319

[77] Dong N, Zhu Y, Lu Q, Hu L, Zheng Y, Shao F. Structurally distinct bacterial TBC-like GAPs link Arf GTPase to Rab1 inactivation to counteract host defenses. Cell. 2012;**150**(5): 1029-1041. DOI: 10.1016/j.cell.2012.06.050

[78] Furniss RC, Slater S, Frankel G, Clements A. Enterohaemorrhagic *E. coli* modulates an ARF6:Rab35 signaling axis to prevent recycling endosome maturation during infection. Journal of Molecular Biology. 2016;**428**(17):3399-3407. DOI: 10.1016/j.jmb.2016.05.023

[79] Viasus D, Di Yacovo S, Garcia-Vidal C, Verdaguer R, Manresa F, Dorca J, et al. Community-acquired *Legionella pneumophila* pneumonia: A single-center experience with 214 hospitalized sporadic cases over 15 years. Medicine (Baltimore). 2013;**92**(1):51-60. DOI: 10.1097/MD.0b013e31827f6104

[80] Ingmundson A, Delprato A, Lambright DG, Roy CR. Legionella pneumophila proteins that regulate Rab1 membrane cycling. Nature. 2007;**450**(7168):365-369. DOI: 10.1038/nature06336

[81] Mihai Gazdag E, Streller A, Haneburger I, Hilbi H, Vetter IR, Goody RS, et al. Mechanism of Rab1b deactivation by the *Legionella pneumophila* GAP LepB. EMBO Reports. 2013;**14**(2): 199-205. DOI: 10.1038/embor.2012.211

[82] Mukherjee S, Liu X, Arasaki K, McDonough J, Galan JE, Roy CR. Modulation of Rab GTPase function by a protein phosphocholine transferase. Nature. 2011;**477**(7362): 103-106. DOI: 10.1038/nature10335

[83] Allgood SC, Romero Duenas BP, Noll RR, Pike C, Lein S, Neunuebel MR. Legionella effector AnkX disrupts host cell endocytic recycling in a phosphocholination-dependent manner. Frontiers in Cellular and Infection Microbiology. 2017;**7**:397. DOI: 10.3389/fcimb.2017.00397

[84] Goody PR, Heller K, Oesterlin LK, Muller MP, Itzen A, Goody RS. Reversible phosphocholination of Rab proteins by legionella pneumophila effector proteins. The EMBO Journal. 2012;**31**(7):1774-1784. DOI: 10.1038/emboj.2012.16

[85] Pan X, Luhrmann A, Satoh A, Laskowski-Arce MA, Roy CR. Ankyrin repeat proteins comprise a diverse family of bacterial type IV effectors. Science. 2008;**320**(5883):1651-1654. DOI: 10.1126/science.1158160

[86] Abrami L, Bischofberger M, Kunz B, Groux R, van der Goot FG. Endocytosis of the anthrax toxin is mediated by clathrin, actin and unconventional adaptors. PLoS Pathogens. 2010; **6**(3):e1000792. DOI: 10.1371/journal.ppat.1000792

[87] Raposo G, Stoorvogel W. Extracellular vesicles: Exosomes, microvesicles, and friends. The Journal of Cell Biology. 2013;**200**(4):373-383. DOI: 10.1083/jcb.201211138

Chapter 5

Aberrant SGK1 Transcription in LNCaP: A Novel Feedback Mechanism of TGF-beta1 Regulation in Prostate Carcinogenesis

Ximena Leighton, Harvey B. Pollard and Meera Srivastava

Additional information is available at the end of the chapter

http://dx.doi.org/10.5772/intechopen.75165

Abstract

SGK1, a serum- and glucocorticoid-inducible kinase implicated in cancer, is regulated by TGF-beta1 and PI3-kinase. In a comparative study of different benign and cancerous breast and prostate cells, we demonstrate in this study that exon 11 deletion in SGK1 occurs only in LNCaP prostate cancer cells in association with the deficient TGF-beta1 mRNA message and FOXO3A-driven promoter activity. Using protein modeling approaches, we discovered that exon11 deletion in SGK1 could redistribute electrostatic surface potential around the major kinase domain and affect phosphorylation of SGK1 target proteins including FOXO3A. Concordantly, we found that LNCaP cells displayed FOXO3A hyperphosphorylation at the Ser218/321 (a site next to Ser315 with the marked SGK1 preference) along with changes in gene expression profile of TGF-beta relevant regulators (such as SMAD2/4, MAD4 and SKIP). Oncomine-interactome analysis further validated a possibility of reciprocal TGF-beta1 regulation by its transcriptional target SGK1 through alterations in FOXO/SMAD and steroid hormone nuclear receptor interactions.

Keywords: SGK1, TGF-beta1, FOXO-SMAD, LNCaP, prostate cancer

1. Introduction

SGK1 plays a major role in carcinogenesis in association with FOXO3A (or FKHRL1), p53 and GR [1–3]. Since TGF-beta1 is turned on by cancer cells from a tumor suppressor into a mediator of metastasis [4], its transcriptional target SGK1 can contribute to pleiotropic TGF-beta actions in homeostasis and carcinogenesis [5]. Glucocorticoid (GC) control of

SGK1 can provide more clues to dual TGF-beta1 effects on the coregulation by endogenous steroids on cell growth. Furthermore, serum and glucocorticoid (GC)-inducible SGK1 regulates ion channel conductance, cell cycling, and apoptosis. Additionally, SGK1 enzymatic activity is also regulated by PI3-kinase [6], and the PI3K/Akt/mTOR cascade is known to be involved in TGF-beta1 resistance in cancer [7]. SGK1 downregulation was identified in prostate carcinogenesis with its mRNA levels specifically reduced in hormone-refractory carcinomas [8, 9]. In the current study, we first examined TGF-beta1 and SGK1 mRNA message and gene expression in benign and cancerous breast and prostate cells differing in their hormone sensitivity. Aberrant SGK1 transcription (Δexon11) in LNCaP prostate cancer cells coincided with alterations in TGF-beta1 mRNA message and FOXO3A-driven promoter activity indicating a possible feedback regulation of TGF-beta1 by SGK1. Our protein simulation studies (DeepView/Swiss-PdbViewer) suggested that the defective translation in the Δexon11-SGK1 could affect its kinase domain and thereby phosphorylation of target proteins including a major TGF-beta1 transcriptional regulator FOXO3A. Consequently, we demonstrated FOXO3A hyperphosphorylation in LNCaP, which suggested FOXO3A deficient transcriptional activity that was concordant to altered gene expression in the FOXO-SMAD and other components of TGF-beta signaling. Analysis of TGF-beta1-SGK1 reciprocal regulatory circuits (Oncomine) suggested possible coregulation of TGF-beta1 by its downstream SGK1 linking FOXO-SMAD to nuclear steroid receptors (AR and GR).

2. Materials and methods

2.1. Cell cultures

Benign as well as cancerous breast and prostate cells (ATCC, Manassas, VA) were routinely grown in media (184B5—MEGM, PrEC—PrEGM; LNCaP—RPMI1640; PC3—F12 K; DU145, MCF7 and MDA-MB-231—MEM; MDA-MB-435—50%DMEM+50%F12) containing FBS and antibiotics (Invitrogen, Carlsbad, CA; Cambrex, East Rutherford, NJ). RNA was extracted (RNAqueous-4 PCR Kit, Ambion, Austin, TX) from confluent cells and used (2 μg) for reverse transcription reactions (SuperScript First-Strand Synthesis System for RT-PCR, Invitrogen, Carlsbad, CA).

2.2. Multiplex PCR and sequencing

Multiplex PCR was performed using following primers for TGF-beta1 (forward—5′-GCCCTGGACACCAACTATTGC-3′ and reverse—5′-GCTGCACTTGCAGGAGCGCAC-3′), SGK1 (forward—5′-CTCCTGCAGAAGGACAGGA-3′ and reverse—5′-GGACAGGCTCTTCGGTAAACT-3′) and beta-actin (forward—5′-CTGGCCGGGACCTGACTGACTACCTC-3′ and reverse—5′-AAACAAATAAAGCCATGCCAATCTCA-3′, ratio to other primers 1:10).

Following TGF-beta1 primers were used to amplify almost entire coding region (1250 bp) or its 3′-fragment (499 bp): forward 5′-AGGCCCTCCTACCTTTTGC-3′ or 5′ ATTGAGGGCTTT CGCCTTAG-3′ with reverse 5′-ACAGCTGCTCCACCTTGG-3′. Both fragments from DU145 control were successfully amplified using 1ul of 0.1× cDNA, whereas amplification with 1ul cDNA from LNCaP produced only the smaller fragment.

http://dx.doi.org/10.5772/intechopen.75165

Sequencing was verified for the SGK1 amplicon with expected size (193 bp) and identified a missing exon11 (90 bp) in the extra amplicon from LNCaP. Amplification and sequencing of full-length SGK1 (~1.4 kbp; primers: forward—5′-TTTGAGCGCTAACGTCTTTCTGT-3′ and reverse—5′-TTGCTAAGCTTCCAGAGATGTGC-3′; *data not shown*) from DU145 and LNCaP confirmed a single exon11 deletion in the apparently smaller amplicon in LNCaP that could cause a lack of following protein sequence: MEIKSHVFFSLINWDDLINKKITPPFNPNV.

2.3. TGF-beta1 promoter analysis

TGF-beta1 promoter (~2400 bp) inspection by the Genomatix software (GmbH, Munich, Germany) identified a single FOXO3A-specific regulatory element (V$FKHRL1.01, core and matrix similarity ~1; within the -350–450) as well as numerous elements with possible modifying effects on TGF-beta transcription (upstream ~600 bp). TGF-beta1 promoter activities were assessed in different cells (MDA-MB-435—N/A) using Firefly Luciferase Reporter System (Promega, Madison, WI) and presented as normalized ratios from quadruple measurements. pGL3-Basic Vector lacking eukaryotic promoter and enhancer sequence was used to insert functional promoters containing first 5 '-UTR nucleotides (ACCTCCCCTCCG) in exon1 in addition to the -323, -453 or -1132 sequences in TGF-beta1 promoter.

2.4. Protein modeling

Using the DeepView/Swiss-PdbViewer, v3.7 software developed at GlaxoSmithKline and available for download through public access at Expasy (http://www.expasy.org/spdbv), we simulated C-terminal SGK1 protein based on a crystallographic model of Rac-beta protein kinase (Kinase Domain 146–460, PDB: 1gzk). According to aminoacid composition, a homologous structure was successfully assigned to SGK1 (UniProtKB/SwissProt Entry: O00141) and C-terminal SGK1 fragment (102–372) was correctly "threaded" on a structural template of the Ser/Thr Rac-beta kinase. In order to complete SGK1 C-terminal (102–376) protein modeling with low threading energy levels, we fixed side chains of some aminoacids with possible clashes and built four 3'end-exon11 SGK1 residues (the NPNV fragment did not have corresponding residues in a structural template). Based on the simulated wt-SGK1, we created a Δexon11-SGK1 (102–346) model that lacked 30 3'end-residues (M347-V376) corresponding to the deleted exon11. In order to predict possible structural effects of the Δexon11 in SGK1 protein, surface (including internal cavities) and electrostatic potential were computed using the DeepView/Swiss-PdbViewer software. In addition, SGK1 nucleotide and protein analysis were performed using databases such as Entrez, Ensembl and Expasy Tools.

2.5. cDNA microarray analysis

cDNA microarray analysis of prostate cancer cells was performed using Atlas Human Cancer 1.2 arrays and the corresponding software AtlasImage 2.01 (Clontech, Palo Arto, CA). Gene expression in two compared arrays was assessed using the ratios of adjusted intensities after subtraction of external background and global normalization based on sum method (signal difference threshold >4000; ratio threshold $R > 2$: upregulation—$R > 2$; downregulation—$R < 0.5$).

2.6. Western blotting

Lysates from LNCaP and DU145 were concentrated by TCA, precipitated and equivalently loaded on polyacrylamide SDS gel (*entire image, left*), then transferred to nitrocellulose membranes for Western Immunoblotting (*enlarged fragment, middle)* with the 1:1000 dilution of Phospho-FOX03A (Ser318/321) antibody (Cell Signaling Technology, Danvers, MA).

3. Results

3.1. In LNCaP prostate cancer cells, aberrant SGK1 transcription was associated with altered TGF-beta1 message and promoter activity

To evaluate the relationship between TGF-beta1 and its transcriptional target SGK1 in prostate and breast cancer cells, we examined their gene expression. Benign prostate (PrEC) and breast (184B5) cells displayed expectedly high TGF-beta1 and low SGK1 gene expression that was maintained in most cancer cells (**Figure 1A**). Among the tested benign and cancerous prostate

Figure 1. SGK1 transcription in association with TGF-beta1 message. (A) Multiplex PCR was performed using primers for TGF-beta1 and SGK1 as described under "materials and methods." (B) sequencing verified that the SGK1 amplicon with expected size (193 bp) was missing exon11 (90 bp) in the amplicon from LNCaP.

(LNCaP, DU145, and PC3) and breast (MCF7, MDA-MB-231, and -435) cells, LNCaP was the only cell line with the almost undetectable TGF-beta1, which coincided with an additional aberrant Δ-exon11-SGK1 transcript of 90 kb (**Figure 1A**). Unlike similar profiles of transcription in breast and prostate cells, mRNA message of SGK1 in the LNCaP prostate cancer cells displayed a double-band for full-length SGK1 cDNA, thereby validating a slightly smaller size of the extra-*SGK1*-transcript. SGK1 amplicon with the expected size (193 bp) and the identified missing exon11 (90 bp) in the extra amplicon from LNCaP were verified by sequencing (**Figure 1B**). Identification of the two PCR amplicons of SGK1 in the LNCaP cells suggests the presence of a heterozygous mutation in genomic DNA that apparently results in an alternative splicing of the SGK1 mRNA.

We analyzed TGF-beta1 promoter (~2400 bp) by the Genomatix software (GmbH, Munich, Germany) and identified a single FOXO3A-specific regulatory element (V$FKHRL1.01, core and matrix similarity ~1; within the -350–450) as well as numerous elements with possible modifying effects on TGF-beta transcription (upstream ~600 bp). Therefore, TGF-beta1 promoter activities were assessed in different cells using the Firefly Luciferase Reporter System (Promega, Madison, WI) and presented as normalized ratios from quadruple measurements. TGF-beta1 promoter activity analysis (**Figure 2A**) identified hormone-sensitive LNCaP as prostate cells with the lowest average activity (~50% compared to the rest). Similarly, hormone-sensitive MCF7 cells had the lowest TGF-beta1 promoter activity among breast cells. Drastically enhanced promoter activity in the -453-fragments compared to -323 in MDA-MB-231 cells in comparison with MCF7 cells can be attributed to the FOXO3A (Genomatix) elements contributing to their hormone-sensitive functionality. Further extension of the promoter fragment (-1132) suggested cell-specific TGF-beta1 transcriptional modulation by auxiliary regulatory elements including SMAD-interacting (FAST-1/FoxH3) and TGF-beta inducible (TIEG/EGR-alpha) proteins as well as Myc/MAX and GR. Remarkably, the FOXO3A-enhanced -453-promoter activity was annulled in the -1132-fragment in the androgen-sensitive LNCaP cells, while the estrogen-sensitive MCF7 breast cancer cells maintained similar TGF-beta1 promoter activity in both fragments. Previous studies have shown that SGK1 co-mediated FOXO3a inactivation [10] contributes to the TGF-beta1-mediated cell survival.

In our further study on the TGF-beta1 message (**Figure 2B**) in LNCaP versus DU145 (two prostate cell lines with most similar TGF-beta1 promoter activity profiles), LNCaP lacked complete TGF-beta1 mRNA but possessed a message which could translate the active form of TGF-beta1 with the 5′-end of its latency-associated peptide responsible for the cell attachment. These results suggested that along with alternative splicing, mRNA processing and stability can be affected by the 5′-UTR sequences (absent in previous amplification, **Figure 1A**) modifying autocrine TGF-beta1 regulation. However, deficient TGF-beta1 message could affect folding and cleavage of the mature TGF-beta-1 in LNCaP, while the remaining latency-associated peptide portion could render it inactive. Consistent with suggested hormonal regulation of TGF-beta1 transcription, TGF-beta mRNA presence and secretion have been previously shown in both androgen-resistant DU145 and PC3, but not in LNCaP [11] where TGF-beta insensitivity was associated with promoter methylation of its cognate receptors [12]. However, LNCaP could secrete active TGF-beta in response to estrogen or androgen [13].

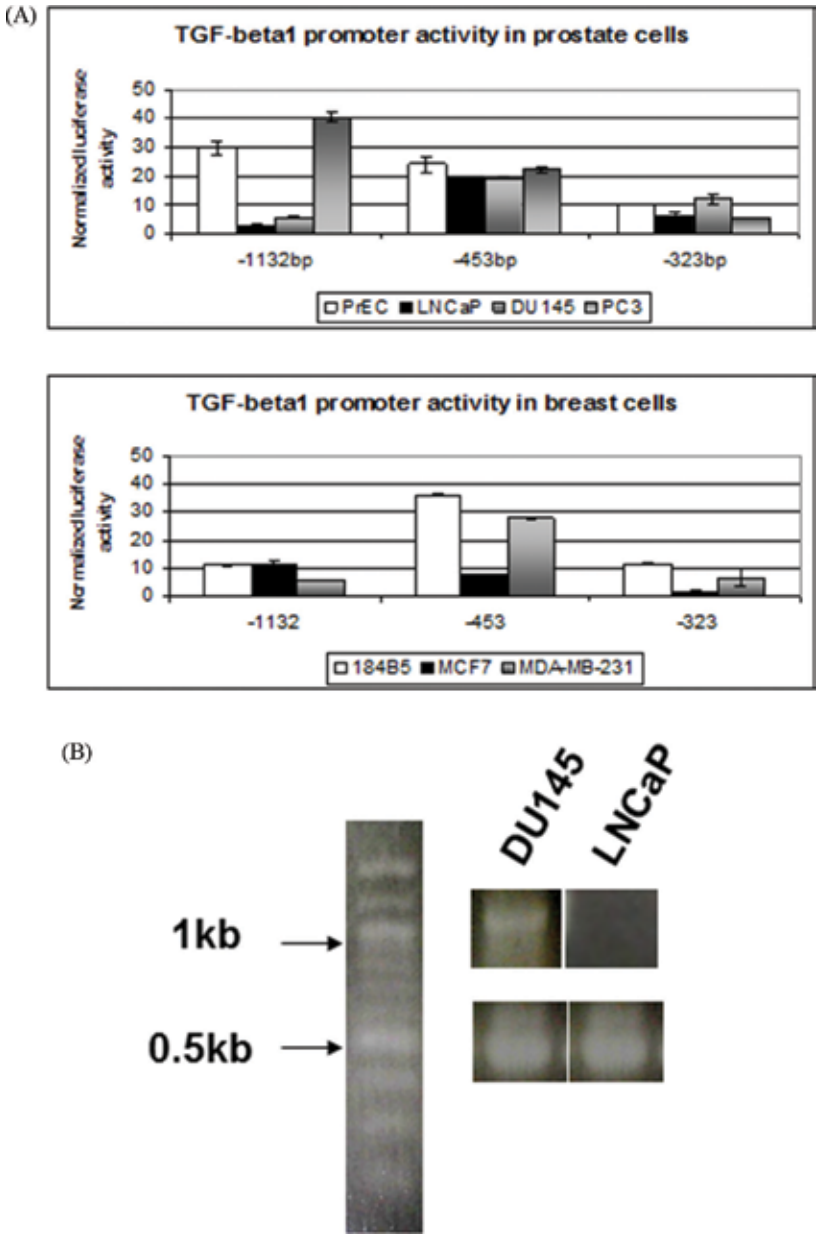

Figure 2. (A) TGF-beta1 promoter activities in prostate and breast cancer cells. TGF-beta1 promoter activities were assessed in different cells using different truncated promoter plasmids as described under "Materials and Methods" and Firefly Luciferase Reporter System (Promega, Madison, WI) and presented as normalized ratios from quadruple measurements. (B) TGF-beta1 cDNA transcripts in DU145 and LNCaP cells. TGF-beta1 primers were used to amplify almost entire coding region (1250 bp) or its 3′-fragment (499 bp) as described under "Materials and Methods." Both fragments from DU145 control (as well as PrEC and PC3, *not shown*) were successfully amplified using 1ul of 0.1× cDNA, whereas amplification with 1ul cDNA from LNCaP produced only the smaller fragment.

3.2. Identified SGK1 exon11 deletion could affect major kinase domain responsible for the phosphorylation of SGK1 target proteins

To our knowledge, this is a first report for alternative transcription of human SGK1 presented by a single transcript (Ensemble: ENSP00000237305) and having effect on TGF-beta. Based on peptide analysis (ExpasyTools), a loss of the 90-bp spanning exon11 is not likely to affect drastically the average MW (reduction only by ~7%) or pI (~8.7 for both). Although none of reported SNPs or mutations implicated the exon11 loss, its missing residues (347–376) in SGK1 protein are included in major Protein Kinase (98–355) or Protein Kinase C (375–427) domains associated with the key phosphorylation function of SGK1 as a Ser/Thr kinase. Defined central SGK1 domain (83–355) included catalytic domain, nuclear localization signal and the PY-domain involved in NEDD4–2 binding [1]. Using DeepView/Swiss-PdbViewer, we simulated both wt- and Δ-SGK1 C-terminals (**Figure 3**). As expected, external area or volume (decrease by 9 and 11%, respectively) as well as disposition and size of internal cavities (images on the left) did not change essentially in the Δ-SGK1 model. However, exon11 deletion reshaped protein surface (*images in the middle*) and redistributed electrostatic potential (images on the right) around the major kinase domain. These changes could influence protein binding and phosphorylation of SGK target proteins (such as FOXO3A and NEDD4–2 involved in the TGF-beta1, GCs or nutrient starvation responses) as well as SGK1 transport between cytoplasm and the nucleus.

3.3. SGK1 aberrant transcription and predicted kinase domain alterations were associated with the increased FOXO3A phosphorylation in LNCaP

As a direct target of SGK1, FOXO3A is phosphorylated in response to PI3K signaling [14]. Unlike two sites (Thr32 and Ser253) in FOXO3A which are catalyzed more effectively by Akt/PKB and are required for FOXO3A binding to 14–3-3 proteins, the Ser315 site next to the nuclear export signal is favored by SGK, which has a primary role in exporting FOXO3A from the nucleus. Consistently, FOXO3A in LNCaP was more phosphorylated at the adjacent Ser318/321 site (**Figure 4**) even when compared to DU145 cells with the most similar reduction profile of TGF-beta1 promoter activity.

3.4. TGF-beta1-specific synexpression profile and interactome associated with aberrant SGK1 and TGF-beta1 mRNA messages in LNCaP

cDNA microarray analysis revealed a distinct TGF-beta1 relevant synexpression pattern in LNCaP as compared to DU145 (**Figure 5**). Most importantly, two major TGF-beta relevant transcriptional regulator SMADs (2 and 4) were greatly reduced in LNCaP consistent with the "logic of TGF-beta signaling" [4] and ability of the SMAD2-lacking cells to escape TGF-beta-mediated growth inhibition [15].

On the other hand, the TGF-beta1 target MAD4 that is upregulated in LNCaP could switch cell growth regulation to Myc pathway [16]. The SMAD3-binding Myc-regulator NOTCH1 [17, 18]

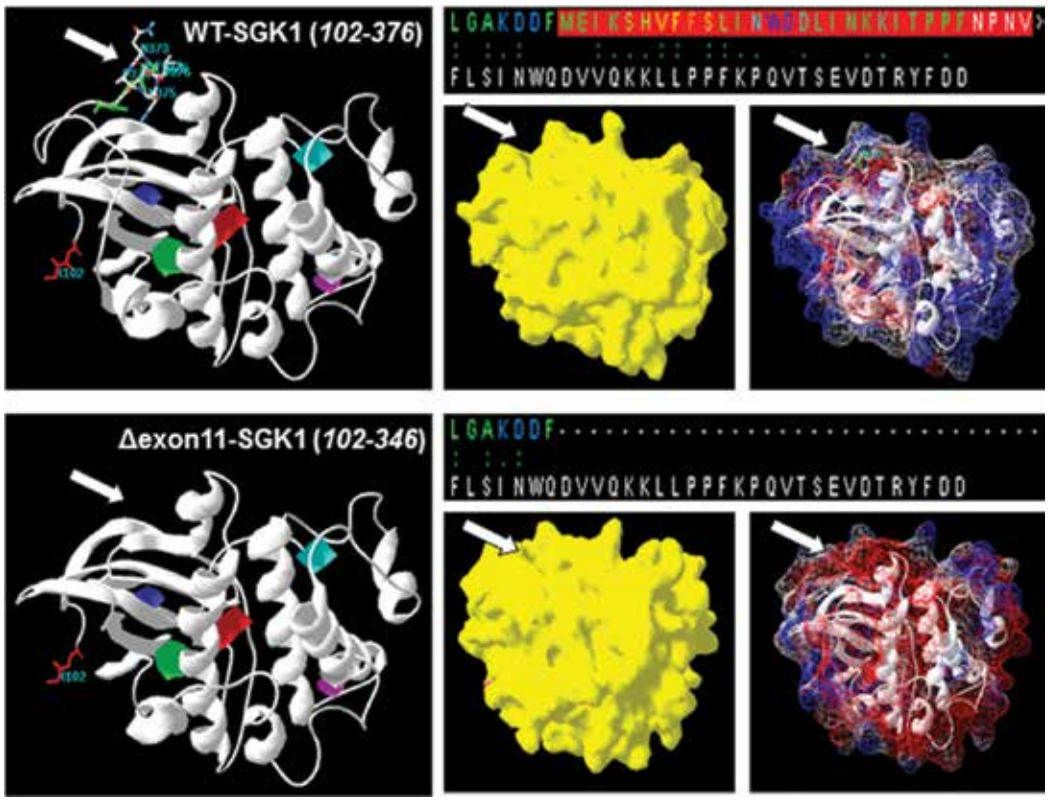

Figure 3. Protein modeling of wt- and Δ-SGK1 C-terminal. In both wt-SGK1 (*top*) and Δ-SGK1 (*bottom*), sequences are colored by threading energy (upper line) except added NPNV residues in the wt-SGK1 (in white). Exon11 residues are highlighted in red in the wt-SGK1 and presented by dots in the Δ-SGK1. Structural template sequences in both models are in white (lower line). In both models, left images represent ribbon structure (in white) with labeled end-residues and internal cavities (in color); middle images—External surface (yellow filled triangles) and right images—The electrostatic potential computed by coulomb method using partial atomic charges (dotted lines, dark red—−1.800 and dark blue—1.800). C-terminals are viewed from the same position with the designated areas corresponding to exon11 (white arrows).

was overexpressed, while two Myc-relevant stress response mediators (GADD-45 and -153) were downregulated in LNCaP cells (data not shown). Intriguingly, spliceosomal component and transcriptional coregulator SNW/SKIP, which activate the SMAD2/3 activity [19], were underexpressed in the LNCaP cells and increased in DU145 pointing to a differential hormonal regulation with aberrantly transcribed SGK1 and TGF-beta1 and reduced SMAD. Gene expression of TGF-beta1 and SGK1 (represented by short downstream 3'UTR fragments) did not change as much accentuating the causative role of alternative RNA processing.

TGF-beta1 and SGK1 interactome (**Figure 6**) substantiated a possible feedback regulation of TGF-beta1 by its transcriptional target SGK1. Alterations in the FOXO3A phosphorylation and following FOXO/SMAD signaling could involve nuclear hormone receptors (GR, AR) and ubiquitination targeting components (UBL1, UBE2L3, UBE2E1) indicating links to steroids and autophagy in the TGF-beta-regulated cell death/proliferation. Consistently, in LNCaP

http://dx.doi.org/10.5772/intechopen.75165

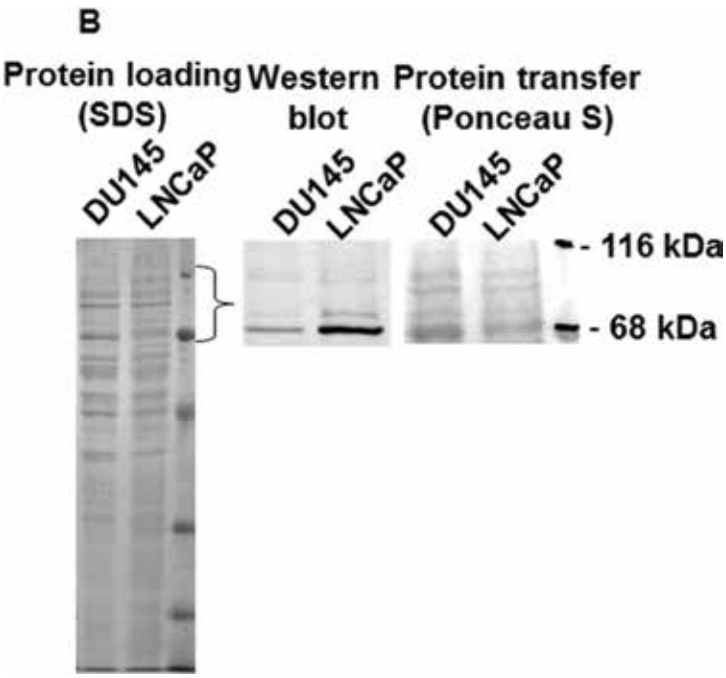

Figure 4. FOXO3A phosphorylation in LNCaP versus DU145. Lysates from LNCaP and DU145 were loaded onto polyacrylamide SDS gel and subjected to immunoblotting (*enlarged fragment, middle)* with the 1:1000 dilution of Phospho-FOX03A (Ser318/321) antibody (Cell Signaling Technology, Danvers, MA). Specific bands with expected size (~97 kDa) were found in the 68–116 kDa gel fragment. Ponceau S staining (*enlarged fragment, right*) marked the standards.

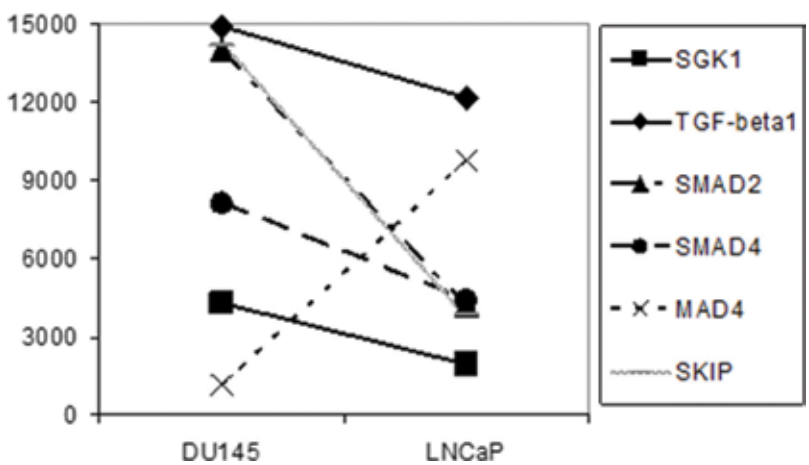

Figure 5. cDNA microarray analysis of prostate cancer cells showing TGF-beta1-relevant synexpression. cDNA microarray analysis of prostate cancer cells was performed using Atlas Human Cancer 1.2 arrays and the corresponding software AtlasImage 2.01 (Clontech, Palo Arto, CA). Gene expression in two compared arrays was assessed using the ratios of adjusted intensities after subtraction of external background and global normalization based on sum method (signal difference threshold >4000; ratio threshold R > 2; upregulation—R > 2; downregulation—R < 0.5). Graphic presentation of adjusted intensities for several listed genes is shown.

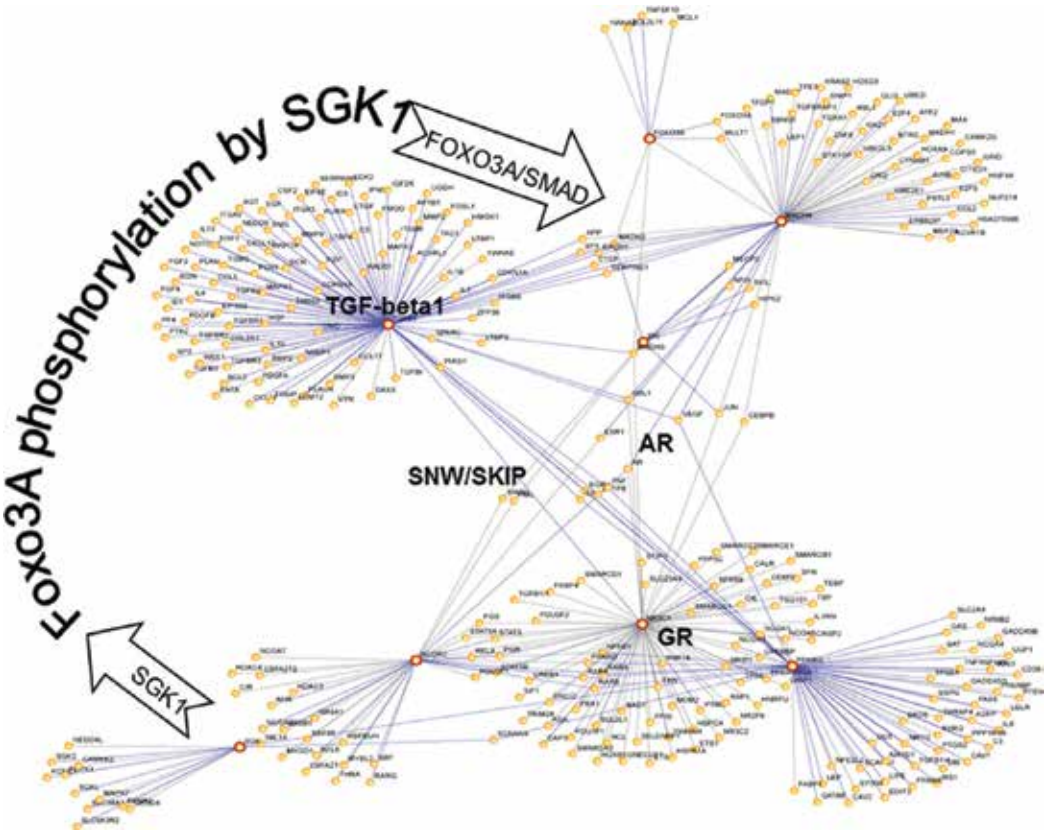

Figure 6. Putative feedback regulation of TGF-beta1 by its transcriptional target SGK1. TGF-beta1 and SGK1 Interactome was created using the Oncomine (http://www.oncomine.org), which represents physically interacting proteins based on the Human Protein Reference Database.

cells with the disturbed PI3K/Akt pathway, the AR-mediated mTOR activation induced cell proliferation, while the serum-induced SGK1 represented modulation of nutrient availability [20]. Our recent studies on cytotoxicity and cell death/proliferation in response to tumor suppressor p53 and ANXA7 suggested deficient PCD-type2 in LNCaP (data not shown).

At last, the spliceosomal regulator SNW/SKIP which mediates TGF-beta, NOTCH, Rb and nuclear hormone receptor signaling [19] may link defective TGF-beta pathway components including FOXO/SMAD to the AR- and GR-dependent alternative splicing in SGK1 and TGF-beta1 RNA in the hormone-sensitive LNCaP.

4. Discussions

Our observations on TGF-beta1 and SGK1 pathways in LNCaP are in line with previously reported evidence that SGK1 altered negative control of FOXO-dependent transcription by Akt/PKB [4]. SGK1 could contribute to the PI3K/Akt and AR controlled cell growth in LNCaP

where constitutive PI3K/Akt activation has been ascribed to phosphatidylinositol-phosphatase PTEN deficiency [21]. Reduced expression and hyperphosphorylation of FOXO3A in progression of LNCaP cells to androgen independence [22] could be also associated with the steroid-regulated SGK1. Correspondent to that, androgen-sensitive and GR-negative LNCaP lacked GC-induced cell growth inhibition unlike the androgen-resistant and GR-expressing prostate cancer cells in which GC could induce TGF-beta1 mRNA [23, 24]. Differential dexamethasone response in LNCaP versus DU145 and PC3 is consistent with the distinct TGF-beta1 and SGK1 mRNA message patterns found in this study. In prostate carcinogenesis, AR and TGF-beta1 interactions were implicated [25], and AR can inhibit TGF-beta-relevant transcription through SMAD3 [26]. Therefore, LNCaP cells could have a shift toward the AR-dominating TGF-beta1 cell survival control where pathological GC-responses could involve SGK1 and GR-mediated FOXO3A inactivation [10].

Another SGK1 target, NEDD4–2 can negatively regulate TGF-beta signaling through the ubiquitin-mediated degradation of SMAD2 and TGF-beta-RI [27], which has intrinsic serine/threonine kinase activity and can stimulate phosphorylation of SMADs [4]. LNCaP cells are defective for conventional TGF-beta-RI (which is not required for TGF-beta1 signaling) but overexpress the TGF-beta-RII in response to dihydrotestosterone [28] that restores cell growth inhibition by TGF-beta1 [29].

Structural changes in SGK1 (which is responsible for phosphorylation in response to various factors including GCs, TGF-beta1 and nutrient starvation) may cause downstream alterations associated with specific target proteins. SGK1 is involved in the cross-talk among FKHRL1 (or FOXO3a), p53 and GR [3, 30] as well as activation of various channels and transporters through the ubiquitin ligase Nedd4–2 [31]. Therefore, suggested electrostatic charge redistribution around a major kinase domain in the Δexon11-SGK1 could affect phosphorylation of the SGK1-related proteins indicating potential targets in a defective response to endogenous steroids with following cell growth imbalance in cancer. Moreover, identified aberrant SGK1 transcription may contribute to prostate carcinogenesis by affecting a reciprocal regulation of TGF-beta by GCs that could uncover a major dysfunction in the homeostatic cell growth control.

5. Conclusions

In summary, LNCaP alternative SGK1 transcription identified in this study may represent a feedback modulation in the TGF-beta1 pathway. Affecting TGF-beta1 signaling by controlling FOXO3A phosphorylation and thereby—nuclear transport and transcriptional activity, SGK1 may uncover cell growth control mechanisms that are lost in cancer. Further studies on the reciprocal TGF-beta-SGK1 associations can elucidate bimodal character of TGF-beta1 responses in the GC and sex hormone coregulated cell death/proliferation in homeostasis and carcinogenesis.

Acknowledgements

This work was supported by the grant DAMD17-03-1-0107 (DOD).

Author details

Ximena Leighton, Harvey B. Pollard and Meera Srivastava*

*Address all correspondence to: msrivastava@usuhs.mil

Department of Anatomy, Physiology and Genetics, Institute for Molecular Medicine, Uniformed Services University of Health Sciences (USUHS), School of Medicine, Bethesda, MD, United States

References

[1] Firestone GL, Giampaolo JR, O'Keeffe BA. Stimulus-dependent regulation of SGK transcription, subcellular localization and enzymatic activity. Cellular Physiology and Biochemistry. 2003;**13**:1-12

[2] Shelly C, Herrera R. Activation of SGK1 by HGF, Rac1 and integrin-mediated cell adhesion in MDCK cells: PI-3K-dependent and -independent pathways. Journal of Cell Science. 2002;**115**:1985-1993

[3] You H, Jang Y, You-Ten AI, Okada H, Liepa J, Wakeham A, et al. p53-Dependent inhibition of FKHRL1 in response to DNA damage through protein kinase SGK1. Proceedings of the National Academy of Sciences of the United States of America. 2004;**101**:14057-14062

[4] Massague J, Gomis RR. The logic of TGFbeta signaling. FEBS Letters. 2006;**580**:2811-2820

[5] Waldegger S, Klingel K, Barth P, Sauter M, Rfer ML, Kandolf R, et al. h-SGK serine-threonine protein kinase gene as transcriptional target of TGF-beta in human intestine. Gastroenterology 1999;**116**:1081-1088

[6] Alliston TN, Gonzalez-Robayna IJ, Buse P, Firestone GL, Richards JS. Expression and localization of SGK in the rat ovary: Relation to follicular growth and differentiation. Endocrinology. 2000;**141**:385-395

[7] Van der Poel HG. Mammalian target of rapamycin and 3-phosphatidylinositol 3-kinase pathway inhibition enhances growth inhibition of transforming growth factor-beta1 in prostate cancer cells. The Journal of Urology. 2004;**172**:1333-1337

[8] Mikosz CA, Brickley DR, Sharkey MS, Moran TW, Conzen SD. Glucocorticoid receptor-mediated protection from apoptosis is associated with induction of the serine/threonine survival kinase gene. The Journal of Biological Chemistry. 2001;**276**:16649-16654

[9] Rauhala HE, Porkka KP, Tolonen TT, Martikainen PM, Tammela TL, Visakorpi T. Dual-specificity phosphatase 1 and serum/glucocorticoid-regulated kinase are downregulated in prostate cancer. International Journal of Cancer. 2005;**117**:738-745

[10] Wu W, Zou M, Brickley DR, Pew T, Conzen SD. Glucocorticoid receptor activation signals through forkhead transcription factor 3a in breast cancer cells. Molecular Endocrinology. 2006;**20**:2304-2314

[11] Wilding G, Zugmeier G, Knabbe C, Flanders K, Gelmann E. Differential effects of TGF beta on human prostate cancer cells in vitro. Molecular and Cellular Endocrinology. 1989;**62**:79-87

[12] Zhang L, Cui R, Cheng X, Du J. Antiapoptotic effect of SGK is mediated by novel mechanism activating I-kappa-B kinase. Cancer Research. 2005;**65**:457-464

[13] Blanchere M, Saunier E, Mestayer C, Broshuis M, Mowszowicz I. Alterations of expression and regulation of TGF-beta in human cancer prostate cell lines. The Journal of Steroid Biochemistry and Molecular Biology. 2002;**82**:297-304

[14] Brunet A, Park J, Tran H, Hu LS, Hemmings BA, Greenberg ME. Protein kinase SGK mediates survival signals by phosphorylating the forkhead transcription factor FKHRL1 (FOXO3a). Molecular and Cellular Biology. 2001;**21**:952-965

[15] Nakao A, Roijer E, Imamura T, Souchelnytskyi S, Stenman G, Heldin CH. Identification of Smad2, a human mad-related protein in the transforming growth factor beta signaling pathway. The Journal of Biological Chemistry. 1997;**272**:2896-2900

[16] Satterwhite DJ, White RL, Aakre ME Moses HL. TGF-beta1 regulates the expression of multiple max-interacting transcription factors in Balb/MK cells: Implications for understanding the mechanism of action of TGF-beta1. Pediatric Research. 2001;**50**:67-75

[17] Blokzijl A, Dahlqvist C, Reissmann E, Falk A, Moliner A, Lendahl U, et al. Cross-talk between the Notch and TGF-beta signaling pathways mediated by interaction of the Notch intracellular domain with Smad3. The Journal of Cell Biology. 2003;**163**:723-728

[18] Palomero T, Lim WK, Odom DT, Sulis ML, Real PJ, Margolin A, et al. NOTCH1 directly regulates c-MYC and activates a feed-forward-loop transcriptional network promoting leukemic cell growth. Proceedings of the National Academy of Sciences of the United States of America. 2006;**103**:18261-18266

[19] Folk P, Puta F, Skruzny M. Transcriptional coregulator SNW/SKIP: The concealed tie of dissimilar pathways. Cellular and Molecular Life Sciences. 2004;**61**:629-640 (Review)

[20] Xu Y, Chen SY, Ross KN, Balk SP. Androgens induce prostate cancer cell proliferation through mammalian target of rapamycin activation and post-transcriptional increases in cyclin D proteins. Cancer Research. 2006;**66**:7783-7792

[21] Yang L, Xie S, Jamaluddin MS, Altuwaijri S, Ni J, Kim E, et al. Induction of androgen receptor expression by phosphatidylinositol 3-kinase/Akt downstream substrate, FOXO3a and their roles in apoptosis of LNCaP prostate cancer cells. The Journal of Biological Chemistry. 2005;**280**:33558-33565

[22] Lynch RL, Konicek BW, McNulty AM, Hanna KR, Lewis JE, Neubauer BL. The progression of LNCaP human prostate cancer cells to androgen independence involves decreased FOXO3a expression and reduced p27KIP1 promoter transactivation. Molecular Cancer Research. 2005;**3**:163-169

[23] Nishimura K, Nonomura N, Satoh E, Harada Y, Nakayama M, Tokizane T, et al. Potential mechanism for the effects of dexamethasone on growth of androgen-independent prostate cancer. Journal of the National Cancer Institute. 2001;**93**:1739-1746

[24] Fakih M, Johnson CS, Trump DL. Glucocorticoids and treatment of prostate cancer: A preclinical and clinical review. Urology. 2002;**60**:553-561

[25] Cardillo MR, Lazzereschi D, Gandini O, Di Silverio F, Colletta G. Transforming growth factor-beta pathway in human renal cell carcinoma and surrounding normal-appearing renal parenchyma. Analytical and Quantitative Cytology and Histology. 2001;**23**:109-117

[26] Chipuk JE, Cornelius SC, Pultz NJ, Jorgensen JS, Bonham MJ, Kim SJ, et al. The androgen receptor represses transforming growth factor-beta signaling through interaction with Smad3. The Journal of Biological Chemistry. 2002;**277**:1240-1248

[27] Kuratomi G, Komuro A, Goto K, Shinozaki M, Miyazawa K, Miyazono K. NEDD4-2 (neural precursor cell expressed, developmentally down-regulated 4-2) negatively regulates TGF-beta (transforming growth factor-beta) signalling by inducing ubiquitin-mediated degradation of Smad2 and TGF-beta type I receptor. The Biochemical Journal. 2005;**386**:461-470

[28] Kim IY, Zelner DJ, Lee C. The conventional transforming growth factor-beta (TGF-beta) receptor type I is not required for TGF-beta 1 signaling in a human prostate cancer cell line, LNCaP. Experimental Cell Research. 1998;**241**:151-160

[29] Guo Y, Kyprianou N. Overexpression of transforming growth factor (TGF) beta1 type II receptor restores TGF-beta1 sensitivity and signaling in human prostate cancer cells. Cell Growth & Differentiation. 1998;**9**:185-193

[30] Maiyar AC, Phu PT, Huang AJ, Firestone GL. Repression of glucocorticoid receptor transactivation and DNA binding of a glucocorticoid response element within the serum/glucocorticoid-inducible protein kinase (sgk) gene promoter by the p53 tumor suppressor protein. Molecular Endocrinology. 1997;**11**:312-329

[31] Vallon V, Lang F. New insights into the role of serum- and glucocorticoid-inducible kinase SGK1 in the regulation of renal function and blood pressure. Current Opinion in Nephrology and Hypertension. 2005;**14**:59-66 (Review)

Chapter 6

Rapid Endosomal Recycling

Hana Mahmutefendić, Gordana Blagojević Zagorac, Senka Maćešić and Pero Lučin

Additional information is available at the end of the chapter

http://dx.doi.org/10.5772/intechopen.75685

Abstract

Peripheral membrane proteins are endocytosed by constitutive processes of membrane invaginations, followed by internalization driven by diverse endocytic machinery available at the cell surface. It is believed that after endocytic uptake, cargo proteins proceed either through the endosomal recycling circuit of the cell or travel toward late endosomes for degradation. In this chapter, we analyzed trafficking of seven cargo molecules (transferrin receptor, fully conformed MHC-I, non-conformed MHC-I, cholera-toxin B subunit, CD44, ICAM1, and G-protein-coupled receptor Rae-1) known to use the distinct endocytic route. For that purpose, we developed the software for multicompartment analysis of intracellular trafficking. We demonstrate that all endocytosed molecules are rapidly recycled and propose that the rapid recycling is a constitutive process that should be considered in the analysis of intracellular trafficking of peripheral membrane proteins.

Keywords: rapid endosomal recycling, clathrin-independent cargo, endosomal recycling, endosomal trafficking, kinetic modeling of endosomal trafficking, transferrin receptor

1. Introduction

Endocytosis is an essential cellular function maintenance of the membranous system and plasma membrane (PM) associated functions, including uptake of nutrients and extracellular material, cell communication and information processing, motility, adhesion, and cell division (reviewed in [1–7]). Endocytic uptake occurs either by ligand binding to cell surface proteins (receptor-mediated endocytosis) or by uptake of extracellular fluid by membrane invaginations (fluid-phase endocytosis) [3]. Endocytosis is initiated by cellular proteins that change PM lipid composition and by the assembly of a series of cytoplasmic proteins,

known as endocytic machinery, which causes membrane deformation and assists pinching off membrane invaginations into endocytic carriers. The best characterized is cytoplasmic protein clathrin that assembles and forms clathrin coat which initiates the rapid development of endocytic carriers, known as clathrin-dependent endocytosis (CDE). Endocytic carriers may be developed without the assistance of the clathrin, known as clathrin-independent endocytosis (CIE), although it is assisted by cellular proteins such as caveolin (known as caveolin-dependent endocytosis) or flotillin (flotillin-dependent endocytosis). Pinching off endocytic carriers is also facilitated by several cellular proteins, including cellular guanosine-triphosphatase (GTPase). Endocytic uptake that requires the dynamin is known as dynamin-dependent endocytosis (DDE), and the endocytic uptake which does not engage dynamin is known as dynamin-independent endocytosis (DIE).

In addition to the endocytic uptake initiated by ligand binding, PM is constitutively endocytosed with the dynamic unique for each cell. Depending on cell type, the whole cell surface is internalized one to five times in an hour [3]. The dynamic of the constitutive uptake, thus, is a cell adaptation to the metabolic and growing conditions. Constitutive endocytic uptake of PM is a part of cellular physiology required for maintenance of PM and membranous organelle composition. PM is internalized into endocytic carriers, which upon endocytic uptake coalesce and together with endocytic carriers derived by receptor-mediated endocytosis form early endosomes (EEs). EEs are highly dynamic intracellular compartments that grow in size, migrate along cytoskeleton, fuse with each other, mix and sort membrane content, mature, and ultimately deliver the membrane content to lysosomes for degradation [1, 8]. Along the endocytic pathway, membranes change composition and form membrane domains, which at some stage of endosomal maturation can form subcompartments [1, 2, 7]. Maturing EEs form larger organelles, which extensively sort membrane cargo, known as sorting endosomes (SEs), by process of endosomal conversion transform into late endosomes (LEs). LEs are a highly dynamic network of membrane domains that also mix and sort membrane cargo and deliver it either toward the *trans*-Golgi network (TGN), cell surface (exocytosis), or lysosomes for degradation [1, 7, 9].

Along the entire endosomal pathway, endosomal membranes develop recycling domains to generate recycling carriers that return membranes back to the cell surface (reviewed in [10–12]). As endocytic uptake, endosomal recycling may be initiated and regulated by a set of cellular proteins representing the recycling machinery and may occur constitutively. At the stage of EEs, a majority of the endocytosed membrane is returned to the cell surface from tubular EEs that directly deliver recycling carriers to PM or transform into the agglomerate of recycling domains near the cell center, known as the endosomal recycling compartment (ERC). EEs and the ERC return the majority of internalized membranes, although recycling may also occur from LEs [13], and only 3–5% of internalized membranes are delivered to lysosomes. Although it is considered that endosomal route through EEs and the ERC represent the endosomal recycling circuit, and LEs represent the feeder system that delivers cargo into degradation [1], it appears that recycling occurs from LEs and the endosomal recycling route can be divided into EE and LE recycling circuits [13].

Constitutive endosomal uptake and recycling are processes utilized by the cell to regulate PM and endosomal organelle composition and represent a fundamental mechanism for cellular adaptation to the metabolic activity and environmental conditions. Maintenance of the

membranous system consumes ~30% of cellular energy [14] and, thus, it is of particular interest for the cell to make these processes energetically efficient. The delivery of endocytosed membranes and membrane cargo along the endocytic pathway should be aligned with the cellular physiology requirements for endosomal compartmentalization, and all membranes and membrane cargo that do not need to enter the distal parts of the endosomal pathway should be returned back to the cell surface as early as possible to minimize cellular energy consumption. Therefore, for a substantial part of an internalized PM, it is essential to be returned quickly after endocytic uptake. This process of membrane return should occur rapidly after both ligand-initiated and constitutive endocytic uptake and may be called rapid recycling.

The term rapid recycling is not clarified in the literature. Although the term rapid recycling can also be assigned to the recycling processes that are characterized by the very fast delivery of membranous content to the PM at any stage of the endocytic tract, we assign the term rapid recycling to a part of the recycling circuit that is activated very early after endocytosis. In this chapter, we used available data from the literature, our experimental data, and kinetic modeling to demonstrate that rapid recycling is a significant constitutive part of post-endocytic itinerary irrespective of the way of membrane endocytic uptake.

2. Plasma membrane dynamics

Early studies on endocytosis suggested that the PM is highly dynamic and the whole PM is internalized one to five times in an hour [2]. Studies using fluorescent lipid analogs demonstrated that the PM system is extremely dynamic and that the half-time for membrane turnover could be as short as 5–10 min [15]. Constitutive endocytic uptake occurs by clathrin-coated pits and by clathrin-independent mechanisms (reviewed in [5, 6]). Thus, it is reasonable to assume that the constitutive uptake does not occur at the entire PM with the same rate. In addition to the wide range of endocytic machinery available in the cell, the rate of PM constitutive uptake would also depend on membrane composition at the site of development of endocytic carriers and attachment of PM to the actin network. For example, requirements for membrane deformation and transformation into an endocytic carrier will be different at lipid-organized membrane microdomains (i.e., lipid rafts) than at more fluid parts of the PM.

Much understanding of the kinetics of the PM uptake came from the studies of CDE cargo, mostly the transferrin receptor (TfR). In general, internalization kinetics of CDE cargo molecules demonstrated that PM uptake at the segments which involves clathrin-coated pits (coat-dependent endocytic uptake) is very fast [4, 15] and occurs with the rate which is in the range of 0.20–0.50 min^{-1} [16–19], although lower [20] and higher [19] rates were determined. Kinetics of the endocytic uptake of CDE cargo, however, does not reflect the average rate of the constitutive uptake of PM. Namely, the coat-dependent route accounts for 40–50% of the constitutive endocytic uptake [5], although recent evidence suggests that at least 95% of cellular endocytic uptake is based on clathrin-coated pits [21] and that different cell surface proteins can be sorted into distinct clathrin-coated pits [2, 4]. On the other hand, the kinetic and physiology of the constitutive endocytic uptake that does not involve clathrin coats (coat-independent pathways) is poorly analyzed. It appears that the rate of the constitutive endocytic uptake is much lower

than in the coat-dependent pathway [22, 23]. However, these rates are mostly determined as the uptake of soluble enzymes or fluorescently labeled molecules and, thereby, may represent the rate of fluid-phase uptake, which is one smaller segment in the coat-independent pathway. Very little quantitative analysis was performed by measuring the constitutive endocytic uptake of coat-independent PM cargo proteins. Even studies based on the incorporation of fluorescent lipid analogs (i.e., sphingomyelin), which are an excellent tool to determine PM dynamics and demonstrated a high rate of the PM uptake [15], did not accurately measured the uptake of the entire PM, but rather PM segments that incorporated the lipid analog.

In general, it is difficult to measure the rate of PM uptake. In fact, most studies determined the internalization rate (IR) which represents the difference between the endocytic rate (ER) and the recycling rate (RR). Thus, any measurement that may account recycling does not represent the rate of PM uptake (ER) but rather IR. Given that the recycling may occur very early after endocytosis (i.e., one or two min. after initiation of the endocytic uptake), any measurement that is longer than 2 min, thus, potentially determines the IR and not the ER. Since it has been shown that membranes labeled with fluorescent lipid analogs rapidly recycle with the high rate, in the range of 0.17–0.70 min^{-1} [15, 18], it can be estimated that the rate of PM uptake must be higher. Thus, understanding the dynamics and activation of the rapid recycling mechanism is essential for understanding the turnover of the PM. Similarly, to understand the cellular physiology of any peripheral membrane protein, including feedback mechanisms that determine its intracellular distribution and consequently function, it is essential to construct its intracellular itinerary, which includes endocytic uptake, inter-endosomal trafficking, and endosomal recycling. Therefore, in addition to PM dynamics, it is essential to understand quantitative aspects of the cellular physiology of the endosomal system, particularly the EE system.

3. The early endosomal system: a brief overview

The early endosomal (EE) system is the complex network of membranous vesicular and tubular structures that continuously exchange cargo and form membrane domains with different functions [1, 8]. The endosomes undergo fusion and fission reactions which shape the number and size of organelles. During these reactions, the cargo is sorted either into tubular domains for recycling to the PM and TGN or into intraluminal vesicles for degradation. Several hundreds of individual endosomes form a dynamic network and create funnel-like system [8] in which endocytosed cargo progressively flow from small endosomes at the cell periphery to large endosomes in the cell center until Rab5-positive EEs convert into Rab7-positive LEs [7, 24]. Recent studies demonstrate that the EE system can be subdivided into at least two stages: proximal comprised of pre-EEs and the distal comprised of EE/SEs [8, 25–27].

3.1. Pre-EEs

We consider pre-EEs as subcortical endosomes which are positive for Rab5, as all EEs, and devoid of early endosomal antigen 1 (EEA1) and phosphatidylinositol-3-phosphate (PI3P) [8, 27]. These endosomes accept CDE cargo, such as TfR [26], epidermal growth factor receptor (EGFR) [2, 25], beta-2-adrenergic receptor (B2AR) [28], and luteinizing hormone receptor (LHR) [27]. A subpopulation of Rab5-positive pre-EEs recruit APPL1 (adaptor protein, phosphotyrosine interaction,

PH domain and leucine zipper containing 1) [29, 30] and represent a stable sorting station, not only intermediate in EE maturation [26]. However, APPL1 endosomes are not the only entry site for clathrin-coated pits, since a significant fraction of clathrin-coated pits do not acquire APPL1 following uncoating [29] and a substantial fraction (approx. 40%) of internalized Tf does not colocalize with APPL1 or EEA1 at early times after internalization [26].

3.2. Early/sorting endosomes

EEs are not the homogenous population of endocytic compartments which accept all internalized cargo without discrimination, but instead are comprised of distinct populations regarding mobility and maturation kinetics [31]. EEs represent a broader profile of tubular and vacuolar compartments that are characterized by the presence of PI3P, EEA1, and Rab5 [31] and form a dynamic network. Endosomes in the central part of this network develop vacuolar and tubular domains [32], undergo fusion and fission reactions [8], and represent earlier stages of endosomal maturation. It also includes dynamic endosomes [31] and APPL1+EEA1 endosomes [29, 30]. Maturation of EEs involves either generation of the tubular endosomal domain which recycles cargo to PM or vacuolization and formation of intraluminal vesicles which ends up with conversion into LEs [24, 31, 32].

The vacuolar domain of EEs retains cargo destined for degradation and sort it into intraluminal vesicles whereby vacuolar EEs become multivesicular endosomes. Limiting membranes of vacuolar EEs generate tubular-sorting endosome (TSE) [32] or tubular endosomal network (TEN) [9] that sorts plasma membrane recycling proteins either into recycling carriers or develop into the ERC. TSE/TEN also sort lysosomal membrane proteins (Lamp1, Lamp2, and CD63), sortilin and M6PR into LEs or TGN [32]. Also, limiting membranes of vacuolar EEs, just before their maturation into LE vacuoles, can develop the endosome-to-TGN transport carriers (ETC) specific for retrograde transport of lysosomal proteins [33]. It has been shown that several CDE cargo molecules can pass through the same EE vacuoles but exit this organelle through different recycling tubules, i.e., the TSE/TEN and ETCs [33].

Live cell imaging [31] and fluorescence resonance energy transfer (FRET) analysis [32] demonstrated the existence of two kinetically distinct populations of EEs, dynamic and static. Dynamic EEs is a smaller peripheral subpopulation of EEs that transfer cargo into LEs with the fast rate, whereas static EEs are multivesicular perinuclear endosomes that undergo an EE-to-LE transition as the latest stage of EE maturation [31, 32]. Static EEs are a pleomorphic structure composed of large vesicles and thin tubular extensions that have membrane invaginations and develop multivesicular appearance [32], sort CDE and CIE cargo, and transport CIE cargo by MICAL1-positive TREs or CDE cargo by Rab11-positive carriers to the ERC or the cell surface [34].

3.3. The endosomal recycling compartment

The endosomal recycling compartment (ERC) is membranous tubulovesicular organelle organized in the pericentriolar region [10, 11]. The ERC is constructed around the MTOC as a network of both partially connected, and individual vesicles and tubules organized [10, 34] which is distinct from membrane-bound tubular recycling endosomes (TREs) [34]. ERC is spatially confined within the Golgi, whereas EEs, LEs, and Ly are excluded from inside the Golgi [35].

4. Endosomal recycling

Early studies of membrane recycling demonstrated that of all endocytosed membrane 95% is eventually recycled, and only 5% is targeted to lysosomes [3]. Most of the knowledge about endosomal recycling routes were generated using conventional assays based on redistribution of receptors, mostly from the TfR (reviewed in [11]). In contrast to CDE cargo proteins, the recycling route was not established or is poorly characterized for many proteins that are endocytosed by the CIE. The best characterized is the recycling route of major histocompatibility class I (MHC-I) proteins [11], although recycling routes of several CIE cargo proteins have been described in the last decade [6, 11, 36].

4.1. Fast and slow endosomal recycling

Recycling route, recycling rate, and recycling efficiency are well established for TfR due to the availability of an excellent tool appropriate for radioactive, chemical, or fluorescent labeling [15, 16]. Recycling of TfR occurs by iterative fractionation during EE trafficking [10, 11, 37] and the recycling kinetics is typically biphasic, with the initial fast and the later slow component [17]. Thus, TfR recycling route is usually divided into two steps: a fast or direct route that occurs from EEs, sometimes called rapid recycling route [11], and slow or indirect route that occurs from the ERC [10–12, 19, 37]. Recycling of TfR from EEs requires the function of Rab4 [7, 10, 11, 18], whereas recycling from the ERC requires the sequential function of multiple regulators including Rab5, Rab11, Rab8a, their effectors (Rabenosyn-5, Rab11-FIP2, and MICAL-L1, respectively), and EHD proteins [34]. TfR can be recycled from both static and dynamic EEs, including those in the process of Rab5 and Rab7 conversion [31]. Some cargo proteins, such as G protein-coupled receptors (GPCRs), require specific sequence and multiple interacting proteins for recycling [28, 38], whereas many proteins may recycle without any sequence and interaction requirements [10, 39], as a part of the bulk membrane flow. Sequence-dependent recycling occurs via tubular microdomains that are distinct from tubular domains that mediate the bulk recycling, even at the same endosome [40].

Using fluorescent lipophilic dyes, Hao and Maxfield [15] demonstrated rapid recycling endosomal membranes very early after endocytosis. They showed after 2 min of pulse internalization of NBD-SM that 30–60% of membranes is rapidly returned (recycled) with very high rate (0.35–0.70 min^{-1}), indicating very early activation of the recycling mechanism. Based on the kinetics of fluorescent dyes trafficking, they concluded that larger endocytic compartment than primary endocytic vesicles is involved in rapid recycling. In addition, a similar study showed rapid and extensive (with similarly high rate) mobilization of the significant fraction of membranes not only in the very early stage of endosomal flow but also from all later stages [39]. Thus, rapid and extensive engagement of membranes into recycling is a general property of the endosomal system, and the exchange of membranes between endosomes and PM is more extensive than it can be derived from studies using single membrane receptor.

4.2. Rapid endosomal recycling

Recent studies using live-cell imaging and total internal reflection fluorescence microscopy (TIRFM), suggest that recycling mechanism may be activated very early in the endocytic tract,

at the stage of pre-EEs or very early endosomes (VEEs). The TIRFM study of GPCRs recorded rapid recycling events as exocytic puffs that appeared at the cell surface 2–3 min after internalization [41], and live cell imaging studies demonstrated that EEA1- and PI3P-negative endosomes and APPL1-positive endosomes represent the very early recycling compartment [27, 40].

Although most of knowledge about recycling was constructed on studies of TfR recycling using radiolabeled or fluorescent ligand (Tf), uncovering the very early recycling step was difficult, because all assays were based on the quantification of the ligand release from the cell as an indication of recycling. However, the release of Tf from TfR only occurs when TfR reaches sufficiently acidic compartment which converts holo- into apo-Tf. Thus, it was long believed that CDE cargoes could recycle back to the cell surface through a pathway that requires Rab4 and Rab35 [11]. Nevertheless, recent studies demonstrated that TfR recycling might occur very early in the endocytic tract, from APPL1 endosomes, downstream APPL1-EEA1 endosomes which receive CIE cargo, and from EEA1 endosomes [8, 26]. The TIRFM study of GPCRs also recorded coincident puffs of fluorescent Tf-labeled receptors, indicating that the earliest recycling of TfR occurs without the release of apo-Tf [41]. These rapid recycling events were invisible by conventional assays, and thus rapid recycling processes were underestimated. The TIRFM imaging enabled visualization of very rapid recycling vesicles, since these vesicles contain endocytic cargo at relatively high concentration, whereas vesicles that mediate slower pathways of recycling or biosynthetic insertions contain cargo at a significantly lower concentration which cannot be detected by the TIRFM imaging. Most evidence for rapid recycling can be derived from studies on the post-endocytic itinerary of G protein-coupled receptors (GPCRs). Activated beta-2 adrenergic receptor (B2AR), a typical representative of the largest GPCR family, is endocytosed by the dynamin-dependent CDE mechanism [28, 38]. Internalized receptors rapidly recycle back to the cell surface in vesicles that concentrate internalized receptor, which recently enabled visualization of the rapidly recycled receptor by the TIRFM microscopy [41]. Also, during each cycle, a fraction of receptors is directed into EE/SEs and either to the ERC from which they are slowly returned to the cell surface or to lysosomes where they are degraded [28, 38]. Not all GPCRs follow the same endocytic itinerary. For example, follicle-stimulating hormone receptors (FSHRs) follow the same route as B2AR, whereas the majority of LHR and δ-opioid receptor (δOR) are targeted from EEs into lysosomes and degraded [27]. However, both types of receptors recycle from EEA1- and PI3P-negative small very-early endosomal (VEEs)/pre-EE compartment [27].

5. Analysis of rapid recycling by kinetic modeling

To analyze rapid recycling, we used kinetic modeling approach, which is based on the accurate measurement of cell surface kinetic and construction of the intracellular itinerary using the software which enables calculation of dynamic distribution through multiple compartments of endosomes [13, 42].

5.1. Selection of peripheral membrane cargo molecules

It is becoming clear that membrane proteins cannot be put into two categories (CDE and CIE cargo) but instead classified into broader spectrum regarding engagement of endocytic machinery, kinetics of the endocytic uptake, and post-endocytic itinerary [6]. Thus, we examined endocytic

itinerary of seven membrane cargo molecules (**Figure 1**) that have been shown to use the distinct endocytic route and that had a distinct post-endocytic itinerary. The route of TfR and GPCRs, CDE cargo proteins, is well defined [4, 9, 43] and involves rapid recycling [15, 27, 41]. Routes of the six CIE cargo molecules (**Figure 1**) are relatively well characterized, but their very-early post-endocytic itinerary is mostly unknown. Internalization pathways of two of these cargo molecules, GM1/CTxB and antibody-clustered GPI-anchored protein (GPI-AP) Rae1-γ [5, 44], require the activity of dynamin (DDE) [45]. These two cargo molecules may not only enter the cell via caveolae but also may be internalized DIE pathway which is regulated by the small GTPase Cdc42 [45]. The Cdc42-regulated pathway, also known as CLIC/GEEC pathway, is controlled by the small GTPase Arf1 and is used for fluid-phase uptake [5, 6]. Constitutive internalization pathway of three membrane proteins (fully-conformed MHC-I molecules, CD44, and ICAM1) is regulated by small GTPase Arf6 (known as Arf6-regulated pathway) [43, 46, 47]. One membrane cargo molecule (empty MHC-I) is internalized by the CIE mechanism, but dynamin requirement and small GTPase regulation are unknown [13, 48].

Irrespective of the way of entry into the cells, cargo molecules have distinct itineraries in the endosomal system upon endocytosis [43] and can be classified into six types according to known endocytic routes. *Type A cargo* proteins are long-lived, travel along the recycling route, and in EE/SEs, nearly all cargo molecules are sorted into recycling tubules or the ERC and returned to the PM, whereas very little enter LEs and lysosomes. *Type B cargo* travels along the bulk route that in EE/SEs, it directs some cargo into recycling tubules and some into LEs and lysosomes for degradation. *Type C cargo* is short-lived, travels along the degradative route, and nearly all cargo is sorted into LE and degraded in lysosomes. *Type D cargo* is long-lived, travels along the TGN retrograde route, and upon entry into EEs, it is sorted either into retrograde tubules to TGN or LEs and delivered to the TGN. *Type E cargo* is long-lived, travels

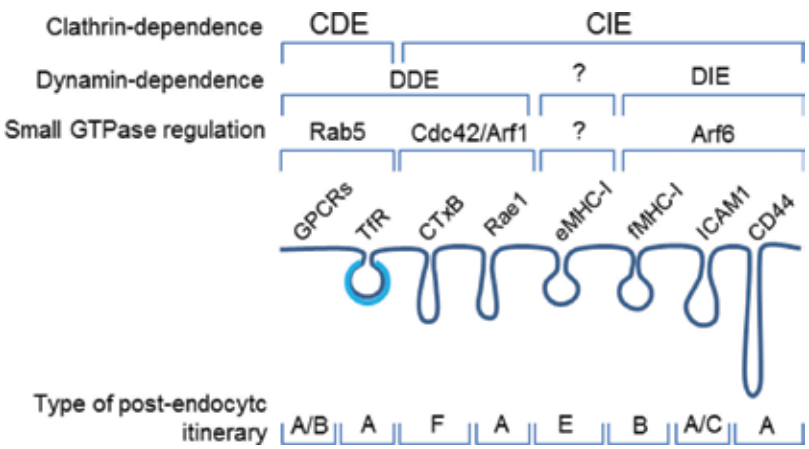

Figure 1. Typology of peripheral membrane cargo molecules used for kinetic analysis. Clathrin dependence during endocytic uptake classifies peripheral membrane cargo for clathrin-dependent endocytosis (CDE) and clathrin-independent endocytosis (CIE). The requirement of dynamin activity during pinching off endocytic carriers classifies cargo molecules as dynamin-dependent (DDE) and dynamin-independent (DIE). Cargo molecules can be classified into at least seven types according to the post-endocytic itinerary (see description in the text).

along the LE route, and in EE/SEs is sorted into LEs and recycled back to the PM either by recycling or exocytic carriers. *Type F cargo* travels along the Golgi retrograde route and from EE/SEs, it is sorted in the ERC from which it is delivered to the Golgi.

According to the classification, GPCRs can be classified as *Type A* and *Type B* [28, 38, 41] cargo, ligand-bound or antibody bound TfR as *Type A* cargo [9, 43], CTxB/GM1 as *Type F* [44]; Rae1 as *Type A* cargo [5, 6], eMHC-I as *Type E* cargo [13, 48], fMHC-I as *Type B* cargo [23, 43, 46, 48], ICAM1 as *Type A* and *Type C* cargo [47], and CD44 as Type A cargo [43, 46].

5.2. Cell surface expression displays internalization rate as integration of endocytic uptake and recycling of membrane proteins

Quantification of distribution of peripheral membrane proteins at the PM and in the endosomal system is critical for analysis and understanding their intracellular itineraries. Unfortunately, the number of techniques for accurate measurement of the number of peripheral membrane proteins in an intracellular compartment is quite limited. On the other hand, techniques based on antibody reagents and radioactively or fluorescently labeled ligands provide quite an accurate method for quantification of the number of peripheral membrane proteins at the cell surface. Thus, kinetic studies of cell surface expression of peripheral membrane proteins are the best available data for quantitative estimation of the intracellular itinerary, as explained below.

The steady state distribution of membrane endocytic cargo components reflects the net effect of endosomal sorting events. The frequency of appearance at the PM and endosomal compartment depends on the rate of transit between compartments and a compartment with the lowest rate of the transit will be a major retention site for cell surface receptor. In general, the distribution of peripheral membrane proteins will depend on the rate of endocytic uptake from the PM and the integrated rate of recycling from endosomal compartments. Receptors with higher endocytic rate will be retained inside the cell and receptors with higher recycling rate will be retained at the cell surface. For example, after rapid endocytic uptake, the TfR almost entirely enters into the recycling circuit, return to the cell surface, and again into endocytic carries. Very little (less than 1%) of internalized TfR is rerouted into LEs and degraded. Thus, TfR circulates from PM through endosomes and back. After several cycles, TfRs established the steady state distribution at the PM and endosomal compartment, and the net result is a redistribution of two-thirds of TfR inside the cell. On the contrary, the rate of recycling of MHC-I proteins overrides the rate of endocytosis, and thus the majority of MHC-I proteins reside at the cell surface. Inhibition of recycling or enhancement of endocytosis, thus, is a mechanism available to the cell to regulate cell surface level of a peripheral membrane protein.

5.3. Kinetic modeling of peripheral membrane protein trafficking

Kinetic models have been used to translate the cell physiology knowledge into mathematical formulas. Accordingly, the knowledge on endosomal compartments determined the number of compartments taken into analysis. Most of the kinetic studies were based on the use of a minimal number of compartments, and the recent expansion on the knowledge about EE system enabled the development of more complex models. The three models can be identified in the literature (**Figure 2**).

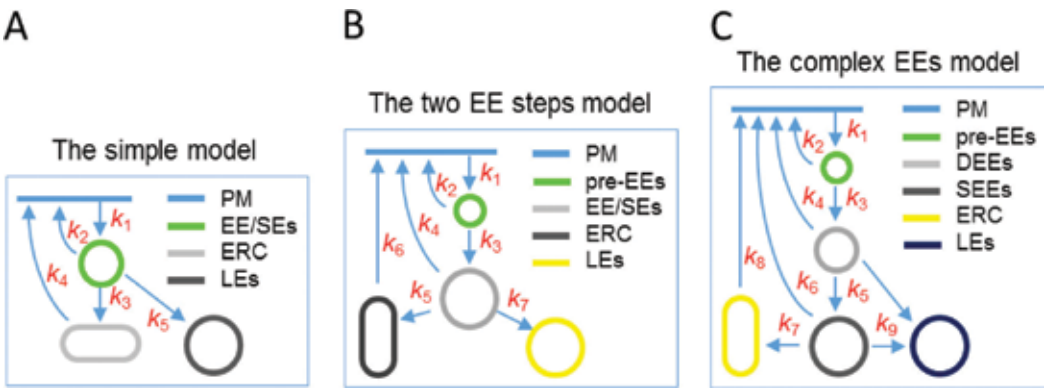

Figure 2. Kinetic models of peripheral membrane protein trafficking. (A) The simple model. (B) The two EE steps model—pre-EEs and EEs as sorting endosome. (C) The complex EEs model—pre-EEs and dynamic and static EEs. PM, plasma membrane; EE/SEs, early/sorting endosomes; ERC, endosomal recycling compartment; LEs, late endosomes; DEEs, dynamic early endosomes; and SEEs, static early endosomes.

The simple model (**Figure 2A**) used EE/SEs, the ERC, and LEs as the only recognized compartments of cargo transit [17]. With the expansion of the knowledge about the endosomal system, it is becoming clear that EEs, LEs, and even the ERC represent a various set of organelles and subcompartments and that the initial categorization into early, late, and recycling endosomes is oversimplified [10, 31, 35]. Recent studies introduced pre-EEs as a stable sorting station that sorts and recycles endocytotic cargo [25–28]. Thus, the EE system can be subdivided into at least two stages: proximal comprised of pre-EEs and the distal comprised of EE/SEs (**Figure 2B**). The more complex organization of the proximal stage (**Figure 3**), for example, has been proposed recently [26]. The funnel-like structure of EE system [8] suggests more complexity and requires separation of the EE system into at least two compartments (**Figure 2C**). Although the degree of biochemical and morphological separation of EEs is still incomplete, live-cell imaging studies [31, 32] suggest that EEs are organized into the more dynamic and static populations (**Figure 2C**).

To analyze endocytic itinerary of the seven peripheral membrane cargo molecules (**Figure 1**), we used the two-step model (**Figure 2B**). A kinetic model was developed which predicts sequential trafficking of peripheral membrane cargo molecules from PM through the endosomal system

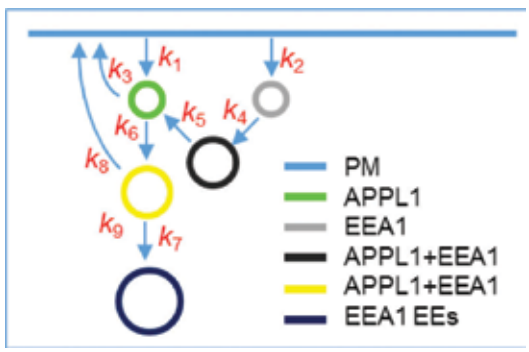

Figure 3. Pre-early endosome model proposed by Kalaidzidis et al. [26].

and that recycling may occur from every step of endosomal trafficking (pre-EEs, EEs/SEs, the ERC, and LEs). Our modeling was based on the following assumptions: (i) each compartment is considered homogenous, "well mixed," and can grow and shrink in size; (ii) cargo enters and leaves the compartments all the time; (iii) the cargo flux is presented as the fraction of cargo in the compartment at any given time; (iv) the velocities can change in space and time, continuously and smoothly; (v) the model does not capture the stochastic, "back and forth" movements of endosomes; (vi) the rates of exit from the compartment should not exceed the rate of entry into the compartment; (vii) different rates of exit from a compartment assume existence of different domains within a compartment; (viii) the predictions must be consistent with values derived from experimental data, including morphological analysis. The model predicts constant flux of cargo from a compartment toward the next compartment with the first-order rate kinetics [16, 17]. We predicted only the forward flux, and the retrograde flux, if exists, was integrated as a sum within the forward flux. Initially, the amount of cargo at the PM was set to 100(%), and the PM was considered as the first compartment. The assigned rate constants are graphically displayed in **Figure 2B**.

We fit the parameters of the model to the kinetic data of cargo molecule determined experimentally by flow cytometry, as cell surface expression of mAb-labeled or ligand-labeled peripheral membrane cargo molecules. To quantify the goodness of any of the models obtained by the described fitting processes, we used the coefficient of determination (R^2). The fitting was based on the adjustment of kinetic parameters until the R^2 value was larger than 0.93.

5.4. Determination of the endocytic rate constant

The endocytic rate constant is defined as the probability of a cell surface receptor to be internalized in 1 min at 37°C [49]. Thus, for kinetic analysis of the earliest post-endocytic events, it was critical to determine the endocytic rate constant (k_1). For experimental measurement of k_1 for peripheral membrane cargo molecules, it was essential to satisfy the following three conditions [49]: (i) internalized and cell surface cargo molecules can be quantitatively discriminated from each other, (ii) there is no degradation at the time of measurement, and (iii) there is no or very little dissociation of primary and secondary reagents during the course of the measurement. Thus, for each cargo molecules, we precisely defined the first step, conditions of ligand binding at the cell surface, since the pool of occupied cell surface molecules is the substrate for endocytosis. All primary and secondary reagents were tested for concentration and time required for saturation of almost all (>98%) PM molecules at 4°C, and dissociation rate of bound primary and secondary reagents at 4°C and at 37°C in the absence of endocytosis.

Experimental identification of k_1 was performed by fitting the predicted curve to the experimental data sets by iterative adjustment of k_1 values and visual alignment by minimization of the sum of square differences (R^2) [13, 42].

5.5. Selection of kinetic parameters

Kinetic parameters, rate constants (k_1-k_8) and the time of the beginning of transition between compartments, were manually chosen by fitting the PM level to the experimental data using the existing knowledge from the literature about endosomal kinetics.

Kinetic parameters for the pre-EE step were based on the following: (i) endocytic vesicles were observed after as little as 20 s of internalization [21]; (ii) after 2 min TfR localize in pre-EEs [25–27]; (iii) in the first 2 min, TfR does not localize in EEA1-positive endosomes, and partial colocalization with EEA1 is evident between 2 and 3 min; (iv) internalized cargo (TfR, EGFR) localize in EEs 3–6 min after endocytosis [17, 25, 27] and EEs are maximally filled with internalized cargo after 5 min [17]; (v) after 5 min, less than 10% of internalized TfRs localize in pre-EEs [27]. The recycling rate constant from pre-EEs (k_2) of 0.17–0.35 min^{-1} was reported for EGFR and of 0.35–0.69 min^{-1} for TfR [15]. The pre-EE-to-EE transition rate constant (k_3) of 0.15–0.35 min^{-1} was reported for TfR [17, 18], 0.69 min^{-1} for HDL, and 0.53 min^{-1} for Glut4 [19].

Kinetic parameters for the EE step were based on the observation that the EE stage of endosomal trafficking ends 6–10 min after endocytosis [25, 37]. The EE recycling rate constant (k_4) of 0.11–0.35 min^{-1} was reported for TfR and B2AR [10, 17, 18, 38]. Several reports suggest that the transition of cargo from SE to the ERC (k_5) occurs with the rate of approx. 0.30–0.35 min^{-1} [37, 39]. The transport from SEs into LEs was reported to occur at the rate of 0.087–0.115 min^{-1} [10, 15, 24, 37].

Kinetic parameters for the ERC step were based on the observation that the ERC is maximally filled at 12–13 min [17]. The ERC recycling rate constant (k_6) was determined in many studies based on loading of Tf-labeled TfRs. Most often reported rate was 0.040–0.080 min^{-1} [10, 15, 17, 39], although lower and higher rates up to 0.3 min^{-1} [19, 39] were reported. Similar externalization rate from the ERC was also reported using the fluorescent lipid analog C6-NBD-SM [39]. Recycling rate from LEs (k_8) of 0.058 min^{-1} was reported for open MHC-I conformers [13].

5.6. Evaluation of the kinetic model by identification of the rapid recycling of the transferrin receptor (TfR)

To evaluate our kinetic model, we analyzed the endocytic itinerary of TfR which is the best characterized CDE molecule in the literature. For quantification, we used its ligand transferrin (Tf) conjugated with the biotin (Tf-biotin) and specific monoclonal antibody (anti-TfR Abs). We used these two reagents since they provide different information about TfRs. Tf-biotin displays internalized receptors at the cell surface that are recycled back to the cell surface from a non-acidic but not from an acidic endosomal compartment. In contrast, anti-TfR Abs display all receptors that recycle back to the cell surface. TfRs were labeled with these two reagents at 4°C, cells were rapidly warmed to 37°C (internalization), and analyzed every minute for the number of labeled TfRs that remained at the cell surface (**Figure 4**).

Rapid loss of Tf-biotin- and anti-TfR-labeled TfRs from the cell surface indicates rapid endocytic uptake (endocytic rate, k_1) with the very high rate. With the estimated endocytic rate of ~0.61 min^{-1}, all receptors should be removed from the cell surface within 10 min. However, after 3 min and later, both Tf-biotin- and anti-TfR-labeled receptors remained at the cell surface (**Figure 4**), suggesting either the arrest of endocytosis or rapid return of labeled receptors back to the cell surface. In the presence of aluminum-fluoride, a potent inhibitor of endosomal recycling [11], labeled receptors did not remain at the cell surface (data not shown) suggesting that endocytosis normally goes on after 3 min and that the reason for the maintenance of the labeled receptors is rapid return by recycling.

To fit the predicted cell surface level to the experimental data, the rapid recycling from the pre-EEs (k_2) should be activated after 2.3–2.4 min after initiation of endocytosis (**Figure 4**).

http://dx.doi.org/10.5772/intechopen.75685

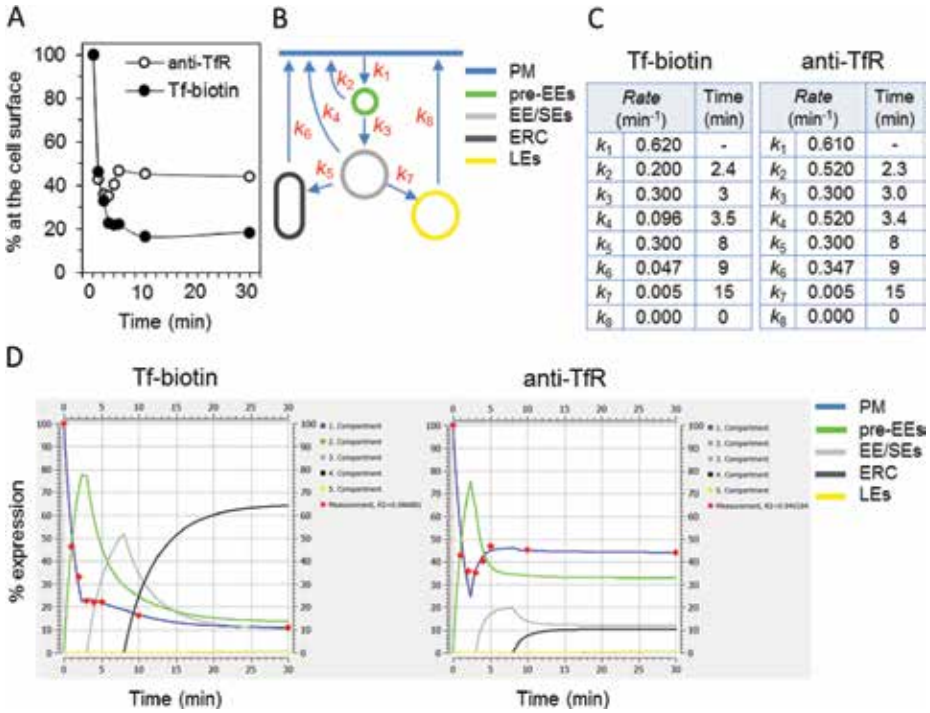

	Tf-biotin Rate (min^{-1})	Tf-biotin Time (min)	anti-TfR Rate (min^{-1})	anti-TfR Time (min)
k_1	0.620	-	0.610	-
k_2	0.200	2.4	0.520	2.3
k_3	0.300	3	0.300	3.0
k_4	0.096	3.5	0.520	3.4
k_5	0.300	8	0.300	8
k_6	0.047	9	0.347	9
k_7	0.005	15	0.005	15
k_8	0.000	0	0.000	0

Figure 4. Evaluation of the kinetic model by analysis of the post-endocytic itinerary of transferrin receptor. (**A**) *Internalization kinetics of TfRs.* Cell surface TfRs were labeled either with Tf-biotin or anti-TfR mAb at 4°C for 30 min, incubated at 37°C from one to 30 min, and stained with AF^{488}-conjugated secondary reagents. Cell surface fluorescence was quantified by flow cytometry. (**B**) *Schematic diagram of the kinetic model used for analysis of TfR post-endocytic itinerary.* (**C–D**) *Outcomes of the kinetic analysis*. Kinetic parameters are presented in table (**C**), and relative distribution within the endosomal system using these parameters is presented in the screen-shots of the kinetic modeling software for multicompartment analysis (**D**) [13, 42]. Experimental data (red diamonds) were plotted into the software, and rate constants (k_1–k_8) and time of the beginning transition between compartments (time) were adjusted to fit the curve of the predicted cell surface level (blue line) to the experimental data. Green, gray, dark gray, and yellow lines represent predicted distribution in corresponding endosomal compartments. The analysis was performed on the J26 fibroblast-like cell line.

Recycling from pre-EEs (k_2) should be active for the whole time of chase and in the absence of this mechanism, it was impossible to simulate the measured receptor levels at later times (data not shown). The estimated recycling rate from pre-EEs (k_2) was significantly lower for Tf-biotin- (~0.20 min^{-1}) than for mAb-labeled (~0.52 min^{-1}) TfRs (**Figure 4**), suggesting that a fraction of Tf-biotin/TfRs was returned to the PM from pre-EEs that are sufficiently acidic to convert *holo*-Tf into *apo*-Tf. Namely, a fraction of TfRs loaded with *apo*-Tf-biotin that was delivered from acidic endosomes would not be detected by flow cytometry as *apo*-Tf is released from the receptor that reached the cell surface. Nevertheless, the kinetic analysis demonstrates that endocytosed TfRs must be rapidly recycled to maintain the cell surface level. The rate of recycling must be rather high to oppose the high endocytic rate.

Entry of internalized TfRs into EEs occurred 3–4 min after endocytic uptake with the rate (k_3) similar to that described in the literature [17–19], followed by immediate activation of recycling from this compartment (k_4). Estimated recycling rate using Tf-biotin (**Figure 4**) represents the rate of TfR recycling sufficient to return *holo*-Tf-biotin-associated receptors that are detected by flow cytometry. Recycling of *holo*-Tf-biotin-associated receptors was also detected from the ERC (k_6).

Thus, Tf-biotin detection at the cell surface suggests that the rate of recycling of TfRs from EEs and the ERC is significantly higher than observed by measuring the *apo*-Tf release [10, 15, 17–19, 38, 39]. This observation is confirmed by estimations of the recycling rates from EEs and the ERC (k_4 and k_6) of mAb-labeled receptors (**Figure 4**). The omitting of any of these recycling rates made impossible to simulate measured cell surface levels of receptors. Thus, kinetic analysis of Tf-biotin- and mAb-labeled TfRs demonstrates the existence of the rapid recycling of TfRs from non-acidic endosomes and recycling with the high rate at the entire recycling circuit.

5.7. Kinetic modeling provides evidence for rapid recycling of clathrin-independent peripheral membrane proteins

We analyzed cell surface kinetics and intracellular itinerary of six CIE cargo molecules, five PM proteins using mAb reagents and GM_1 using biotinylated CTxB. The PM kinetics was measured using flow cytometry as described for TfR. The incubation conditions and the shift in temperature (i.e., from 4°C to 37°C and vice versa) were carefully controlled to minimize the time required for warming or cooling. Experimental details and validation of protocols have been published in several papers [13, 22, 23, 42, 48].

Experimentally acquired values were imported into the kinetic modeling software [13, 42], and kinetic analysis of trafficking through five membranous compartments (**Figure 4**) was performed. The fitting of kinetic parameters (rate constants and transition time) was based on data from the immunofluorescence analysis of intracellular itinerary and data from the literature. The experimental data and the outcome of the fitting procedure (including distribution throughout the compartments) for each cargo molecule are presented in graphs of **Figure 5**, and parameters that best fit to the experimental data in the table of **Figure 5**.

PM kinetics of six CIE cargo molecules, which are endocytosed by distinct mechanisms, demonstrated different rates of disappearance from the cell surface (k_1). CDE and DDE cargo, such as TfR, disappeared with the very high rate (0.573 min^{-1}) also in murine embryonal fibroblasts (**Figure 5**) and other cell lines used for analysis (data not shown). CIE and DDE cargo (such as GM_1/CTxB and ICAM1) disappeared with the moderate rate, whereas CIE and DIE cargo (CD44, fMHC-I, and Rae1) disappeared from the cell surface six times slower than TfR (**Figure 5**). Although the contribution of dynamin in the endocytic uptake of eMHC-I has not been proven, kinetic of their disappearance from the cell surface suggests that they belong to the group of CIE and DDE cargo and may use the similar route as ICAM1 and GM_1/CTxB (**Figure 5**).

The rate of disappearance from the cell surface represents the rate of endocytosis (k_1). The observed rates (k_1 for all six CIE cargo molecules) would lead to the kinetics of the loss (internalization) from the plasma membrane as presented by blue dashed lines in the graphs of **Figure 5**. Apparently, the measured kinetics of cell surface expression of all cargo molecules is distinct to this calculated kinetics, and all cargo molecules remain at the cell surface much longer than predicted by the calculated kinetics. As described above for TfR, the prolonged retention of cargo molecules at the cell surface is not due to the arrest in the endocytic uptake, since under conditions of inhibited recycling by aluminum-fluoride [11], all cargo molecules disappeared from the cell surface with the rate similar to that predicted by the calculated kinetics (data not shown). Thus, the reason for the prolonged maintenance of cargo molecules at the cell surface is the activation of the recycling mechanism, which returns internalized cargo to the cell surface.

http://dx.doi.org/10.5772/intechopen.75685

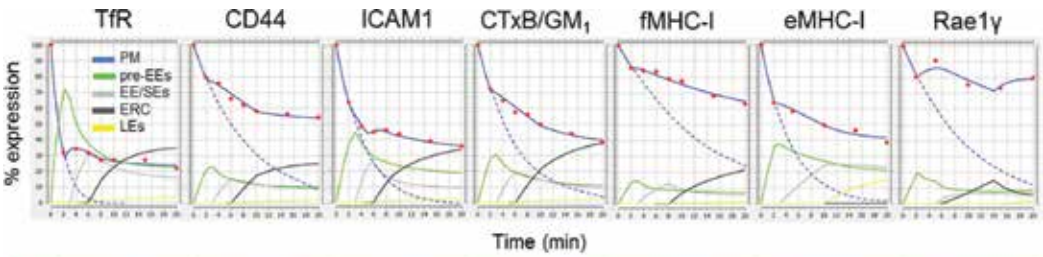

	TfR		CD44		ICAM1		CTxB		fMHC-I		eMHC-I*		Rae1γ**	
	min^{-1}	time	min^{-1}	time	min^{-1}	time	min^{-1}	time	min^{-1}	time	min^{-1}	time	min^{-1}	time
k_1	0.573	0	0.120	0	0.231	0	0.165	0	0.073	0	0.210	0	0.101	0
k_2	0.355	2.2	0.330	2	0.145	2	0.310	2	0.375	2	0.320	2.1	0.655	2.2
k_3	0.250	3	0.310	3	0.310	3	0.310	3	0.310	3	0.110	3	0.310	5
k_4	0.108	4	0.038	4	0.315	5	0.058	4	0.088	4	0	0	0.088	5
k_5	0.250	6	0.310	6	0.310	6	0.310	6	0.310	8	0	0	0.310	10
k_6	0.108	8	0.105	10	0.068	9	0.058	10	0.038	10	0	0	0.388	14
k_7	0.010	15	0.010	15	0.010	20	0.010	15	0.010	15	0.110	10	0.060	15
k_8	-	-	-	-	-	-	-	-	-	-	0.130	10	-	-

Figure 5. Analysis of the early post-endocytic itinerary of clathrin-dependent and clathrin-independent cargo molecules. PM proteins were labeled with specific mAbs and ganglioside M_1 (GM_1) with AF^{488}-CTxB at 4°C, and cell surface expression was quantified by flow cytometry after indicated time of internalization at 37°C. The experimental data (red diamonds) were loaded into the software for multicompartment analysis [13, 42], five endosomal compartments setup as described in **Figure 4**, and kinetic parameters were adjusted by fitting the curve of the predicted cell surface level (full blue line) to the experimental data. Kinetic rates (k_1–k_8) and the time of the beginning of transport between compartment (time) are shown in the table. Dashed blue lines represent predicted cell surface expression in the absence of recycling. The analysis was performed on murine embryonal fibroblasts except for eMHC-I (*), which was analyzed on L^d-transfected L-cells (L-L^d), and Rae1γ (**), which was analyzed on Rae1γ-transfected NIH 3 T3 cells.

Alignment of kinetic parameters to the experimental data between 2 and 5 min after initiation of internalization, demonstrated that recycling mechanism should be activated approx. within 2 min for all CIE cargo molecules to explain experimentally measured value at 5 min (**Figure 5**). Therefore, our analysis demonstrates that also CIE cargo, irrespective of the involvement of the dynamin in the endocytic uptake, enter into endosomes that may recycle cargo back to the cell surface very early after endocytosis. Apparently, the recycling mechanism is activated from pre-EEs, since at 2 min, none of the cargo molecules should be expected in EEs. The estimated rate of exit from pre-EEs indicates rather a high rate (more than 0.3 min^{-1}), which is in agreement with previously observed rapid recycling kinetic [15, 17–19]. The only exception was ICAM1 which activates very fast recycling mechanism later. The distinct rate of the return from pre-EEs indicates that pre-EEs are not the homogenous population of endosomes. This is not surprising since distinct endocytic routes lead to distinct endocytic carriers which have membrane composition that correspond to the piece of the PM taken up into endocytic carriers. Altogether, this analysis indicates that rapid recycling mechanism exists for all CIE cargo molecules and occurs very early after endocytosis with a very high rate.

Analysis of further steps (5 min after internalization) in the endocytic itinerary demonstrate that additional recycling should be activated, from EEs and later from the ERC, to maintain the measured cell surface level. The kinetics of recycling from these compartments (k_4 and k_6) differ among cargo molecules, indicating that EEs and the ERC may have distinct domains or subcompartments that generate recycling carriers with distinct rates. Although cargo molecules

used for this analysis differ in their post-EE endocytic itinerary, we did not add this complexity into the analysis since our intention in this discussion was to demonstrate that all endocytic cargo undergoes into the rapid recycling circuit. The rapid recycling circuit is, apparently, distinct from the conventional recycling circuit [1] and also recycles cargo that is excluded from the conventional recycling circuit. For example, although eMHC-I molecules are excluded from the recycling circuit that involves EEs and the ERC [48] and recycles from LEs [13], they are included onto the rapid recycling circuit and recycled from pre-EEs with the relatively high rate (**Figure 5**). Given that the conventional recycling circuit has the capacity of conformation-based sorting (i.e., sorting of membrane proteins that changed conformation and can be considered as misfolded), this type of endosomal sorting does not operate in the rapid recycling circuit.

Altogether, our analysis of post-endocytic itinerary of seven cargo molecules that utilize distinct endocytic machinery and undergo distinct post-endocytic itinerary demonstrated that all endocytic cargo molecules enter into the rapid recycling circuit and are rapidly returned to the cell surface after endocytosis. Thus, a critical segment of post-endocytic trafficking of peripheral membrane proteins and other membrane components was underestimated in the past and should be considered in the explanation of the cellular physiology of peripheral membrane proteins and related physiological and pathophysiological processes.

6. Physiological significance of the rapid endosomal recycling

Very early activated recycling (rapid recycling) is apparently an important cellular physiology mechanism to reduce energy consumption for the maintenance of plasma membrane composition. The vast majority of the energetic cost for the maintenance of the cells is associated with protein synthesis and maintenance of membranes (i.e., ~30% cellular energy budget is spent on membranes) [14]. Therefore, there is an evolutionary rationale to evolve mechanism(s) which will reduce energy consumption in the membrane trafficking pathways. For example, although the bulk recycling route may provide sufficient amount of a protein at the cell surface, for some cellular proteins (i.e., proteins that maintain cell–cell contacts), it is not reasonable to enter deep inside the cell and travel throughout the entire recycling circuit. It would be more energy efficient to return internalized proteins back to the cell surface as soon as possible. To maintain the steady-state distribution of a protein at the cell surface, which is determined by the post-endocytic itinerary, it is essential to synthesize enough proteins to fill all compartments that are on the route. Thus, the size of the cellular pool of a protein would depend on the length of a route intracellular trafficking of a protein. The rapid return would require less protein synthesis and would reduce a load of endosomal compartments by a protein, which may be important for fidelity of post-endocytic sorting events. Therefore, rapid recycling may reduce energy consumption by the shortening of the recycling circuit for many membrane components and by reducing the number of membrane proteins required to fill the membranous system of the cell properly.

Rapid recycling is also essential for the cellular physiology of cholesterol homeostasis, which requires efficient binding of lipoproteins (LDL and VLDL remnants) to LDL receptor (LDLR), their internalization, the release of lipoproteins in the endocytic compartment, and the return of receptors to the cell surface for further rounds of lipoprotein uptake. Quantitative fluorescence imaging study [50] demonstrated that lipoprotein release occurs before the entry of LDLRs

into EEs. The failure of LDLRs recycling results in the loss of receptors by rerouting into the lysosomal degradation pathway and several therapeutic strategies were explored in order to minimize LDLRs degradation. The failure of pre-EE recycling route also may result in reduced LDL clearance. Thus, understanding the rapid LDLRs' recycling pathway may lead to the identification of new therapeutic targets that can be exploited to prolong LDLR half-life and, thereby, enable treatment of atherosclerosis-based diseases, including coronary artery disease.

Very early activation of recycling is undoubtedly vital in shaping cellular receptor-mediated signaling via GPCRs. Rapid endocytic recycling determines the number of functional receptors at the PM [28, 38] and the rapid recovery of functional signaling after ligand-activated endocytic uptake [28, 38]. Even more, a rapid recycling process that delivers receptors at high concentration may be particularly suited for dynamic regulation of localized receptor signaling.Rapid recycling may be essential for assembly and maintenance of cell-cell contacts. The very fast rate of endocytic uptake may result in the redistribution of molecules that maintain cell contact, and slow recycling processes may make cell contacts weaker. It has been shown that recycling processes are important for regulation of trafficking of various cell adhesion molecules, including cadherins and integrin receptors (reviewed in [51]). Alteration of recycling processes has been shown to be associated with the loss of cell adhesion increased motility and cell migration, which are the characteristics of epithelial-mesenchymal transition and invasive cancer cells [51]. Many of these processes may be assigned to the rapid recycling. Thus, misregulation of the rapid recycling can result in human disease when it compromises important cellular functions, such as lipid homeostasis, cellular signaling, movement, or division.

7. Conclusion(s)

Although significant progress has been made in understanding the endosomal recycling, characterization of endosomal recycling routes of peripheral membrane proteins is still poorly integrated into the cellular physiology, especially into the higher-order physiology [11]. The increasing number of molecules with characterized recycling routes indicates that recycling may occur very early in the endocytic tract, suggesting more complexity of the endosomal recycling circuit and the need for its integration into physiology and pathophysiology of many cellular processes.

Our study demonstrates that the constitutive endocytic uptake of peripheral membrane proteins occurs with much higher rate and the overall low internalization rate is primarily maintained by rapid recycling prior their entry into structured EE network. Internalization rates and endocytic rates described in the literature, in fact, represent the combination of endocytic uptake and the (rapid) recycling processes. Rapid recycling, therefore, should be taken into consideration when analyzing and estimating many important cellular processes, including physiology cell motility and adhesion, receptor signaling, lipoprotein metabolism, and signal transduction.

Acknowledgements

This work was supported in part by the Croatian Science Foundation (grant IP-2014-9-9564) and by the University of Rijeka (grants 13.06.1.1.4, 13.06.2.1.55, and 13.06.2.1.56).

Conflict of interest

The authors declare that they have no conflict of interest.

Notes/Thanks/Other declarations

We apologize to all authors whose work has not been cited owing to space restrictions, and for not always citing primary literature.

Abbreviations

Ab	antibody
AF	alexa-fluor
CDE	clathrin-dependent endocytosis
CIE	clathrin-independent endocytosis
CTxB	cholera-toxin B subunit
DDE	dynamin-dependent endocytosis
DIE	dynamin-independent endocytosis
EE	early endosome
ERC	the endosomal recycling compartment
GPCR	G protein-coupled receptor
GTPase	guanosine-triphosphatase
LE	late endosome
mAb	monoclonal antibody
MHC-I	major histocompatibility class I
PM	plasma membrane
pre-EE	pre-early endosome
SE	sorting endosome
Tf	transferrin
TfR	transferrin receptor
TGN	the *trans*-Golgi network

Author details

Hana Mahmutefendić[1], Gordana Blagojević Zagorac[1], Senka Maćešić[2] and Pero Lučin[1,3]*

*Address all correspondence to: pero.lucin@medri.uniri.hr

1 Department of Physiology and Immunology, University of Rijeka, Faculty of Medicine, Rijeka, Croatia

2 Department of Mathematics, Physics, Foreign Languages and Kinesiology, University of Rijeka, Faculty of Engineering, Rijeka, Croatia

3 University North, University Center Varaždin, Varaždin, Croatia

References

[1] Huotari J, Helenius A. Endosome maturation. The EMBO Journal. 2011;**30**:3481-3500. DOI: 10.1038/emboj.2011.286

[2] Doherty GJ, McMahon HT. Mechanisms of endocytosis. Annual Review of Biochemistry. 2009;**78**:857-902. DOI: 10.1146/annurev.biochem.78.081307.110540

[3] Steinman RM, Mellman IS, Muller WA, Cohn ZA. Endocytosis and the recycling of plasma membrane. The Journal of Cell Biology. 1983;**96**:1-27

[4] Kirchhausen T, Owen D, Harrison SC. Molecular structure, function, and dynamics of clathrin-mediated membrane traffic. Cold Spring Harbor Perspectives in Biology. 2014;**6**:a016725. DOI: 10.1101/cshperspect.a016725

[5] Mayor S, Pagano RE. Pathways of clathrin-independent endocytosis. Nature Reviews. Molecular Cell Biology. 2007;**8**:603-612. DOI: 10.1038/nrm2216

[6] Maldonado-Báez L, Williamson C, Donaldson JG. Clathrin-independent endocytosis: A cargo-centric view. Experimental Cell Research. 2013;**319**:2759-2769. DOI: 10.1016/j.yexcr.2013.08.008

[7] Wandinger-Ness A, Zerial M. Rab proteins and the compartmentalization of the endosomal system. Cold Spring Harbor Perspectives in Biology. 2014;**6**:a022616. DOI: 10.1101/cshperspect.a022616

[8] Villaseñor R, Kalaidzidis Y, Zerial M. Signal processing by the endosomal system. Current Opinion in Cell Biology. 2016;**39**:53-60. DOI: 10.1016/j.ceb.2016.02.002

[9] Bonifacino JS, Rojas R. Retrograde transport from endosomes to the trans-Golgi network. Nature Reviews. Molecular Cell Biology. 2006;**7**:568-579

[10] Maxfield FR, McGraw TE. Endocytic recycling. Nature Reviews. Molecular Cell Biology. 2004;**5**:121-132. DOI: 10.1038/nrm1315

[11] Grant BD, Donaldson JG. Pathways and mechanisms of endocytic recycling. Nature Reviews. Molecular Cell Biology. 2009;**10**:597-608. DOI: 10.1038/nrm2755

[12] Vale-Costa S, Amorim MJ. Recycling endosomes and viral infection. Virus. 2016;**8**:64. DOI: 10.3390/v8030064

[13] Mahmutefendić H, Blagojević Zagorac G, Grabušić K, Karleuša L, Maćešić S, Momburg F, Lučin P. Late endosomal recycling of open MHC-I conformers. Journal of Cellular Physiology. 2017;**232**:872-887. DOI: 10.1002/jcp.25495

[14] Lynch M, Marinov GK: Membranes, energetics, and evolution across the prokaryote-eukaryote divide. eLife. 2017;**6**:e20437. DOI: 10.7554/eLife.20437

[15] Hao M, Maxfield FR. Characterization of rapid membrane internalization and recycling. The Journal of Biological Chemistry. 2000;**275**:15279-15286

[16] Ciechanover A, Schwartz AL, Dautry-Varsat A, Lodish HF. Kinetics of internalization and recycling of transferrin and the transferrin receptor in a human hepatoma cell line. Effect of lysosomotropic agents. The Journal of Biological Chemistry. 1983;**258**:9681-9689

[17] Sheff DR, Daro EA, Hull M, Mellman I. The receptor recycling pathway contains two distinct populations of early endosomes with different sorting functions. The Journal of Cell Biology. 1999;**145**:123-139

[18] Ward DM, Perou CM, Lloyd M, Kaplan J. "Synchronized" endocytosis and intracellular sorting in alveolar macrophages: The early sorting endosome is a transient organelle. The Journal of Cell Biology. 1995;**129**:1229-1240

[19] Brewer PD, Habtemichael EN, Romenskaia I, Mastick CC, Coster AC. Glut4 is sorted from a Rab10 GTPase-independent constitutive recycling pathway into a highly insulin-responsive Rab10 GTPase-dependent sequestration pathway after adipocyte differentiation. The Journal of Biological Chemistry. 2016;**291**:773-789. DOI: 10.1074/jbc.M115.694919

[20] Magadán JG, Barbieri MA, Mesa R, Stahl PD, Mayorga LS. Rab22a regulates the sorting of transferrin to recycling endosomes. Molecular and Cellular Biology. 2006;**26**:2595-2614. DOI: 10.1128/MCB.26.7.2595-2614.2006

[21] Bitsikas V, Corrêa IR Jr, Nichols BJ. Clathrin-independent pathways do not contribute significantly to endocytic flux. eLife. 2014;**3**:e03970. DOI: 10.7554/eLife.03970

[22] Mahmutefendić H, Blagojević G, Kučić N, Lučin P. Constitutive internalization of murine MHC class I molecules. Journal of Cellular Physiology. 2007;**210**:445-455. DOI: 10.1002/jcp.20877

[23] Zagorac GB, Mahmutefendić H, Tomaš MI, Kučić N, Le Bouteiller P, Lučin P. Early endosomal rerouting of major histocompatibility class I conformers. Journal of Cellular Physiology. 2012;**227**:2953-2964. DOI: 10.1002/jcp.23042

[24] Rink J, Ghigo E, Kalaidzidis Y, Zerial M. Rab conversion as a mechanism of progression from early to late endosomes. Cell. 2005;**122**:735-749. DOI: 10.1016/j.cell.2005.06.043

[25] Leonard D, Hayakawa A, Lawe D, Lambright D, Bellve KD, Standley C, Lifshitz LM, Fogarty KE, Corvera S. Sorting of EGF and transferrin at the plasma membrane and by cargo-specific signaling to EEA1-enriched endosomes. Journal of Cell Science. 2008;**121**:3445-3458. DOI: 10.1242/jcs.031484

[26] Kalaidzidis I, Miaczynska M, Brewińska-Olchowik M, Hupalowska A, Ferguson C, Parton RG, Kalaidzidis Y, Zerial M. APPL endosomes are not obligatory endocytic intermediates but act as stable cargo-sorting compartments. The Journal of Cell Biology. 2015;**211**:123-144. DOI: 10.1083/jcb.201311117

[27] Jean-Alphonse F, Bowersox S, Chen S, Beard G, Puthenveedu MA, Hanyaloglu AC. Spatially restricted G protein-coupled receptor activity via divergent endocytic compartments. The Journal of Biological Chemistry. 2014;**289**:3960-3977. DOI: 10.1074/jbc.M113.526350

[28] von Zastrow M, Williams JT: Modulating neuromodulation by receptor membrane traffic in the endocytic pathway. Neuron. 2012;**76**:22-32. DOI: 10.1016/j.neuron.2012.09.022

[29] Zoncu R, Perera RM, Balkin DM, Pirruccello M, Toomre D, De Camilli P. A phosphoinositide switch controls the maturation and signaling properties of APPL endosomes. Cell. 2009;**136**:1110-1121. DOI: 10.1016/j.cell.2009.01.032

[30] Miaczynska M, Christoforidis S, Giner A, Shevchenko A, Uttenweiler-Joseph S, Habermann B, Wilm M, Parton RG, Zerial M. APPL proteins link Rab5 to nuclear signal transduction via an endosomal compartment. Cell. 2004;**116**:445-456

[31] Lakadamyali M, Rust MJ, Zhuang X. Ligands for clathrin-mediated endocytosis are differentially sorted into distinct populations of early endosomes. Cell. 2006;**124**:997-1009. DOI: 10.1016/j.cell.2005.12.038

[32] Cullen PJ. Endosomal sorting and signalling: An emerging role for sorting nexins. Nature Reviews. Molecular Cell Biology. 2008;**9**:574-582. DOI: 10.1038/nrm2427

[33] Mari M, Bujny MV, Zeuschner D, Geerts WJ, Griffith J, Petersen CM, Cullen PJ, Klumperman J, Geuze HJ. SNX1 defines an early endosomal recycling exit for sortilin and mannose 6-phosphate receptors. Traffic. 2008;**9**:380-393. DOI: 10.1111/j.1600-0854.2007.00686.x

[34] Xie S, Bahl K, Reinecke JB, Hammond GR, Naslavsky N, Caplan S. The endocytic recycling compartment maintains cargo segregation acquired upon exit from the sorting endosome. Molecular Biology of the Cell. 2016;**27**:108-126. DOI: 10.1091/mbc.E15-07-0514

[35] Kobayashi H, Fukuda M. Arf6, Rab11 and transferrin receptor define distinct populations of recycling endosomes. Communicative & Integrative Biology. 2013;**6**:e25036. DOI: 10.4161/cib.25036

[36] Reineke JB, Xie S, Naslavsky N, Caplan S. Qualitative and quantitative analysis of endocytic recycling. Methods in Cell Biology. 2015;**130**:139-155. DOI: 10.1016/bs.mcb.2015.04.002

[37] Salzman NH, Maxfield FR. Fusion accessibility of endocytic compartments along the recycling and lysosomal endocytic pathways in intact cells. The Journal of Cell Biology. 1989;**109**:2097-2104

[38] Marchese A, Paing MM, Temple BR, Trejo J. G protein-coupled receptor sorting to endosomes and lysosomes. Annual Review of Pharmacology and Toxicology. 2008;**48**:601-629. DOI: 10.1146/annurev.pharmtox.48.113006.094646

[39] Mayor S, Presley JF, Maxfield FR. Sorting of membrane components from endosomes and subsequent recycling to the cell surface occurs by a bulk flow process. The Journal of Cell Biology. 1993;**121**:1257-1269

[40] Puthenveedu MA, Lauffer B, Temkin P, Vistein R, Carlton P, Thorn K, Taunton J, Weiner OD, Parton RG, von Zastrow M: Sequence-dependent sorting of recycling proteins by actin-stabilized endosomal microdomains. Cell. 2010;**143**:761-773. DOI: 10.1016/j.cell.2010.10.003

[41] Yudowski GA, Puthenveedu MA, Henry AG, von Zastrow M. Cargo-mediated regulation of a rapid Rab4-dependent recycling pathway. Molecular Biology of the Cell. 2009;**20**:2774-2784. DOI: 10.1091/mbc.E08-08-0892

[42] Blagojević Zagorac G, Mahmutefendić H, Maćešić S, Karleuša LJ, Lučin P. Quantitative analysis of endocytic recycling of membrane proteins by monoclonal antibody-based recycling assays. Journal of Cellular Physiology. 2017;**232**:463-476. DOI: 10.1002/jcp.25503

[43] Donaldson JG, Johnson DL, Dutta D. Rab and Arf G proteins in endosomal trafficking and cell surface homeostasis. Small GTPases. 2016;**7**:247-251. DOI: 10.1080/21541248.2016.1212687

[44] Matsudaira T, Niki T, Taguchi T, Arai H. Transport of the cholera toxin B-subunit from recycling endosomes to the Golgi requires clathrin and AP-1. Journal of Cell Science. 2015;**128**:3131-3142. DOI: 10.1242/jcs.172171

[45] Kirkham M, Fujita A, Chadda R, Nixon SJ, Kurzchalia TV, Sharma DK, Pagano RE, Hancock JF, Mayor S, Parton RG. Ultrastructural identification of uncoated caveolin-independent early endocytic vehicles. The Journal of Cell Biology. 2005;**168**:465-476. DOI: 10.1083/jcb.200407078

[46] Eyster CA, Higginson JD, Huebner R, Porat-Shliom N, Weigert R, Wu WW, Shen RF, Donaldson JG. Discovery of new cargo proteins that enter cells through clathrin-independent endocytosis. Traffic. 2009;**10**:590-599. DOI: 10.1111/j.1600-0854.2009.00894.x

[47] Ghaffarian R, Muro S. Distinct subcellular trafficking resulting from monomeric vs multimeric targeting to endothelial ICAM-1: Implications for drug delivery. Molecular Pharmaceutics. 2014;**11**:4350-4362. DOI: 10.1021/mp500409y

[48] Mahmutefendić H, Blagojević G, Tomaš MI, Kučić N, Lučin P. Segregation of open major histocompatibility class I conformers at the plasma membrane and during endosomal trafficking reveals conformation-based sorting in the endosomal system. The International Journal of Biochemistry & Cell Biology. 2011;**43**:504-515. DOI: 10.1016/j.biocel.2010.12.002

[49] Wiley HS, Cunningham DD. The endocytotic rate constant. A cellular parameter for quantitating receptor-mediated endocytosis. The Journal of Biological Chemistry. 1982;**257**:4222-4229

[50] Pompey S, Zhao Z, Luby-Phelps K, Michaely P. Quantitative fluorescence imaging reveals point of release for lipoproteins during LDLR-dependent uptake. Journal of Lipid Research. 2013;**54**:744-753. DOI: 10.1194/jlr.M033548

[51] Schweitzer JK, Sedgwick AE, D'Souza-Schorey C. ARF6-mediated endocytic recycling impacts cell movement, cell division and lipid homeostasis. Seminars in Cell & Developmental Biology. 2011;**22**:39-47. DOI: 10.1016/j.semcdb.2010.09.002

Chapter 7

Folding and Binding Properties of Human Complement Receptor Type 1 Extracellular Domain

Noriyuki Ishii

Additional information is available at the end of the chapter

http://dx.doi.org/10.5772/intechopen.75120

Abstract

Complement receptor type 1 (CR1 or CD35) is a peripheral glycosylated membrane protein that regulates the complement activation in the control of immune responses. The author would like to overview the folding and binding properties of the soluble form of CR1, so-called as sCR1, introducing our development of the high-yield overexpression and purification methods as well as the investigation to its molecular structure. Although sCR1 prepared through our method showed the highest binding affinity against C3b, it is quite difficult to be crystallized for X-ray structure analysis. In spite of many attempts, only microcrystals have been obtained so far. Considering the usefulness to understand factors within the difficulty, the primary sequence of sCR1 has been reexamined from the viewpoints both of secondary structure predictions and recent findings of intrinsically disordered proteins (IDPs) or natively unfolded proteins (NUPs). As an example, the theoretically predicted structure of a short consensus repeat (SCR) of a binding domain, SCR-15–17 in sCR1 is compared with the reported solution structure by NMR. The discussion is extended to protein structure studies with proteins containing ID regions, which are unfolded state without taking uniformly decided structures.

Keywords: complement receptor type1, CR1, sCR1, innate immunity, dissociation constant, binding affinity, overexpression, molecular structure, secondary structure prediction, crystallization

1. Introduction

Many cellular proteins are believed to fold autonomously to a certain specific three-dimensional structures in order to realize their unique biologically important functions [1, 2]. In the field of protein structural chemistry or structural biology, protein crystallography is fraught with challenge,

whereby various kinds of proteins are known to be difficult to be crystallized. The difficulty may be caused either by polymorphic conformations that the protein takes or movement of regions participating in the contact between molecules in a crystal field [3, 4].

On the other hand, wholly or partly unstructured proteins *in vivo* have been known for a long time and have been recently reevaluated and designated as intrinsically disordered proteins (IDPs) or natively unfolded proteins (NUPs) [5, 6]. It has been revealed that a large number of proteins contain at least a region that does not fold into uniformly converged sophisticated three-dimensional structures. Those regions are sometimes called random coils, which usually indicate globular proteins adopting an unfolded state. It is also not so rare for regions to form chain-like conformations as long as several hundred residues. Since the first review by Wright and Dyson [7], analyses by NMR studies and followed by computational analyses have revealed the importance of IDPs or NUPs in protein structural biochemistry. According to the recent computational survey of primary sequences, it is predicted that the total number of NUPs is approximately one-third of eukaryotic proteins [8].

From the viewpoint of studying functions of proteins, how to recognize and distinguish between self and non-self is still reminded mysterious. Recently, it has become apparent that extracellular membrane vesicles such as exosomes, released from cells are also involved in information transmission between cells in the immune system as well as cancer metastasis [9–12]. In this chapter, the author would like to limit the subject protein to a complement regulatory peripheral membrane protein of innate immunity. Immune adherence was first described at the beginning of the twentieth century and was rediscovered in the 1950s [13, 14]. The binding of serum-exposed particles to blood cells, which is a fundamental step for initiating and promoting the destruction of invasion microbes and for activating an adaptive immune system. This interaction is dependent on the coating of the antigenic particle with the complement, and the recognition by a factor on the erythrocyte surface, namely the immune adherence receptor [15, 16]. Recently, not only infectious microorganisms such as Salmonella, pathogenic *Escherichia coli*, influenza virus and so forth but also causative substances of pollinosis and allergies are widely known as a trigger, further similar causes are increasing including artificial nanoparticles. The complement system, comprised of over 35 protein components present in the plasma or bound to cell surfaces, forms an integral part of the early innate immune response. Three major complement cascades such as classical-, alternative-, and mannose-binding lectin pathways are known to activate the complement pathway and for excluding harmful invaders.

Complement receptor type 1 (CR1 or CD35) is a glyco-membrane protein that plays a role as a regulator of complement activation in the control of immune responses through its binding to C3b/C4b-opsonized foreign antigens [17]. The existence of allotypes is known to CR1, and the molecular mass varies from 160 to 250 kDa depending on its types. The extracellular portion of the most common allotype has about molecular mass of 220 kDa and is comprised of 30 modules, a series of tandem arranged short consensus repeat (SCR) (**Figure 1**). The sequence of each SCR shows approximately 45% homogeneity on average. The feature to be noted is the existence of four conserved cysteine residues in each SCR, as the first and third, and the second and fourth cysteines from the N terminus are covalently linked through disulfide bonds [17]. Weisman et al. reported a construction of human CR1 plasmid (pBSCR1c/pTCSgpt) by

http://dx.doi.org/10.5772/intechopen.75120

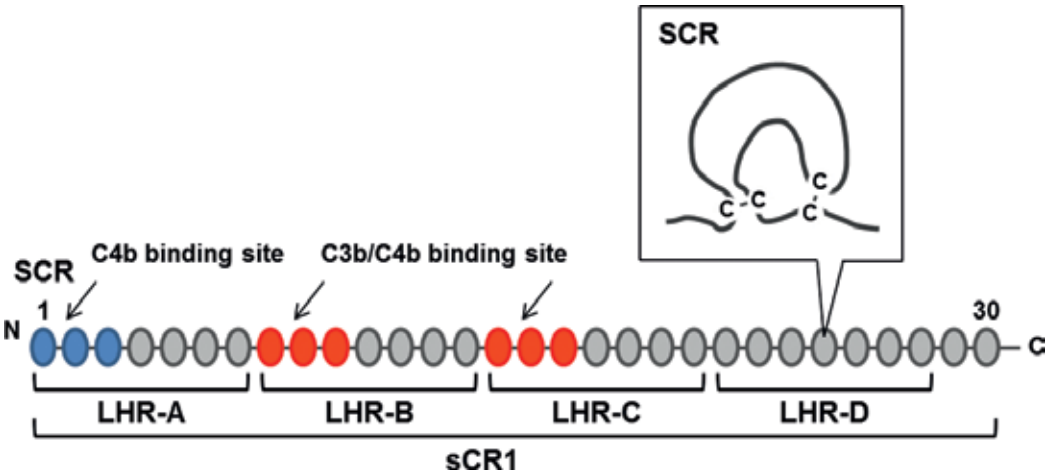

Figure 1. A schematic diagram showing the structural features of human sCR1. The extracellular domain consists of 30 short consensus repeats (SCRs). The amino-terminal 28 SCRs constitute four long homologous repeats (LHRs). The regions of LHR-A through LHR-D are indicated in the brackets. The predicted binding domains to complement proteins C3b, and C4b are indicated, respectively. The inset shows the enlargement of the triple loop structure of SCR with the predicted disulfide bonds.

cloning a soluble CR1 gene to plasmid pTCSgpt, in which a stop codon was inserted before the transmembrane and cytoplasmic domains [18]. As shown in **Figure 1**, the schematic drawing of the predicted structure of human sCR1 shows sCR1 consisting of four long homologous repeats (LHRs) constituted with seven SCRs, which are referred as LHR-A, -B, -C, and -D from N terminus. A binding domain to complement fragment C4b resides near N-terminus in LHR-A, and two domains to C3b reside LHR-B and LHR-C. The C3b binding domains appear to bind C4b but more weakly than C3b.

Although sCR1 may not fall exactly within the category of NUPs (or IDPs) because it has structured domains arranged at intervals tandemly, we think that it is important to consider the analysis of sCR1 from the perspective of NUPs (or IDPs).

2. Materials and methods

2.1. Preparation of human sCR1 from the cultivation with CHO cells

The cell line of Chinese hamster ovary (CHO) (CRL-10052) that carries the human sCR1 gene was purchased from American Type Culture Collection (ATCC) and was cultured under the ATCC's instructions. The human sCR1 was overexpressed using our novel cell culture method comprised of two-stage cell culture of CHO cells expressing sCR1 [19, 20]. The first stage involves cells grow up to 70–80% confluent in the medium with fetal bovine serum (FBS), and during the second stage, the cells produce sCR1 extensively and secrete it in a serum-free medium. For the first stage of cell growth culture, cells were cultivated in a medium containing α-MEM (Sigma-Aldrich Co. LLC., MO) supplemented with 10% FBS (Hyclone Lab. Inc., UT), 60 U/mL penicillin

and 60 μg/mL streptomycin (Pen Strep, Gibco, Life Technologies Corp., CA). Medium used for CHO cell culture was especially chosen, without deoxyribonucleoside and ribonucleoside. For the second stage of protein production, the cells were cultured in a serum-free medium such as ASF104 without albumin (Ajinomoto Co. Inc., Tokyo, Japan) supplemented with 1 μM methotrexate. Cell culture was performed in the incubator with 5% CO_2 at 37°C.

The serum-free medium which contains the secreted human sCR1 was recovered after a filtration (pore size of 0.22 μm). Subsequently, the purification of human sCR1 was performed by affinity column chromatography using HiTrap Heparin HP (GE Healthcare, PA). Briefly, the filtered medium solution was applied to the column that had been pre-equilibrated with 20 mM Tris-HCl buffer (pH 7.5) containing 0.05% CHAPS (Dojindo Molecular Technologies, Inc., Kumamoto, Japan). The column was washed with the equilibration buffer containing 100 mM NaCl, and the bound protein was eluted with 20 mM Tris-HCl buffer (pH 7.5) containing 0.05% CHAPS and 200 mM NaCl. Each eluted fraction sample was examined with sodium dodecyl sulfate polyaclylamide gel electrophoresis (SDS-PAGE) and subsequent Coomassie Brilliant Blue (CBB) staining. Though in most cases, a single or a considerably major band which corresponds to human sCR1 can be observed at this stage, to achieve the buffer exchange concurrently and further examine the purity, the fractions containing sCR1 gathered from the eluents from the heparin column was injected to HPLC gel filtration column chromatography (TSK gel G3000SWxl, Tosoh Corp., Tokyo, Japan). The single peak fraction at around the elution volume of 5.75 ml with a flow rate of 0.5 ml/min was collected as a purified human sCR1 [21]. Complement protein C3b was purchased from Calbiochem Research Biochemicals (EMD Bioscience, Inc., La Jolla, CA), and used after HPLC gel filtration column chromatography (TSK gel G3000SWxl, Tosoh Corp., Tokyo, Japan).

2.2. Characterization of binding affinity of sCR1 for C3b, and suppression effect of cell necrosis by sCR1

In order to investigate the binding affinity of the human sCR1 prepared by our protocol mentioned above, binding assay was performed by the use of a BIACORE X (GE Healthcare UK Ltd., Buckinghamshire, UK) using C3b as an analyte. The measurement was carried out using sCR1 as a ligand, immobilized on a substrate by the amine coupling method, and following the manufacturer's operation manual. In addition, assuming heterogeneous ligand parallel reaction, data analysis was performed by the software, BIAevaluation attached to the device.

The suppression effect of sCR1 on complement activation was examined as follows: a stroma cell derived from mouse skull bone marrow was used for this assay. PA-6 cells were seeded and allowed to grow in the medium containing α-MEM (Sigma-Aldrich Co. LLC., MO) with 10% FBS for 1 day. After three washes with PBS, cells were added with serum-free medium (900 μL of α-MEM) as well as 100 μL of PBS solution containing sCR1 and normal human serum (NHS) at a ratio of 1:9, or 100 μL of PBS solution containing sCR1 and heat-inactivated NHS at a ratio of 1:9. After 1 h incubation at 37°C, the suppression effect on the necrosis of cells was observed with a microscope (Zeiss Axiovert 200 M and Nikon DP50-WMED) following the previous methods [22–24].

2.3. Crystallization trials

Crystallization using thus obtained human sCR1 was carried out with a normal sitting drop vapor diffusion technique in the combination with a random-screening protocol with screen packages such as the Hampton Crystal Screen, Hampton Crystal Screen II (Hampton Research, CA), and Structure Screen 1 and Structure Screen 2 (Molecular Dimensions, Suffolk, UK) after the condensation to the protein concentration of around 3.5 mg/mL by means of centrifugal concentrator (Centri-plus 20, Merck Millipore Corp., MA). The incubation temperature for the crystallization trials was kept at around 23°C [4, 25].

2.4. Secondary structure prediction of human sCR1

The secondary structure predictions of human sCR1 on the basis of its primary sequence were performed by the use of PArallel Protein Information Analysis (PAPIA) system (http://cbrc3.cbrc.jp/papia/), parallel calculation using EnterPrise 4000 with 250 MHz UltraSPARC II 9pu, at the Computational Biology Research Center, AIST [26, 27]. The computing strategies employed were Chou-Fasman algorithm, and the joint prediction method where the protein secondary structure results of five different independent prediction methods were evaluated. In the latter calculation, the most likely secondary structure element for each amino acid sequence region of interest is decided from five independent answers depending on the decision by majority. The five methods incorporated are Qian-Sejnowski, Ptitsyn-Finkelstein, Nisikawa-Ooi, SSthread (prediction of protein secondary structure using threading), and Gibrat-Garinier-Robson methods. They were chosen from different methodologies on the basis of their performance.

3. Results and discussion

3.1. Characterization of sCR1 binding affinity for C3b

The intrinsic state, that is, if the protein is in the original structural state, its activity should be retained. Therefore, it can be considered that the purified protein assumes the same three-dimensional structure as when it is present *in vivo*. The binding affinity of the overproduced and purified human sCR1 for the complement C3b was investigated by biophysical interaction analysis with BIACORE X. The scheme in **Figure 2(a)** shows an outline of the measurement, and **Figure 2(b)** shows one of the typical results of sensorgram. In the light of the manufacture's protocol for data analysis, we have analyzed the data on the assumption of heterogeneous ligand parallel reaction and found that the dissociation constants of sCR prepared according to our production and purification method were $Kd = 3.03 \times 10^{-10}$ M for C3d dimer, and $Kd = 4.59 \times 10^{-9}$ M for C3b monomer, which are higher affinity than any values reported so far [18, 28–32]. It turned out that the binding affinities for C3b of the sCR1 prepared by our developed procedure are remarkably strong. We consider that the reason is due to the rapid and efficient purification method developed by us that can preserve sCR1 in an intact state.

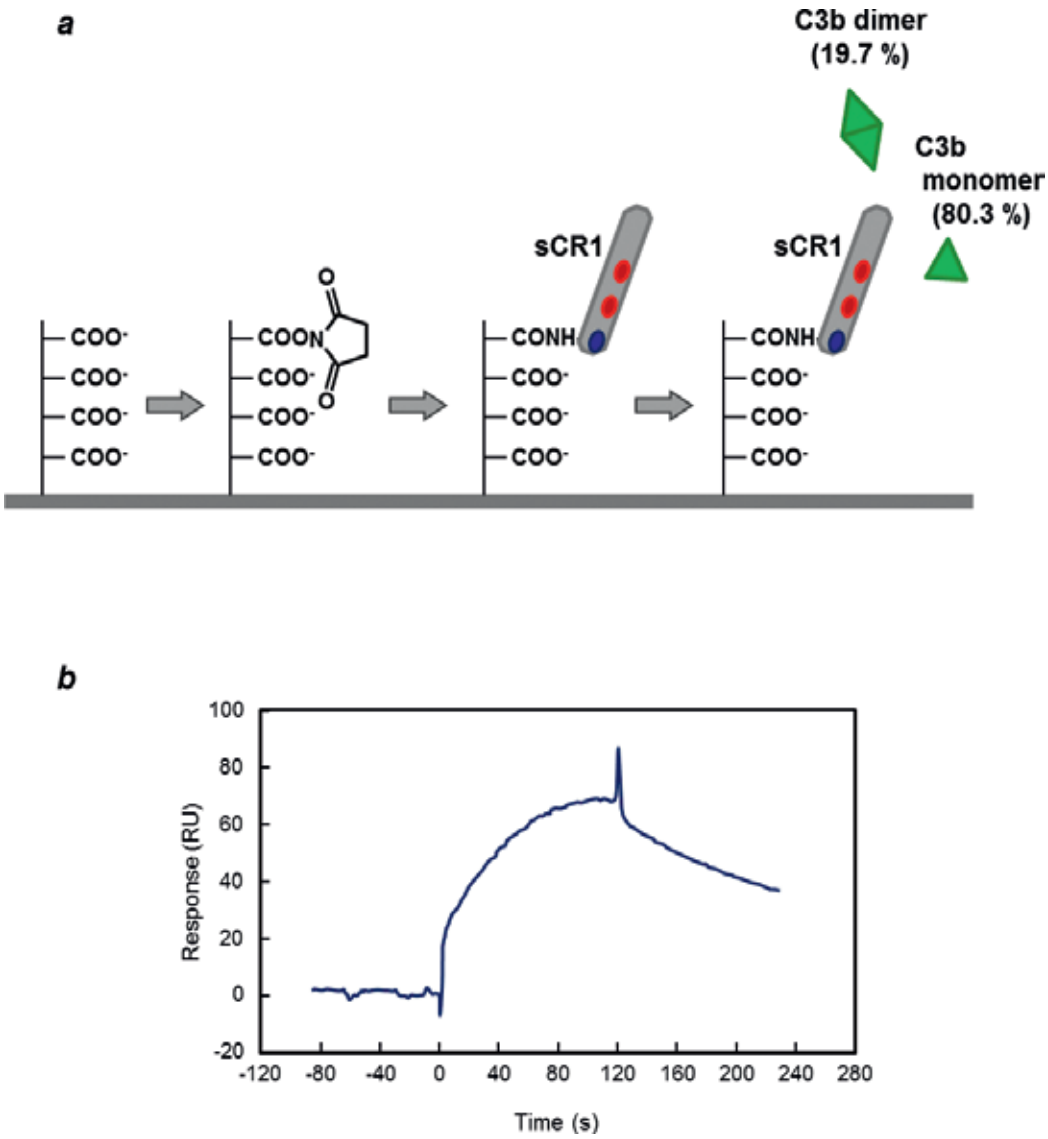

Figure 2. (a) A schematic drawing of the binding assay measurement by BIACORE. In complement C3b solution used as an analyte, monomeric and dimeric forms in C3b are recognized. The existence ratio between C3b monomer and C3b dimer was confirmed on HPLC gel permeation column chromatography. (b) A typical result of sensorgram from the biophysical interaction analysis with BIACORE X.

3.2. Characterization of sCR1 suppression effect of cell necrosis

In order to investigate the suppression effect of sCR1 on complement activation, a stroma cell PA-6 derived from mouse skull bone marrow was used for the assay. Human serum comprises complement proteins C1–C9, which trigger the activation of complement pathways and attack invading target microbes or non-self-cells. The complement pathway ends with the

necrosis of target cells due to the attack by C5b-9 membrane attack complex (MAC) [22, 23]. MAC is an important innate immune effector of the complement terminal pathway that forms cytotoxic pores on the surface of microbes. Similarly to CR1, the conformation in three-dimension of MAC is also unknown. In order to determine whether the purified human sCR1 retains its activity to bind complement C3b and/or C4b and suppresses the necrosis of cells by blocking complement pathway, sCR1 was added to PA-6 cells before the addition of the normal human serum (NHS). The results are shown in **Figure 3**. Cells cultured in medium were used as a control (**Figure 3(a)**), and cells cultured with inactivated NHS show similar results as the control; all cells grew well and maintained their normal morphology (**Figure 3(b)**). This fact implies that the inactivated complements in the serum cannot trigger any complement pathway. However, cells cultured with NHS reveal remarkable necrosis (**Figure 3(c)**). It implies that NHS triggers the activation of complement pathway and MAC attacks the cell membrane and causes cell death. On the other hand, when cells were cultured in the presence of NHS as well as the purified sCR1, cells showed normal morphology without any necrosis although most of cells appeared slim in their shape (**Figure 3(d)**). These results proved that the purified sCR1 has an activity to bind C3b and C4b in NHS and play a role as a blocker to the activation of MAC.

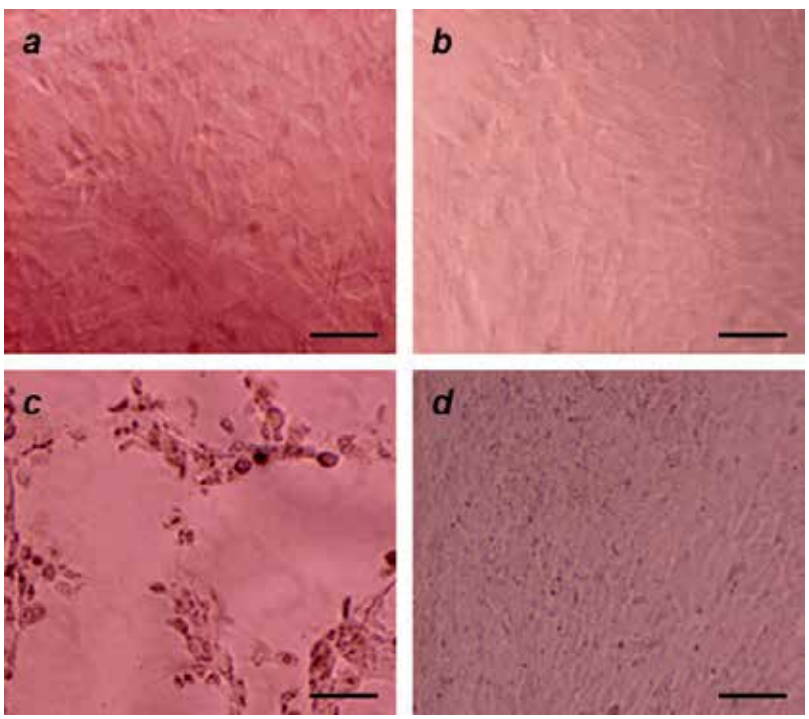

Figure 3. Suppression effect of cell necrosis by sCR1 on stroma cell PA-6. Phase contrast micrographs of PA-6 cells in (a) α-MEM media (control), (b) in the presence of heat inactivated NHS, (c) in the presence of NHS, and (d) in the presence of NHS plus the purified sCR1. Cell necrosis is observed when the formation of membrane attack complex (MAC) located at the complement terminal pathway is not inhibited. The scale bars correspond to 100 μm.

3.3. Crystallization trials

Although we have not yet fully succeeded in obtaining crystals of sCR1 suitable for X-ray crystallographic experiments, the microcrystals have been obtained more than 10 years after the continuous re-innovation of cell culture methods and protein purification strategies. **Figure 4** shows the micrographs of thus obtained microcrystals of sCR1. These crystals are obtained under the conditions where sulfate and polyethylene glycol (PEG) of low polymerization degree were used as precipitants (Kato and Ishii, unpublished data). Those microcrystals diffract X-ray up to several tens of angstrom units, only in a small angle region (data not shown) [33].

Furtado et al. reported the structural model as a partly folded back solution structure of human sCR1 by using a combination of small angle X-ray scattering and analytical ultracentrifugation analyses [34]. They constructed the sCR1 model using a SCR segment as a building block unit. The average model of the consensus SCR domain used was derived from 27 different experimental SCR structural templates and 49 residue consensus SCR sequence from 124 human complement sequences. They connected the SCRs and build the sCR1 model so as to give a better hit to the X-ray solution scattering profiles. Although they emphasize that one out of the five models is the most likely conformation in a free environment, these five models do not seem to overlap three-dimensionally with each other at all. Their solution structure of human sCR1 reported appears not to be rigid at each inter-SCR connection. The realization of structure

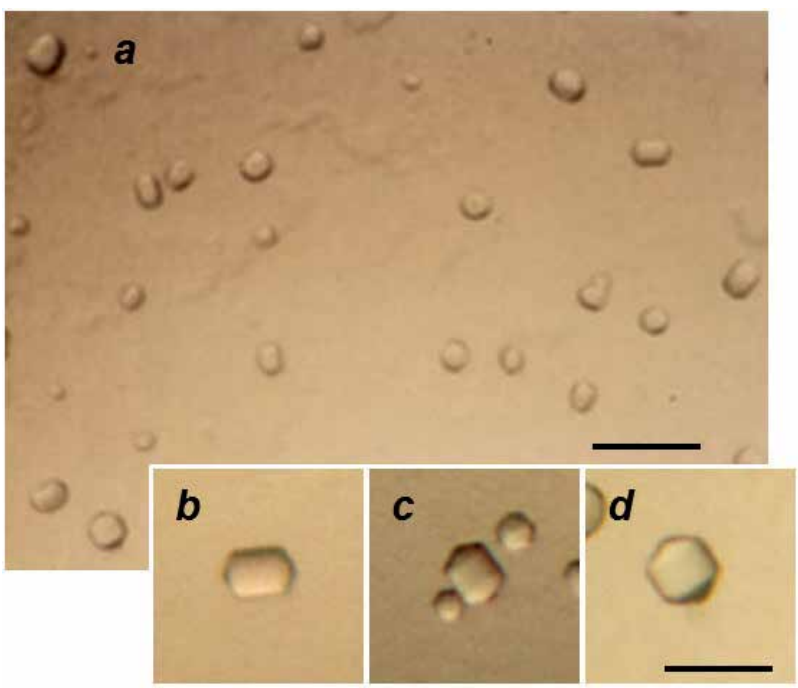

Figure 4. Microcrystals of human sCR1. Approximate dimension of the typical crystals were 29 × 29 × 33 μm. The scale bar in panel (a) corresponds 100 μm, and that for the enlargement, (b)–(d) corresponds 50 μm. Those microcrystals diffract X-ray poorly and spots could be recorded in a small angle range (not shown).

at an atomic resolution of human sCR1 as determined with X-ray crystallography appears very difficult without once forming a rigid complex structure with a complement ligand like C3b, although it is unknown what three-dimensional structured complex would be formed between sCR1 and C3b.

3.4. Secondary structure simulation of human sCR1

To change tactics, it may be useful to compute the secondary structure prediction for the amino acid sequence of a protein whose tertiary structure is not determined [26]. First, we tried the prediction method of Chou-Fasman. The results of secondary prediction for each SCR (from SCR-1 through SCR-30) are exhibited in **Figure 5**. According to the Chou-Fasman method, the content of α-helices is 13.6%, and that of β-strands is 24.9%. Taking a look at the distribution along the sequences of the predicted secondary elements, similarity is recognized between every seventh SCRs. Typically, the homogeneity among the every seventh SCRs between SCR-8–SCR-11 and SCR-15–SCR-18 are remarkable. These regions are considered as a C3b/C4b binding site, thus the conservation in the secondary elements between the above regions is convincible consistent with this observation.

The structural model of the domain from SCR-15 through SCR-17 of human sCR1 was built by Smith et al. [35]. Before building the structural model of the three consecutive SCR domains, they had determined the solution structure of SCR-15–SCR-16, and SCR-16–SCR-17, independently by NMR analyses. As shown in **Figure 6(a)**, the model reveals three complement control modules (SCR-15–17) in extended head-to-tail arrangement with flexibility at the SCR-15–SCR-16, and the SCR-16–SCR-17 junction. **Figure 6(b)** shows the result of quantitative electrostatic calculations. The view orientation is the same as **Figure 6(a)**. In this view angle, the negatively charged surface regions appear to be dominant and appear to be concentrated on the surface of SCR-15, and SCR-17. **Figure 6(c)** is a presentation of SCR-15–16–17 from a different orientation (turned 180°) as shown on the right side of **Figure 6(b)**. The corresponding electrostatics to **Figure 6(c)** is shown in **Figure 6(d)**. At this angle, the positively charged surface regions appear to be connected with one-side surface of SCR-15 through SCR-17. It is said that the positively charged region on SCR-15 is critical for C4b binding, and further, together with basic amino acid residues exposed on the same surface of SCR-16 are requisite for C3b binding [35]. Negatively charged regions are also seen scattered on the surface. The domain architecture and the manner of charged states appear important and may provide clues to the functional aspect of C3b binding.

At this stage, it appears interesting to examine the secondary structure predictions with the model built from the solution structures by NMR analyses. The domain SCR-15–17 (indicated with a box in **Figure 5**) is from a prediction using the Chou-Fasman method (**Figure 5**). α-Helices are not assigned with the solution structure at all (**Figure 6**), though the existence is predicted by the Chou-Fasman method. However, it is interesting that the number of predicted secondary structural elements is almost comparable. We then tried another structure prediction method, that is, the joint prediction method, which had higher precision. **Figure 7** shows the results of secondary prediction for each SCR (from SCR-1 through SCR-30) by the use of the joint prediction method. The content of α-helices is 6.0%, and that of β-strands is

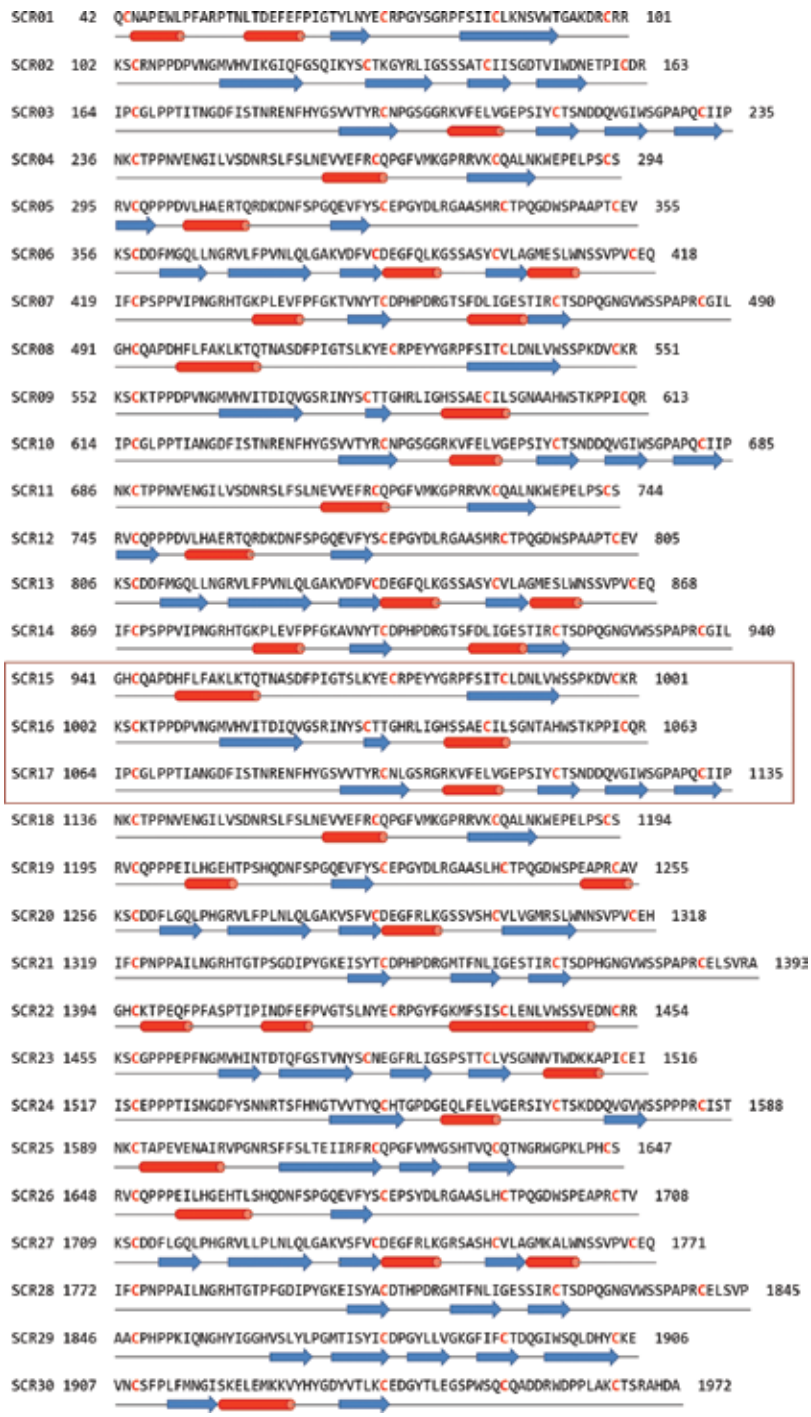

Figure 5. Secondary structure prediction for each SCR (from SCR-1 through SCR-30) in human sCR1 by the use of the Chou-Fasman method. The sequence predicted as α-helix or β-strand is shown with a cylindrical shape or fat arrow, respectively. The predicted sequence except the secondary structural element is a coil shown as a simple rod. The conserved Cys residues in each SCR are highlighted in red. The portion of SCR-15–17 discussed in the text is indicated with a box.

http://dx.doi.org/10.5772/intechopen.75120

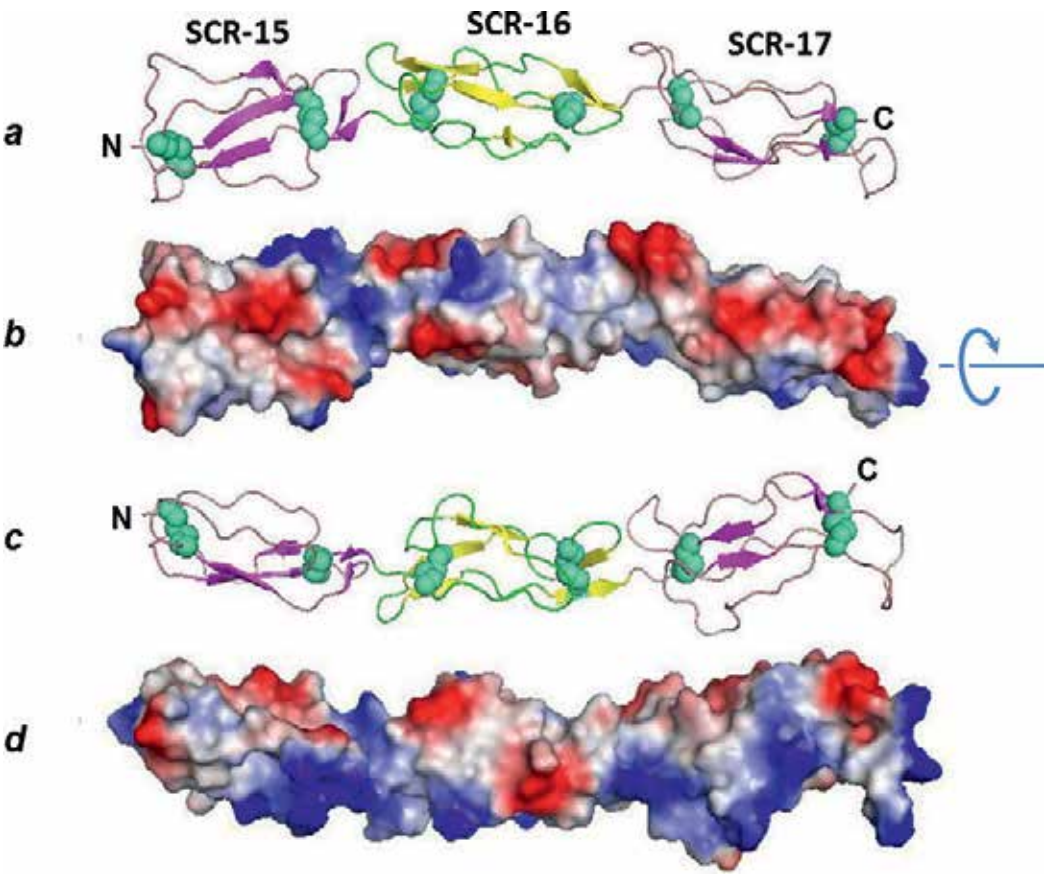

Figure 6. Diagrams of solution structure of domains SCR-15–17 (PDB ID: 1GOP). (a) Cα trace of SCR-15–17 with secondary structural elements (β-strand is indicated with arrow) and disulfide bonds (indicated with spheres). (b) An electrostatic presentation of SCR-15–17; the same view as (a). The protein domains are shown as an electrostatic surface colored blue in the positive regions and red in the negative regions. (c) Cα trace with secondary structural elements and disulfide bonds of SCR-15–17 made to rotate 180° as shown on the right side of (b). (d) An electrostatic presentation of SCR-15–17; the same view as (c). Atomic coordinates were obtained from the RCSB protein data Bank (www.rcsb.org/pdb/home/home.do) and imaged using PyMol (the PyMOL molecular graphics system, version 0.99, DeLano scientific, LLC).

19.3%. The accuracy of results from the joint prediction methods is better than a single method such as Chou-Fasman method, Garinier-Osguthorpe-Robson method, and Lim method [27]. Since the final assessment of whether a certain amino acid sequence forms a secondary structure element is determined by majority rule between five different prediction algorithms, the precision success rate is rather high while the adoption rate as secondary structure elements is low compared to the prediction results by Chou-Fasman method on the whole. Looking at the prediction of SCR-15–17 for example (as indicated with a box in **Figure 7**), all but one predicted secondary elements as β-strands, suggesting that precision rose. The content of α-helices was predicted in the half ratio in comparison with that of β-strands by the Chou-Fasman method, but the prediction of α-helices improved in one-third or less compared with the content of β-strands using the joint method. In the algorithms of the joint prediction method, the most likely secondary structure element for each amino acid sequence region is decided depending

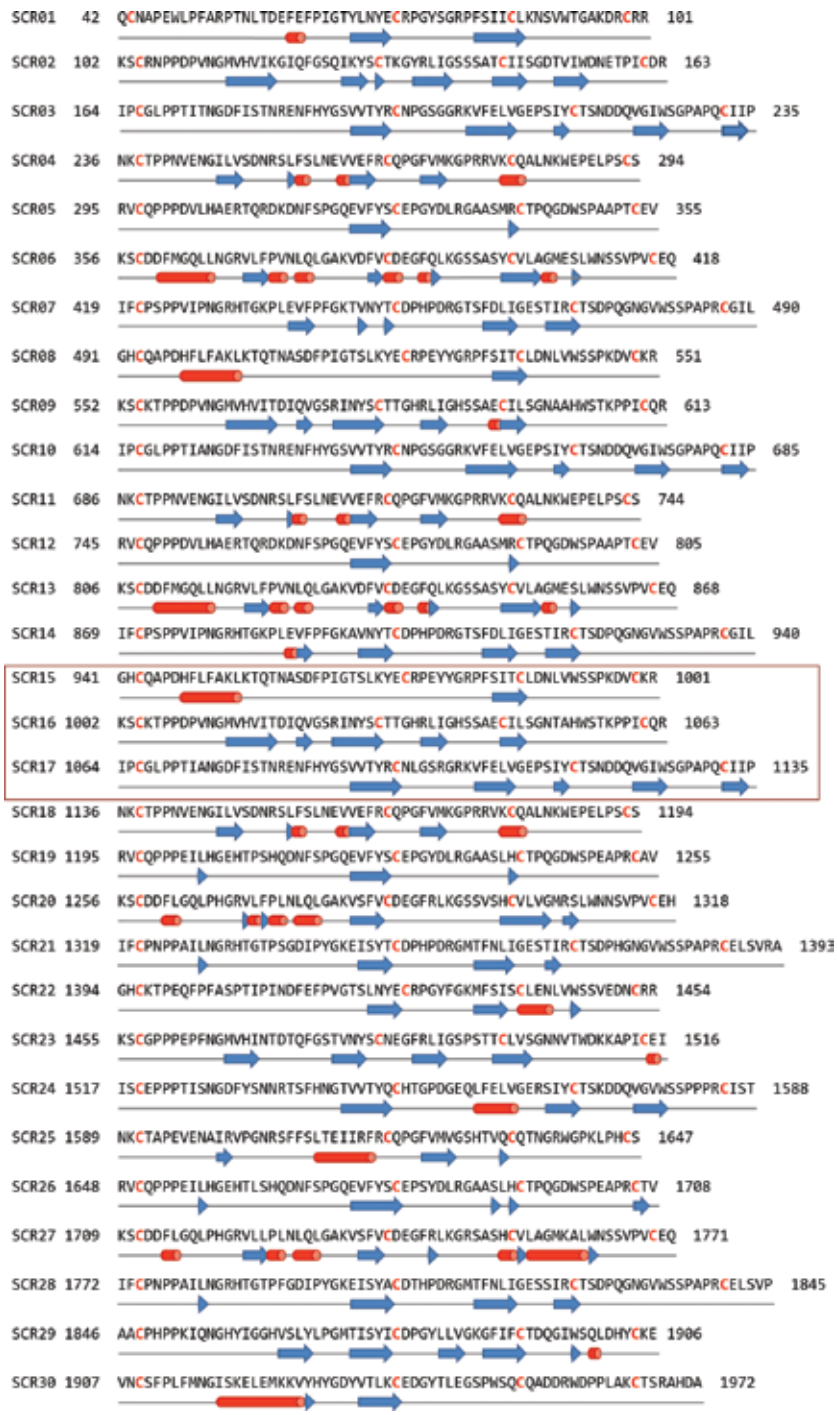

Figure 7. Secondary structure prediction for each SCR (from SCR-1 through SCR-30) in human sCR1 by the use of the joint prediction method. The sequence predicted as α-helix or β-strand is shown with a cylindrical shape or fat arrow, respectively. The predicted sequence except the secondary structural element is a coil shown as a simple rod. The conserved Cys residues in each SCR are highlighted in red. The portion of SCR-15–17 discussed in the text is indicated with a box.

on the decision by majority votes against five independent answers, from Qian-Sejnowski, Ptitsyn-Finkelstein, Nisikawa-Ooi, SSthread, and Gibrat-Garinier-Robson methods. Therefore, a sequence will not be qualified as a secondary structure, either α-helix or β-strand, unless getting an approval from majority solutions. Therefore, the number of region predicted as secondary structured elements as a whole will be decreased, but higher reliability will be expected. The tendencies in the order and distribution of the predicted secondary elements are recognized to be almost the same between every seventh SCRs, especially among the every seventh SCRs between SCR-8–SCR-11 and SCR-15–SCR-18.

3.5. Structural biological aspect of human sCR1

As discussed earlier, determinations of three-dimensional structure of each SCR, and the confidence with subsequent modeling of sCR1 appears severely difficult due to the sequence variation, and the orientation and flexibility of neighboring SCRs with respect to one another appear to easily change considerably, and are thus unpredictable. sCR1 is one of the very difficult targets for structure analysis, but we are convinced that such a goal has some promise once its three-dimensional molecular structure is determined.

Recently, a large number of NUPs have been found, and those appear to be connected with signaling and regulation of gene expression [8]. As exemplified above with sCR1, there are a lot of proteins involved in the immune system whose three-dimensional structure has not yet been revealed by X-ray crystallography. One of the reasons is the difficulties in the preparation of crystals suitable for X-ray diffraction methods probably due to the large flexibility (that may correspond to large values in B factor) of functional and reactive domains and is thus subject to conformational changes. The conceptual importance of NUPs is that various proteins interact with other proteins via intrinsically disordered regions. It means the ID region is an unfolded state without a definitive structure, but when a ligand peptide or partner protein coexists, the region interacts with it to form a complex by changing the random coil segments to secondary structures. It is suggested that disorder in a free state may actually be advantageous for the binding process, and that the rate of macromolecular association is enhanced by the presence of disorder region [36, 37]. As a way out of the situation, co-crystallization with some sort of ligands may work. That is, we should utilize the property of NUPs-like protein that is easy to change conformations by letting the protein change its structures, and by guiding it to a structure that is easier to be crystallized. The structural atlas of the protein promotes and deepens an understanding of the interaction between the complement proteins, which are involved in the human immune system, and drives novel drug development. Direct structural studies of the interaction between C4b and sCR1, or between C3b and sCR1 are desired to realize these goals [38].

4. Conclusions

Proteins like sCR1 are difficult targets to lead crystallization suitable for X-ray crystallography. The recognition of NUPs has imposed the view that proteins consist not only of structured domains but also of ID regions. The ID region is an unfolded state without a definitive structure, but when a ligand peptide or partner protein coexists, the region interacts with it

to form a complex by changing the random coil segments to rigid structured secondary structures. As a way out of the situation, co-crystallization with some sort of ligands or partner protein molecule may work. That is, we should utilize the flexible conformation property of NUPs-like protein, let the protein change its structures, and guide it to the structure that is easy to be crystallized. Once the structural detail of interest is obtained at hand, the atlas of the protein promotes and deepens the understanding of the interaction between the complement proteins which are involved in the immune system.

Acknowledgements

The author deeply thanks Dr. Kenneth S. Kim for discussion and critical reading of the manuscript. He also thanks Prof. Dr. Pi-Chao Wang, and Dr. Mutsuo Tanaka for stimulating discussion. This study was partly supported by a Grant-in-Aid for Scientific Research (B) (Grant Number 17370043), a Grant-in-Aid for Challenging Exploratory Research (Grant Number 25650042), and Challenging Research (Pioneering) (Grant Number 17H06242) from Japan Society for the Promotion of Science (JSPS), Ministry of Education, Culture, Sports, Science and Technology (MEXT) of Japan.

Conflict of interest

The author declares that he has any financial or personal relationships with people of organization that can inappropriately influence his work or the conclusions drawn from this investigation.

Author details

Noriyuki Ishii

Address all correspondence to: n.ishii@aist.go.jp

Biomedical Research Institute, Department of Life Science and Technology, National Institute of Advanced Industrial Science and Technology (AIST), Tsukuba, Ibaraki, Japan

References

[1] Anfinsen CB. Principles that govern the folding of protein chains. Science. 1973;**181**:223-230. DOI: 10.1126/science.181.4096.223

[2] Ellis RJ. Proteins as molecular chaperones. Nature. 1987;**328**:378-379. DOI: 10.1038/328378a0

[3] Akiba T, Ishii N, Rashid N, Morikawa M, Imanaka T, Harata K. Structure of RadB recombinase from a hyperthermophilic archaeon, *Thermococcus kodakaraensis* KOD1: An implication for the formation of a near-7-fold helical assembly. Nucleic Acids Research. 2005;**33**:3412-3423. DOI: 10.1093/nar/gki662

[4] Ishii N. Crystallization, structure and functional robustness of isocitrate dehydrogenases. In: Chandrasekaran A, editor. Current Trends in X-Ray Crystallography. Croatia: InTech; 2011. pp. 309-332. DOI: 10.5772/32635

[5] Dyson HJ, Wright PE. Intrinsically unstructured proteins and their functions. Nature Reviews Molecular Cell Biology. 2005;**6**:197-208. DOI: 10.1038/nrm1589

[6] Wright PE, Dyson HJ. Linking folding and binding. Current Opinion in Structural Biology. 2009;**19**:31-38. DOI: 10.1016/j.sbi.2008.12.003

[7] Wright PE, Dyson HJ. Intrinsically unstructured proteins: Re-assessing the protein structure-function paradigm. Journal of Molecular Biology. 1999;**293**:321-331. DOI: 10.1006/jmbi.1999.3110

[8] Nishikawa K. Natively unfolded proteins: An overview. Biophysics. 2009;**5**:53-58. DOI: 10.2142/biophysics.5.53

[9] Hoshino A, Costa-Silva B, Shen TL, Rodrigues G, Hashimoto A, Mark MT, Molina H, Kohsaka S, Di Giannatale A, Ceder S, Singh S, Williams C, Soplop N, Uryu K, Pharmer L, King T, Bojmar L, Davies AE, Ararso Y, Zhang T, Zhang H, Hernandez J, Weiss JM, Dumont-Cole VD, Kramer K, Wexler LH, Narendran A, Schwartz GK, Healey JH, Sandstrom P, Labori KJ, Kure EH, Grandgenett PM, Hollingsworth MA, de Sousa M, Kaur S, Jain M, Mallya K, Batra SK, Jarnagin WR, Brady MS, Fodstad O, Muller V, Pantel K, Minn AJ, Bissell MJ, Garcia BA, Kang Y, Rajasekhar VK, Ghajar CM, Matei I, Peinado H, Bromberg J, Lyden D. Tumour exosome integrins determine organotropic metastasis. Nature. 2015;**527**:329-335. DOI: 10.1038/nature15756

[10] Welton JL, Khanna S, Giles PJ, Brennan P, Brewis IA, Staffurth J, Mason MD, Clayton A. Proteomics analysis of bladder cancer exosomes. Molecular & Cell Proteomics. 2010; **9**:1324-1338. DOI: 10.1074/mcp.M000063-MCP201

[11] Melo SA, Luecke LB, Kahlert C, Fernandez AF, Gammon ST, Kaye J, LeBleu VS, Mittendorf EA, Weitz J, Rahbari N, Reissfelder C, Pilarsky C, Fraga MF, Piwnica-Worms D, Kalluri R. Glypican-1 identifies cancer exosomes and detects early pancreatic cancer. Nature. 2015;**523**:177-182. DOI: 10.1038/nature14581

[12] Ishii N, Fitrilawati F, Manna A, Akiyama H, Tamada Y, Tamada K. Gold nanoparticles used as a carrier enhance production of anti-hapten IgG in rabbit: A study with azobenzene-dye as a hapten presented on the entire surface of gold nanoparticles. Bioscience, Biotechnology, and Biochemistry. 2008;**72**:124-131. DOI: 10.1271/bbb.70499

[13] Nelson RA Jr. The immune adherence phenomenon. Science. 1953;**118**:733-737. DOI: 10.1126/science.118.3077.733

[14] Nelson DS. Immune adherence. In: Dixon DS, Humphrey JH Jr, editors. Advances in Immunology. Vol. 3. New York: Academic Press Inc.; 1963. pp. 131-180

[15] Fearon DT. Regulation of the amplification C3 convertase of human complement by an inhibitory protein isolated from human erythrocyte membrane. Proceedings of the National Academy of Sciences of the United States of America. 1979;**76**:5867-5871. PMCID: PMC411753

[16] Fearon DT. Identification of the membrane glycoprotein that is the C3b receptor of human erythrocyte, polymorphonuclear leukocyte, B lymphocyte, and monocyte. The Journal of Experimental Medicine. 1980;**152**:20-30. PMCID: PMC2185895

[17] Krych-Goldberg M, Atkinson JP. Structure-function relationship of complement receptor type 1. Immunological Reviews. 2001;**180**:112-122. DOI: 10.1034/j.1600-065X.2001.1800110.x

[18] Weisman HF, Bartow T, Leppo MK, Marsh HC Jr, Carson GR, Concino MF, Boyle MP, Roux KH, Weisfeldt ML, Fearon DT. Soluble human complement receptor type 1: In vivo inhibitor of complement suppressing post-ischemic myocardial inflammation and necrosis. Science. 1990;**249**:146-151. DOI: 10.1126/science.2371562

[19] Kato H, Inoue T, Ishii N, Murakami Y, Matsumura M, Wang PC. A novel simple method to purify recombinant soluble human complement receptor type 1 (sCR1) from CHO cell culture. Biotechnology and Bioprocess Engineering. 2002;**7**:67-75. DOI: 10.1007/BF02935882

[20] Yamaguchi A, Takagawa H, Iwakaji H, Miyagawa S, Wang PC, Ishii N. Construction of the plasmid, expression by Chinese hamster ovary cell, purification and characterization of the first three short consensus repeat modules of human complement receptor type 1. Journal of Biochemistry. 2009;**145**:533-542. DOI: 10.1093/jb/mvp006

[21] Ishii N, Kato H, Wang PC. Observation by electron microscopy on recombinant soluble human complement receptor type 1 (sCR1) and its derivative, aglyco-sCR1, from CHO cells. Enzyme and Microbial Technology. 2003;**33**:482-487. DOI: 10.1016/S0141-0229(03)00152-2

[22] Mevorach D, Mascarenhas JO, Gershov D, Elkon KB. Complement-dependent clearance of apoptotic cells by human macrophages. Journal of Experimental Medicine. 1998;**188**:2313-2320. DOI: 10.1084/jem.188.12.2313

[23] Carrington CA, dos Santos Cruz G. Effect of cell surface concentration of human DAF on transgenic pig aortic endothelial cells on the degree of protection afforded against human complement deposition. Xenotransplantation. 2001;**8**:100-105. DOI: 10.1034/j.1399-3089.2001.00086.x

[24] Huang J, Gou D, Zhen C, Jiang D, Mao X, Li W, Chen S, Cai C. Protection of xenogeneic cells from human complement-mediated lysis by the expression of human DAF, CD59 and MCP. FEMS Immunology and Medical Microbiology. 2001;**31**:203-209. DOI: 10.1111/j.1574-695X.2001.tb00521.x

[25] Ishii N, Umemura K, Miyazaki K. Supramolecular complex formation and crystallization of isocitrate dehydrogenase from *Thermus thermophilus* HB8: Preliminary studies with X-ray crystallography and atomic force microscopy. Bioscience, Biotechnology, and Biochemistry. 2008;**72**:2369-2376. DOI: 10.1271/bbb.80269

[26] Nishikawa K, Noguchi T. Predicting protein secondary structure based on amino acid sequence. Methods in Enzymology. 1991;**202**:31-44. DOI: 10.1016/0076-6879(91)02005-T

[27] Ito M, Matsuo Y, Nishikawa K. Prediction of protein secondary structure using the 3D-1D compatibility algorithm. Computer Applications in the Biosciences. 1997;**13**:415-424

[28] Klickstein LB, Barbashov SF, Liu T, Jack RM, Nicholson-Weller A. Complement receptor type 1 (CR1, CD35) is a receptor for C1q. Immunity. 1997;**7**:345-355. DOI: 10.1016/S1074-7613(00)80356-8

[29] Makrides SC, Scesney SM, Ford PJ, Evans KS, Carson GR, Marsh HC Jr. Cell surface expression of the C3b/C4b receptor (CR1) protects Chinese hamster ovary cells from lysis by human complement. Journal of Biological Chemistry. 1992;**267**:24754-24761

[30] Reilly BD, Makrides SC, Ford PJ, Marsh HC Jr, Mold C. Quantitative analysis of C4b dimer binding to distinct sites on the C3b/C4b receptor (CRl). Journal of Biological Chemistry. 1994;**269**:7696-7701

[31] Wong WW, Farrell SA. Proposed structure of the F′ allotype of human CR1. Loss of a C3b binding site may be associated with altered function. Journal of Immunology. 1991;**146**:656-662

[32] Reilly BD, Mold C. Quantitative analysis of C4Ab and C4Bb binding to the C3b/C4b receptor (CR1, CD35). Clinical and Experimental Immunology. 1997;**110**:310-316. DOI: 10.1111/j.1365-2249.1997.tb08333.x

[33] Ishii N, Saijo S, Sato T, Tanaka N, Harata K. Crystallization and preliminary X-ray studies of V_1-ATPase of *Thermus thermophilus* HB8 complexed with Mg-ADP. Journal of Structural Biology. 2001;**134**:88-92. DOI: 10.1006/jsbi.2001.4358

[34] Furtado PB, Huang CY, Ihyembe D, Hammond RA, Marsh HC, Perkins SJ. The partly folded back solution structure arrangement of the 30 SCR domains in human complement receptor type 1 (CR1) permits access to its C3b and C4b ligands. Journal of Molecular Biology. 2008;**375**:102-118. DOI: 10.1016/j.jmb.2007.09.085

[35] Smith BO, Mallin RL, Krych-Goldberg M, Wang X, Hauhart RE, Bromek K, Uhrin D, Atkinson JP, Barlow PN. Structure of the C3b binding site of CR1 (CD35), the immune adherence receptor. Cell. 2002;**108**:769-780. DOI: 10.1016/S0092-8674(02)00672-4

[36] Shoemaker BA, Portman JJ, Wolynes PG. Speeding molecular recognition by using the folding funnel: The fly-casting mechanism. Proceedings of the National Academy of Sciences of the United States of America. 2000;**97**:8868-8873. DOI: 10.1073/pnas.160259697

[37] Pontius BW. Close encounters: why unstructured, polymeric domains can increase rates of specific macromolecular association. Trends in Biochemical Sciences. 1993;**18**:181-186. DOI: 10.1016/0968-0004(93)90111-Y

[38] Ishii N, Sato T. Anisotropic intersubunit and inter-ring interactions revealed in the native bullet-shaped chaperonin complex from *Thermus thermophilus*. Biochimica et Biophysica Acta. 1830;**2013**:2907-2916. DOI: 10.1016/j.bbagen.2013.01.003

Edited by Shihori Tanabe

The peripheral membrane proteins transduce the extracellular signaling into the cells. The peripheral membrane proteins include the G protein-coupled receptors, receptor tyrosine kinases, channels and transporters. The signals, which are transduced via the peripheral membrane proteins, activate several pathways including G protein signaling, MAPK signaling, TNF signaling, TGFβ signaling, Wnt signaling and Hedgehog signaling. The peripheral membrane proteins transduce the signaling from the extracellular ligands into the cells. This book intends to provide a comprehensive overview of the features and signaling of peripheral membrane proteins, which includes the molecular structure and interaction. The insights into membrane proteins associated with diseases and therapeutics and the effects of drugs and chemicals are also discussed in this book.

Published in London, UK

IntechOpen

ISBN 978-1-83881-617-9